
Neurobiology and vision of jumping spiders (Araneae: Salticidae)

David E. Hill¹

¹ 213 Wild Horse Creek Drive, Simpsonville SC 29680, USA, *email* platycryptus@yahoo.com

Introduction

As with other spiders (Araneae), the paired segmental ganglia of jumping spiders (Salticidae) are fused into a single nerve mass, or central nervous system (CNS), surrounding the esophagus. In this respect, salticids are not remarkable. What is really unique about salticid spiders is their development of high-resolution visual systems, and the visual system of the *anterior medial eyes* (AME, also known as the *primary eyes*) in particular. The modern study of the salticid AME began with two benchmark papers written by Michael F. Land (1942-2020) in the late 1960's (Land 1969a, 1969b), which revealed the structure of a multi-layered retina in these eyes. Here we will review many subsequent studies of these eyes, but it is fair to say that our understanding of their function has not proceeded very far beyond the important questions raised in those benchmark papers. Apart from the visual systems of salticids, most of our understanding of the senses and neurobiology of spiders has emerged from the study of spiders in other families, and I will review some of these as well to the extent that they apply to our understanding of the Salticidae. This paper also includes introductory material on the salticid CNS that I presented in earlier papers (Hill 1975, 2006).

It is important that students of salticid behavior are familiar with *what is known* of the function of the eyes of these animals, but it is also true that few arachnologists have a sufficient understanding of either visual optics or color vision as experienced by our own species, both subject to active research programs at the present time. The study of the AME is certainly difficult. Beginning with Land's (1969a) work, most models of the visual optics of the AME have relied on key assumptions, readily confused by the casual reader with actual observations. It is necessary to carefully separate observation from assumption, and fact from hypothesis, in a critical review of this subject. To allow the reader to follow this discussion I have included some introductory material here, particularly on the subjects of optics and color vision with respect to our own species.

As the many studies of David Blest (e.g., Blest 1983, 1984, 1985a, 1985b) have revealed, there is considerable variation in the development of vision within the Salticidae. This is something that we should expect, given the importance of vision to the success of these spiders, and its key role in their evolution (Hill & Richman 2009). *Structural or functional findings with respect to one salticid species do not necessarily apply to all salticids.*

Vision-mediated behavior of salticids

Robert R. Jackson has recalled that the late Michael F. Land, while in Berkeley, *casually said something about how watching a salticid scan feels almost like watching it think* (Jackson & Harland 2009). Many who have closely observed these active spiders share this impression as, like us, these are decidedly visual animals. I would add that, as one observes more of the behavior and implicit decision-making of these spiders, the notion that one is *watching them think* grows stronger. And, *they turn to look at you*. They have faces, and they turn to look at our own faces (Figure 1).



Figure 1. Faces of two jumping spiders of the North American genus *Phidippus* C. L. Koch 1846. **1**, Adult male *P. pacosauritus* Edwards 2020, Paco's Reserva de Flora y Fauna, Mazatlán, Sinaloa, Mexico. **2**, Adult female *P. putnami* (Peckham & Peckham 1883), southern Greenville County, South Carolina, USA.

Many papers have been written to describe the unique vision-mediated behaviors of salticids, and several extensive reviews of the subject are available (e.g., Richman & Jackson 1992; Harland & Jackson 2000; Harland, Li & Jackson 2012). Some of these behaviors are listed here for reference (Table 1).

Table 1. Some vision-mediated behaviors of salticid spiders. Behaviors that appear to be more complicated or sophisticated are placed toward the bottom of this list.

behavior	selected references
Lateral (α) turn to face a moving object with the anterior eyes, with stepping movements	Land 1971, 1972; Duelli 1978; Hill 1978, 1979, 2010a; Bennett & Lewis 1979
Dorso-ventral (β), or combined (α , β) turn to face a moving object with the anterior eyes, with or without stepping movements	Hill 1978, 1979, 2010a
Rotation (ρ) around body axis to change alignment of eyes while facing an object	Hill 1978, 1979, 2010a
Determine distance of prey or other object faced with the anterior eyes	Hill 1978, 1979, 2010a, 2010b
Avoid areas associated with specific colors	Nakamura & Yamashita 2000
Jump accurately to capture sighted prey at a distance	Peckham & Peckham 1895; Robinson & Valerio 1977; Hill 2010b, 2018a, 2018b; Hill, Glaser and Galvão, 2021
Recognize and communicate visually with conspecific males or females at a distance	Richman 1982; Crocker & Skinner 1984; Clark & Uetz 1993; Taylor, Hassan & Clark 2000, 2001; Clark & Morjan 2001; Lim 2006; Lim & Li 2006a, 2006b; Elias <i>et al.</i> 2006, 2012; Lim, Li & Li 2007; Nelson & Jackson 2007; Li <i>et al.</i> 2008; Nelson 2010; Hill & Otto 2011; Girard, Kasumovic & Elias 2011; Otto & Hill 2012; Hill 2018a
Recognize and evaluate predators or prey at a distance	Kästner 1950; Drees 1952; Gardner 1966; Hill 1978, 2010a, 2018a; Jackson & Blest 1982; Bartos 2000; Jackson 2000; Harland & Jackson 2000, 2001a, 2001b, 2002; Li & Lim 2005; Lim 2006; Nelson & Jackson 2007, 2009; Nelson 2010
Visually evaluate routes of movement or pursuit	Hill 1978, 1979, 2010a; Jackson & Wilcox 1993; Tarsitano & Jackson 1994
Recognize local landmarks or plant configurations	Hill 1978, 1979, 2010a; Hoefler & Jakob 2006

Facing turns represent the most defining behavior of an alert salticid spider. Even a rapidly moving ant mimic like *Peckhamia* Simon 1900 reveals its true salticid nature when it turns to look at something. These turns bring the visual capabilities of the four anterior or *facial* eyes (AME, ALE) to bear on an object of interest, whether that represents a conspecific male or female, potential prey, a threat, or just a part of the local vegetation. Although they have many other senses, there can be no doubt that salticids are profoundly dependent upon their vision.

Segmentation and cellular components of the central nervous system (CNS)

Early students of the spider CNS (e.g., Hanström 1921, 1935) thought that they could identify structures, such as the *corpora pedunculata*, that were homologous with structures of similar shape and position associated with the insect or even the annelid brain. Later others (e.g., Meier 1967; Hill 1975, 2006) noted that the *corpora pedunculata* of spiders were quite different in structure and function from those of insects and annelids. In insects, these structures are primarily associated with the processing of sensory input from the antennae (Scheiner et al. 2001), whereas in spiders they are part of the lateral eye visual system (Hill 1975, 2006). With the recent discovery of bilaterian Hox genes, we are now able to obtain a much better view of homologies related to the anterior-posterior segmentation of both insects and spiders (Table 2). This reveals that the antennal segment of the insect is homologous to the cheliceral segment, and not to a missing second segment of the spider. From DNA studies of molecular phylogeny (Giribet, Edgecombe & Wheeler 2001; Halanych & Janosik 2006), we now know that annelids are only distantly related to arthropods, and insects are closely related to the paraphyletic Crustacea, which do not have *corpora pedunculata* (Strausfeld et al. 1998).

Table 2. Anterior (top) to posterior segmentation of spiders (Araneae: *Achaearanea tepidariorum* and *Cupiennius salei*) compared to insect segmentation, based on expression of Hox genes (after Damen et al. 1998; Telford & Thomas 1998; Damen and Tautz 1999; Damen 2002; Angelini et al. 2005; Schwager et al. 2007; Schwager 2008). The number of abdominal segments may vary in insects, with 11 reported in the hemipteran *Oncopeltus fasciatus* (Angelini et al. 2005). The *mode of segmentation* is based on the analysis of spider development by Schwager (2008). *Opisoma* is used here as a convenient contraction of *opisthosoma*, the rear part of the arachnid body that is sometimes called the *abdomen*.

segment	description	mode of segmentation	CNS structures	homologous insect segment
Oc	ocular segment	prosomal mode: simultaneous development of segments as in insects	protocerebrum (all precheliceral lobes)	Oc, ocular segment
Ch	chelicerae		cheliceral ganglia (deutocerebrum)	An1, first antennal
Pp	pedipalps		pedipalpal ganglia	Ic (An2), intercalary
L1	legs I		leg I ganglia	Md, mandibles
L2	legs II		leg II ganglia	Mx, maxillae
L3	legs III	opisomal mode: sequential development of segments as in vertebrates	leg III ganglia	Lb, labium
L4	legs IV		leg IV ganglia	T1, first thoracic
O1	opisoma I		corresponding ganglia of <i>cauda equina</i> (CE)	T2, second thoracic
O2	opisoma II			T3, third thoracic
O3-O12	opisoma III-XII	A1-A10, abdominal segments		

It is quite likely that future studies of regulatory genes associated with the development of the precheliceral lobes (Table 2, first or ocular segment) will reveal some homologies between these nerve centers and those of other arthropods. In fact, at some point it may be possible to use a complete chart of the temporal differentiation of associated neurons to do this. Here I will describe the nerve centers of the precheliceral lobes as discrete structures within a *protocerebrum* comprising all preoral (or supraesophageal) centers. The cheliceral ganglia are very similar in appearance to those of the pedipalps and legs, and are similarly joined by a postoral (behind the esophagus) commissure (Rempel 1957). Thus they are not included in the protocerebrum here. The chelicerae actually migrate on either side of the mouth, to the front of the spider, during embryonic development (Liu, Maas & Waloszek 2009), so their anterior or preoral position in the fully-developed spider does not reflect their proper association with the postoral second segment (Table 2, *Ch*).

It is important to recognize that in many respects the structures of the spider nervous system are much like highways than are travelled by the processes of individual neurons, or *neurites*. The individual neurons that (with associated glial cells) comprise these structures frequently traverse several different body or appendage segments, and they may branch profusely. From the examination of stained serial sections, we can identify many *tracts* comprised of neurites in transit. Outside of the CNS, we refer to these tracts as *nerves*. Within the CNS, we may call them *commissures* (if they join left and right parts of the CNS), or we may label them by their direction (longitudinal, descending, ascending). In most parts of the CNS, areas (*neuropiles*) where neurites are connected with intercellular *synapses* are relatively unstructured or complex. In several places, however, neuropiles are very structured, and it is in these areas that we are most tempted to try to interpret the meaning of the observed structure. Fortunately for purposes of this exercise, the most structured (or patterned) neuropiles of the salticid CNS are associated with the eyes.

General structure of the CNS

The spider CNS (Figures 2-13) is a compact mass, comprised of a preoral or supraesophageal protocerebrum containing the visual centers and the fused, postoral segmental ganglia of the prosoma and opisoma. In salticids, the eyes and visual centers are particularly large.

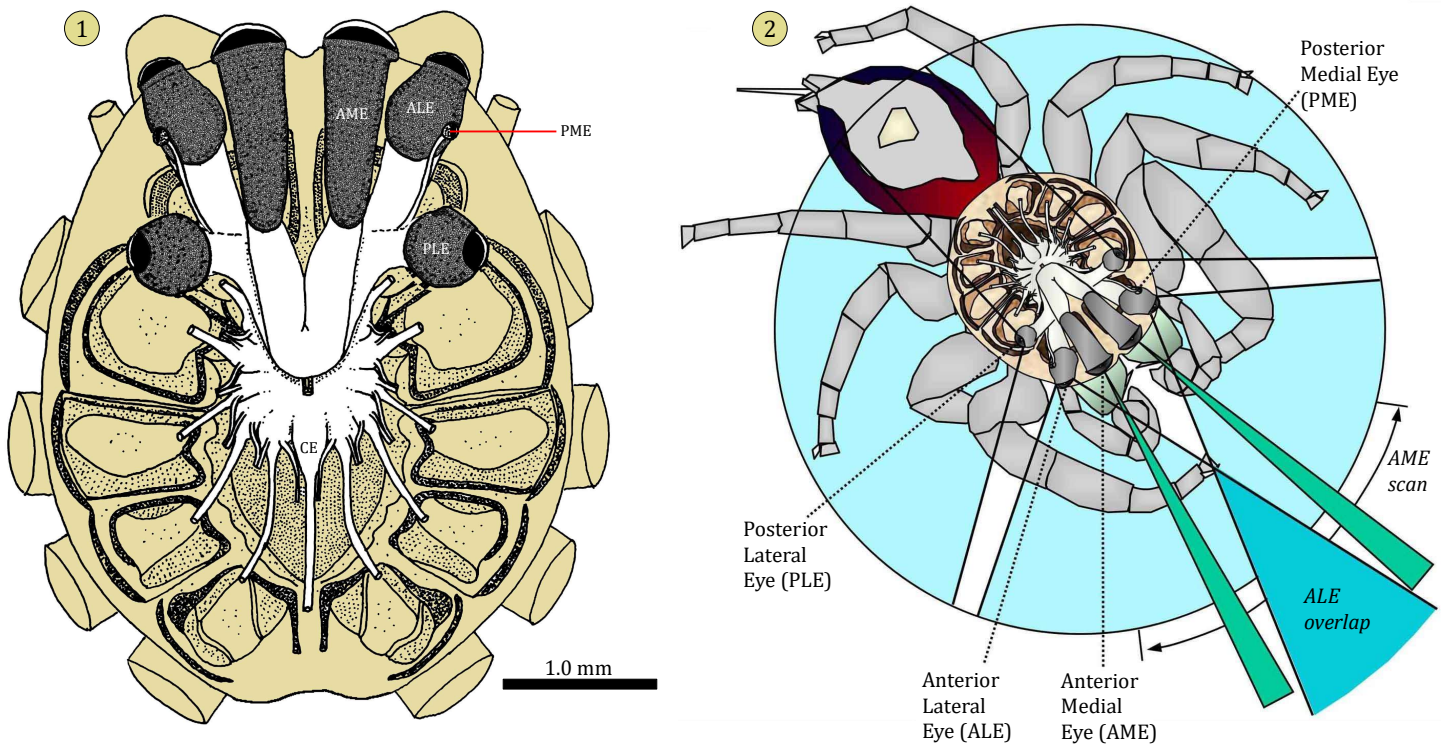


Figure 2. Semi-schematic views of the CNS exposed in a dissection of the prosoma of *Phidippus* jumping spiders. **1**, Adult female *Phidippus clarus* Keyserling 1885. The optic nerves of the anterior medial eyes (AME) lead directly to the rear, to the AME neuropiles I and II at the top of the CNS. Below these are the wide optic nerves of the anterior and posterior lateral eyes (ALE and PLE, respectively), and the small optic nerves of the posterior medial eyes (PME). In most salticids the PME are small as shown here, but in some they are much larger. The fused opisomal ganglia (CE, or *cauda equina*) lie at the rear of a suboral, ventral mass of fused pedipalp and leg ganglia. **2**, Visual fields of the respective eyes. The PLE have wide fields of vision, the ALE much narrower fields that overlap in front of the spider. The tubular AME have narrow fields, but are moved up and down and side to side to scan a larger field. After Hill (1975, 2006).

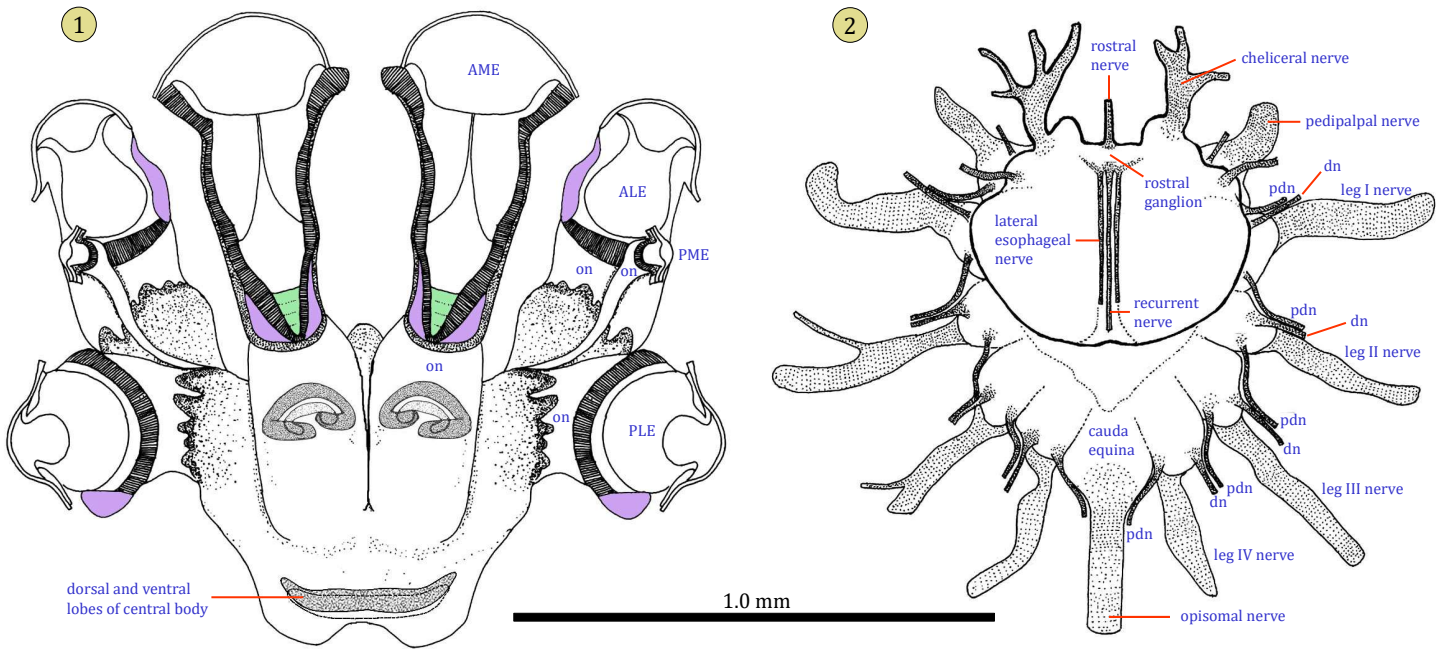


Figure 3. Semi-schematic dorsal views of the CNS of a fifth instar *Phidippus clarus*, based on reconstruction from serial sections. **1**, Protocerebrum and eyes (shown in section). Areas containing cell bodies of retinal photoreceptors are shown in purple. The tiered retinae of the AME are shaded in green. The optic nerve (*on*) associated with each eye leads to a respective first neuropile, where sensory neurons synapse with interneurons. For the lateral eyes, these neuropiles are folded or convoluted, increasing the surface area available for synapses. Neuropile I of each AME includes two concentric lobes, shown at center. **2**, Preoral rostral and postoral segmental ganglia. The rigid esophagus (not shown) is surrounded by two lateral esophageal nerves, and a dorsal recurrent nerve, all originating from the preoral rostral ganglion. In addition to the primary segmental nerves, each prosomal segment is associated with a small dorsal nerve (*dn*), and a postero-dorsal nerve (*pdn*) that joins the dorsal nerve of the next, posterior segment. After Hill (1975, 2006).

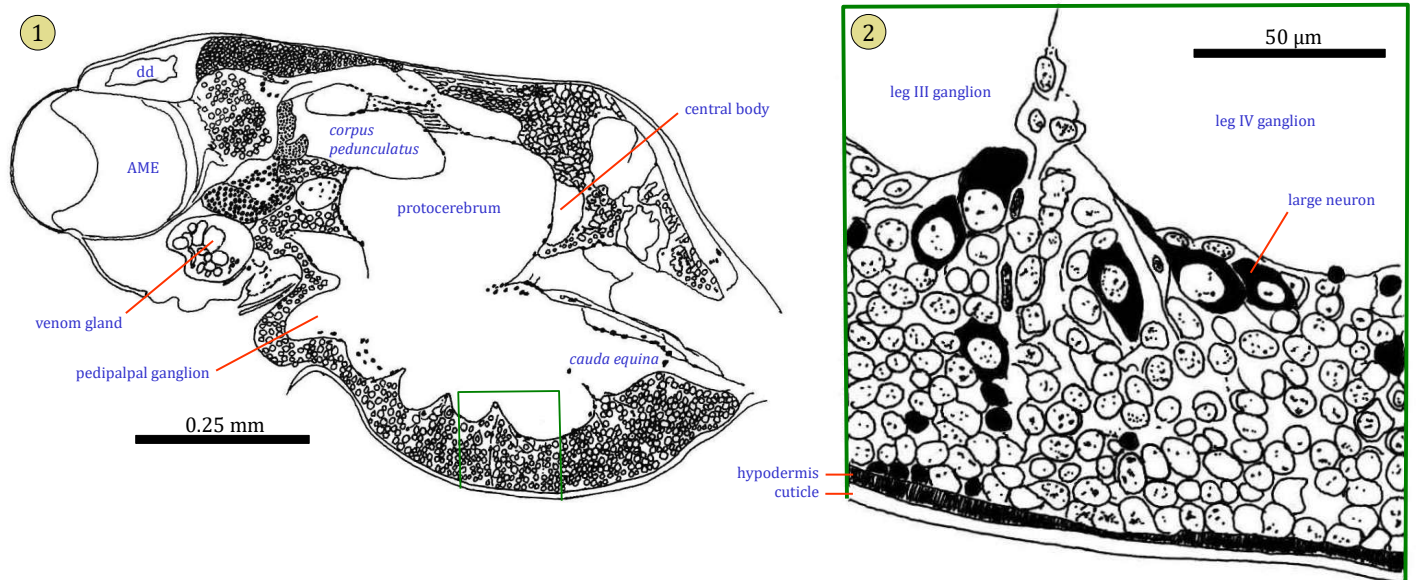


Figure 4. Camera lucida drawing of a parasagittal section through the prosoma of a second instar (emergent) *Phidippus clarus*. **1**, At this stage, the CNS occupies nearly the entire medial volume of the prosoma. **2**, Detail of inset from (1) showing a cluster of large neuron cell bodies in the cortex of the third and fourth leg ganglia, surrounded by smaller neurons. After Hill (1975, 2006).

With few exceptions, the neurons that comprise the spider CNS are *unipolar*. The neurites of each cell originate with a single process that leaves the cell body. The neuron cell bodies, readily identified by their compact, chromatin-rich nuclei, are packed together, external to the central tracts and neuropiles of the CNS. One notable exception to this pattern are the *bipolar* sensory neurons of the AME (anterior medial eyes). Each of these neurons sends one process bearing light-sensitive stacked membranes (*rhabdoms*) toward the retina, and a second process to the rear, where it synapses with the visual cortex (primary neuropile) of the AME.

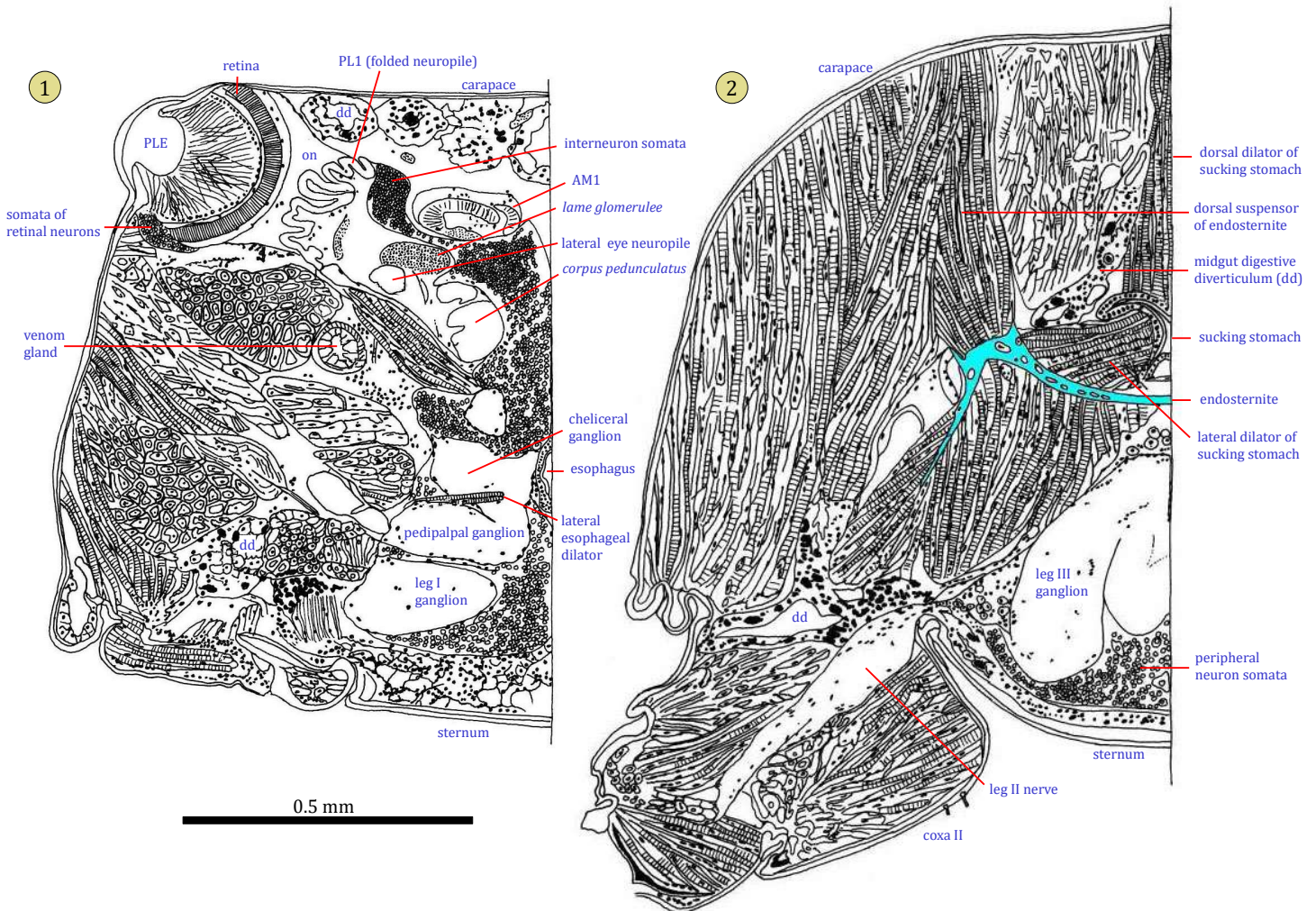


Figure 5. *Camera lucida* drawings of half transverse (frontal or cross) 10 μm sections of the prosoma of a fifth instar *Phidippus clarus* (1), and a sixth instar *P. johnsoni* Peckham & Peckham 1883 (2). In each drawing the midline is at the right. **1**, Section through the posterior lateral eye (PLE). The short optic nerve of each lateral eye (ALE and PLE) has its own folded first neuropile (PL1 for the PLE). interneurons associated with this neuropile are associated with tracts leading to both the glomerular synapses (or *glomeruli*) of the *corpora pedunculata*, and to a lateral eye neuropile. **2**, Section through the sucking stomach. The CNS is separated from the sucking stomach by the endosternite, an internal skeletal element comprised of a cartilage-like material. This view emphasizes the powerful musculature that fills much of the prosoma. Many of these striated muscles are attached to the endosternite. After Hill (1975, 2006).

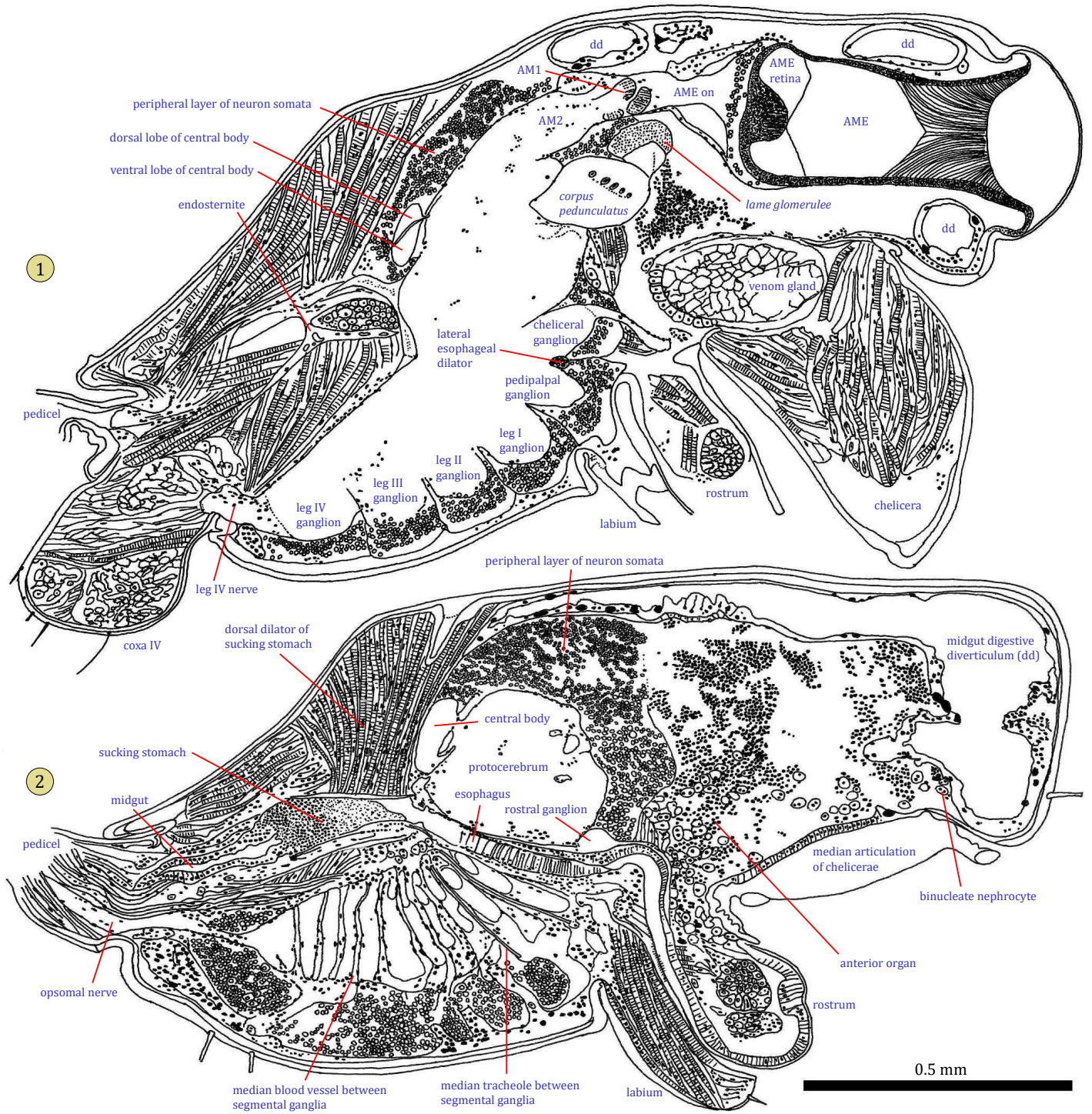


Figure 6. Camera lucida drawings of 10 μ m sections of the prosoma of a fifth instar *Phidippus clarus*. **1**, Parasagittal section. Visual centers of the ALE (AM1, AM2) lie at the top of the protocerebrum. Each *corpus pedunculatus* lies beneath the ALE neuropiles, and forms compact synapses (glomeruli of the *lame glomerulee*) with the ipsilateral lateral eyes (ALE and PLE). A lateral esophageal dilator separates the cheliceral and pedipalpal ganglia on each side. The dorsal and ventral lobes of the central body are situated at the rear of the protocerebrum. Densely packed neuronal cell bodies are peripheral to the mass of the CNS. In this vertical section, only the dorsal and ventral extensions of layers I and II of the retina of the ALE can be seen. **2**, Sagittal (midsagittal) section. The rostral ganglion, situated above the anterior esophagus, sends the recurrent nerve to the rear just above the esophagus, and the rostral nerve to the front. Commissures of the respective segmental ganglia are separated by blood vessels, associated with tracheoles that originate with the opisomal tracheal spiracle. These tracheoles pass between the sucking stomach and the mass of fused segmental ganglia, then turn ventrally to penetrate that mass at the midline. After Hill (1975, 2006).

Histology. The somata of the unipolar neurons forming the mass of the CNS are situated in a peripheral cortex, distinct from the central mass of fibers and synapses. These somata are found in greatest numbers at the bottom of the postoral ganglia, in front of the nervous mass, and above the preoral portion of the CNS. Neuroglia are associated with the neuron somata, but are generally lacking in the central mass of fibers. The inner fiber portion and outer cortex of the CNS are separated and collectively enclosed by a single layer of flattened epithelial cells comprising the *neurilemma*. This thin neurilemma is typical of araneomorphs (Saint Remy 1890; Legendre 1959), whereas a much thicker multilayered neurilemma capsule is found in mygalomorphs (Babu 1965; Legendre 1961). This neurilemma surrounds nerves leading from the CNS, and also forms the lining of a series of dorso-ventral blood vessels penetrating the postoral CNS in a sagittal plane. Tracheoles leading from the spiracle just anterior to the spinnerets at the rear of the opisoma also pass through the CNS in these blood vessels (Figure 6:2; Hill 2020). In front of the CNS is situated a curious group of loosely attached or clustered binucleate nephrocytes and small endocrine cells, collectively termed the anterior organ (Figure 6:2; Legendre 1959, 1971).

Unipolar neuron types (Table 3) are categorized according to nuclear size and nucleo-cytoplasmic ratio. This classification agrees with similar schemes proposed by Legendre (1959) and Babu (1965), although Babu described much larger neurons in the large theraphosid spider *Poecilotheria*. This classification serves to emphasize the great disparity in size of neurons associated with different structures in the CNS. According to Legendre (1959), the largest neurons are the last to be elaborated from neuroblasts. A cluster of relatively large neuron somata from a second instar *Phidippus clarus* are shown in Figure 4:1. It has been suggested that some of the largest of these neurons in spiders are neurosecretory (Gabe 1954; Kuhne 1959; Legendre 1959, 1971), but their specific functions are not known and it is also possible that they are motor neurons (Meier 1967). I have not found any related studies of these cells in the Salticidae.

Table 3. Unipolar neuron types observed in the CNS cortex of an adult female *Phidippus clarus* (after Hill 1975, 2006).

size of cell body	location in CNS	nuclear diameter	nucleo-cytoplasmic ratio
small	interneurons originating with first lateral eye neuropile	4-5 μm	much greater than 1
small	interneurons (<i>globuli cells</i>) originating in glomeruli of <i>corpora pedunculata</i>	4-5 μm	much greater than 1
small	massed under central body	5-6 μm	greater than 1
medium	at periphery of protocerebrum	7-8 μm	near 1
medium	under leg ganglia	7-8 μm	near 1
large	under leg ganglia	~10 μm	less than 1
giant	in groups under leg ganglia	~15 μm	much less than 1

Post-embryonic growth of the CNS. The migration of opisomal ganglia into the prosoma, characteristic of araneids, is completed in the late embryo, by the end of inversion (Rempel 1957; Legendre 1959). When a young salticid and its siblings molt and emerge from the brood sac as second instars, they already have a complete nervous system, but a very compact one (Figures 4,7; Goté et al. 2019). According to Legendre (1959), there is no further elaboration of neurons from neuroblasts after this stage. During the life of the salticid, the CNS will only double in length, while the length of the prosoma increases by a factor of about 4 to 10. Similar changes are seen in the development of other Araneae (Eberhard & Wcislo 2011; Quesada et al. 2011). Peters (1969) demonstrated that the coordinated ability to produce webs in *Zygiella x-notata* (Cl.) develops during the brooding of second instars. Similarly in *Phidippus* the second instars may remain in the brood sac for several weeks, retaining the gregarious behavior characteristic of the first instars. When they finally emerge, the second instar jumping spiders are fully capable of spinning shelters and capturing prey, just as orb weavers of this age produce miniature webs of perfect construction.

With age, salticids acquire an increasing number of setae. This must correspond to continued development of associated sensory neurites. Proportions of many structures, including the eyes, continue to change as a salticid grows (Hill 1975, 2006; Goté et al. 2019). As can be seen in a comparison of the parasagittal sections shown in Figure 7, both the length of the AME tubes and the shape of the corneal lens of these eyes changes considerably. Optic nerves of the AME also elongate considerably, and individual sensory neurites within these nerves double their diameter (from 0.8 to 1.5 μm) between the fifth instar and the adult stage of *P. clarus*. The glomerular synapses at the anterior end of the *corpora pedunculata* (glomeruli of the *lame glomerulee*), a secondary neuropile of the lateral eyes, are only about 3 μm in diameter in the second instar, growing in diameter to about 4 μm in by the fifth instar, and about 5 μm in the adult *P. clarus*. Quesada et al. (2011) document many other changes in the size of CNS structures associated with the growth of other Araneae.

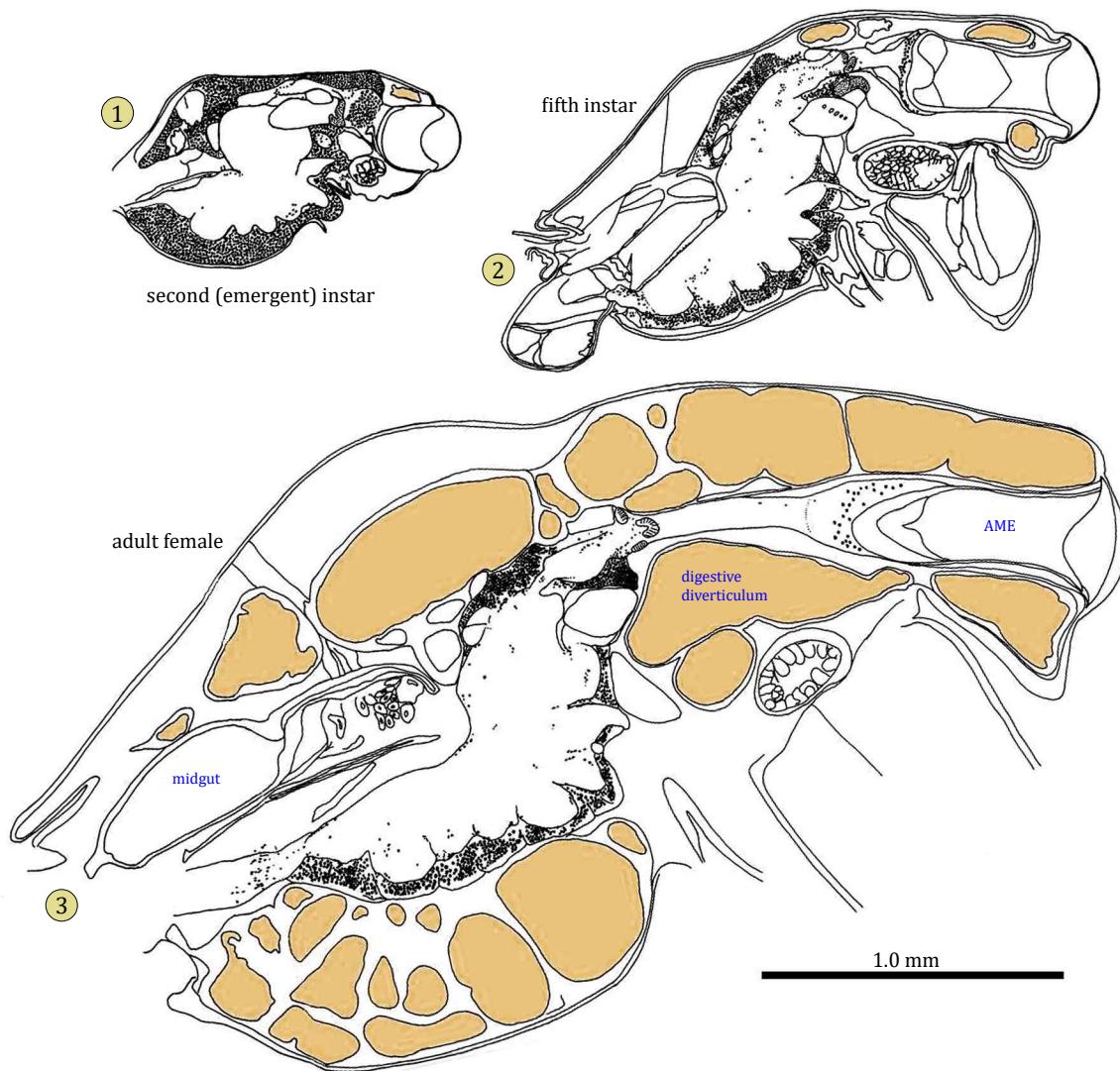


Figure 7. Camera lucida drawings of parasagittal sections through the prosoma of *Phidippus clarus* at three different stages of development. Relative to body size, the CNS of the adult is relatively small. The prosoma of the adult is packed with midgut digestive diverticulae (highlighted in orange) above, below, and in front of the CNS. In the adult female, these supplement the diverticulae of the opisoma, as developing ova occupy an increasing portion of the opisomal volume. Recent studies have shown that adult and juvenile salticids have similar numbers of visual receptor cells, more tightly packed in the latter (Goté et al. 2019). After Hill (1975, 2006).

abbreviations	
ALE, AL1	anterior lateral eye, ALE neuropile 1
AME, AM1, AM2	anterior medial eye, AME neuropiles 1,2
ao	anterior organ
bn	binucleate nephrocytes
br	bridge between <i>corpora pendunculata</i>
bv	vertical blood vessel through median CNS
cb	central body (or arcuate body)
CE	<i>cauda equina</i> , or fused opisomal ganglia
CHc	commisure between cheliceral ganglia
CHn	primary nerve of cheliceral ganglion
cl	corneal lens of respective eye
cp	<i>corpus pendunculatus</i>
e	esophagus, a rigid tube
es, esd	endosternite, dorsal suspensor of endosternite
I-IV, In-IVn	leg I-IV ganglion, primary nerve of leg I-IV
lenp	lateral eye neuropile
lg	<i>lame glomerulee</i> (glomerular synapses)
lnp	lateral neuropile of protocerebrum
m	mouth
on	optic nerve connecting retina to neuropile 1
OPn	opisomal nerve
P, Pn	pedipalp ganglion, primary nerve of pedipalp
pat	paturon, basal segment of chelicera
pc	protocerebrum
pd	pharyngeal dilator
pe	pedicel
PLE, PL1	posterior lateral eye, PLE neuropile 1
PME, PM on, PM1	posterior medial eye, PME optic nerve, PME neuropile 1
r, rt	retina of respective eye, tiered retina of AME
rz	ramification zone for neuropile I to II interneurons
ss, ssd, ssl	sucking stomach, ss dorsal and ss lateral dilators
vd, vg	venom duct, venom gland

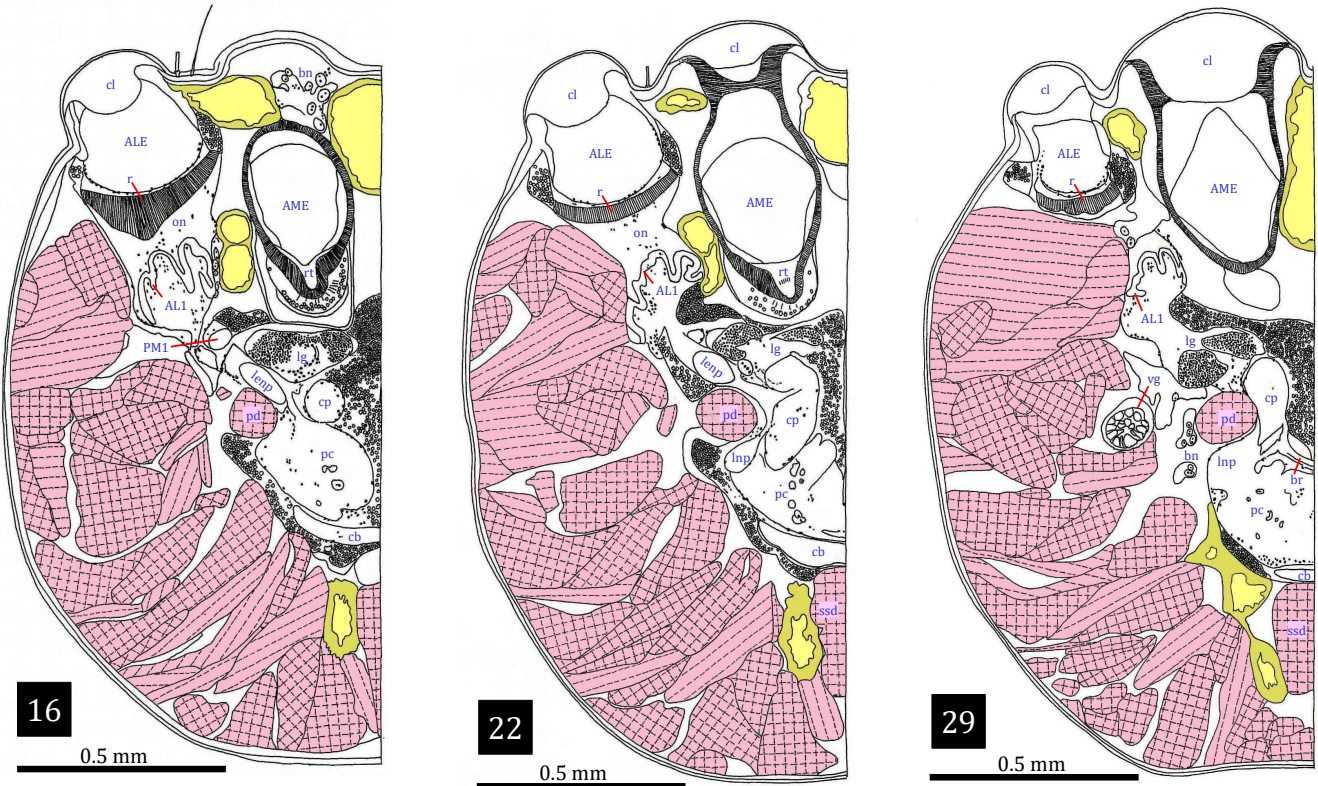
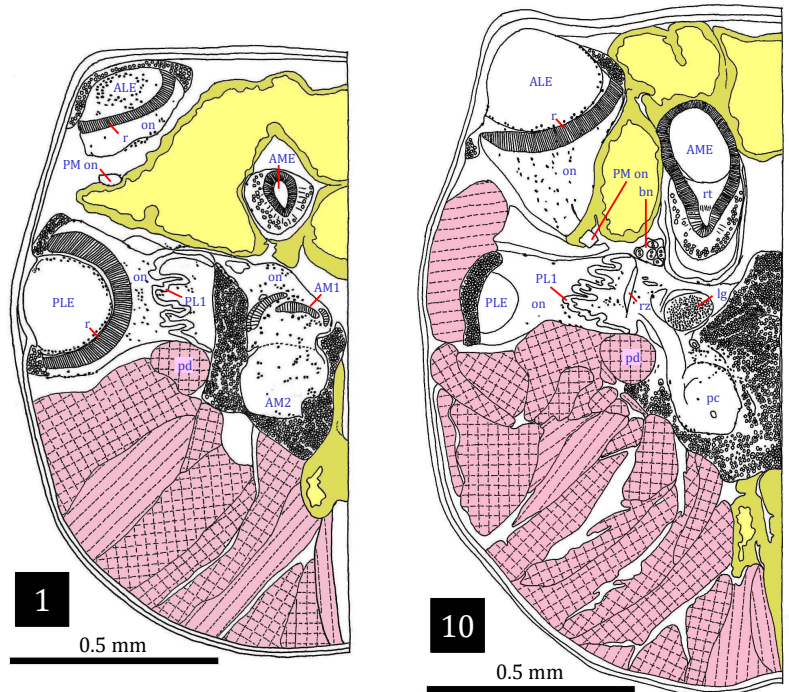


Figure 8 (continued on next page). Semi-schematic *camera lucida* drawings of a series of 10 μ m half-horizontal sections through the prosoma of a fifth instar *Phidippus johnsoni*. In each drawing the midline or sagittal plane is shown at right. Numbers in rectangles (1-102) indicate the relative vertical position of each section in the series. These drawings illustrates the relative position of the CNS at various levels. Musculature in the plane of each section is shown in red, digestive diverticulae of the midgut in yellow. Nuclei of the unipolar neurons that surround the otherwise fibrous nerve masses are shown as small circles.

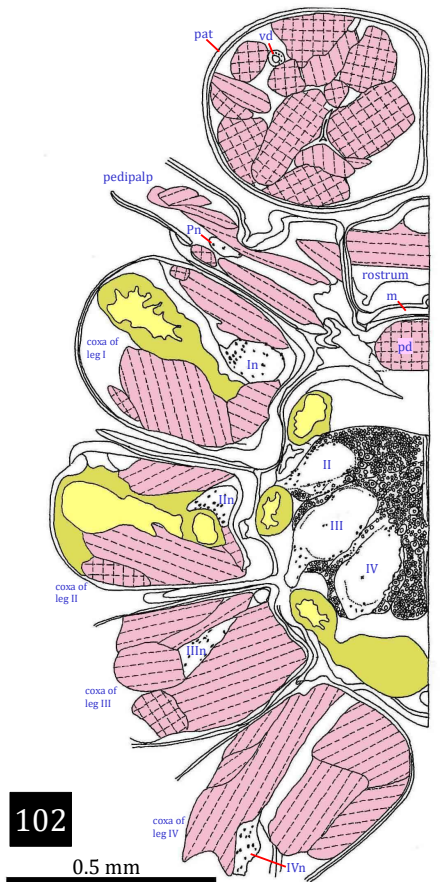
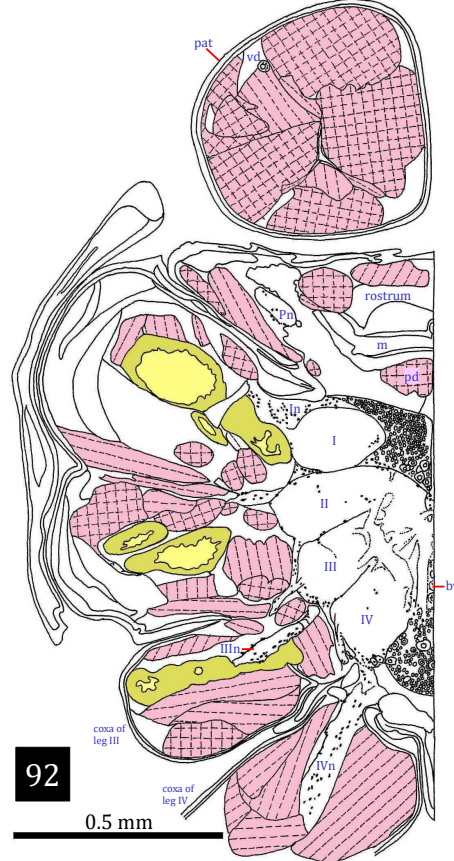
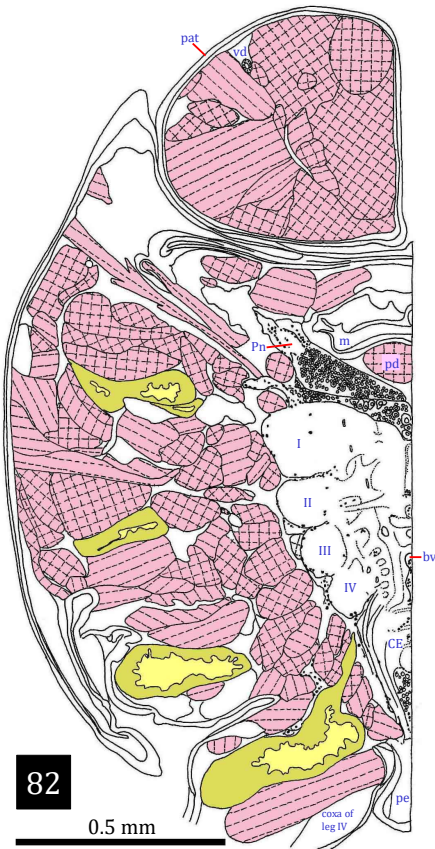
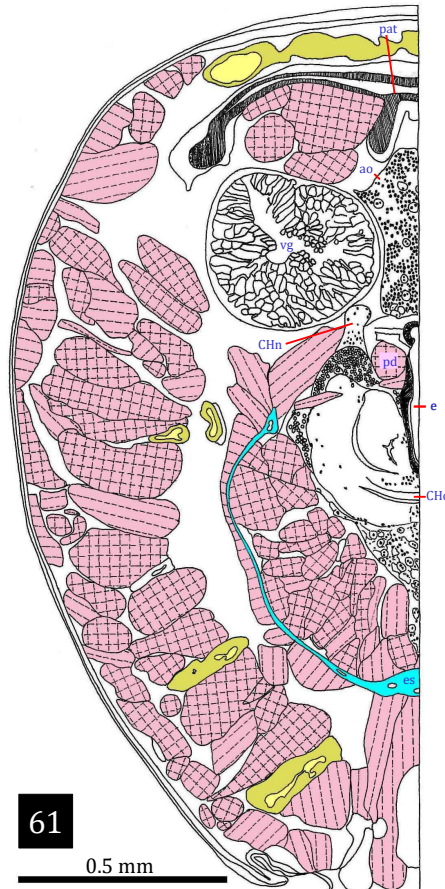
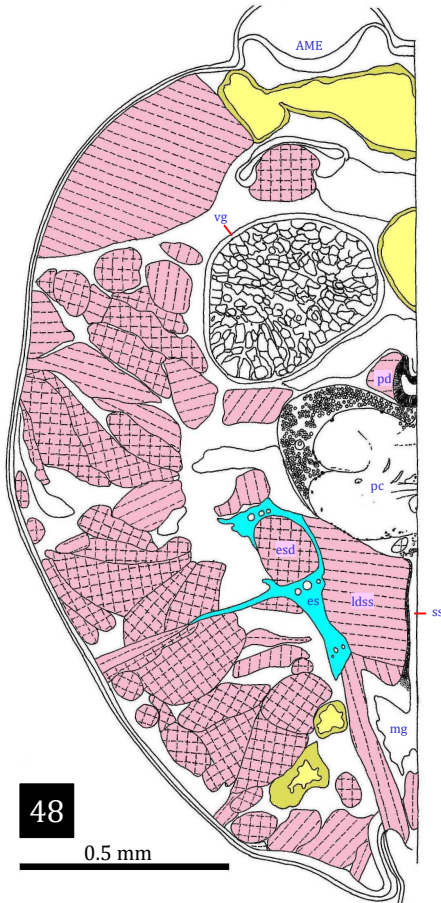


Figure 8 (continued from previous page).

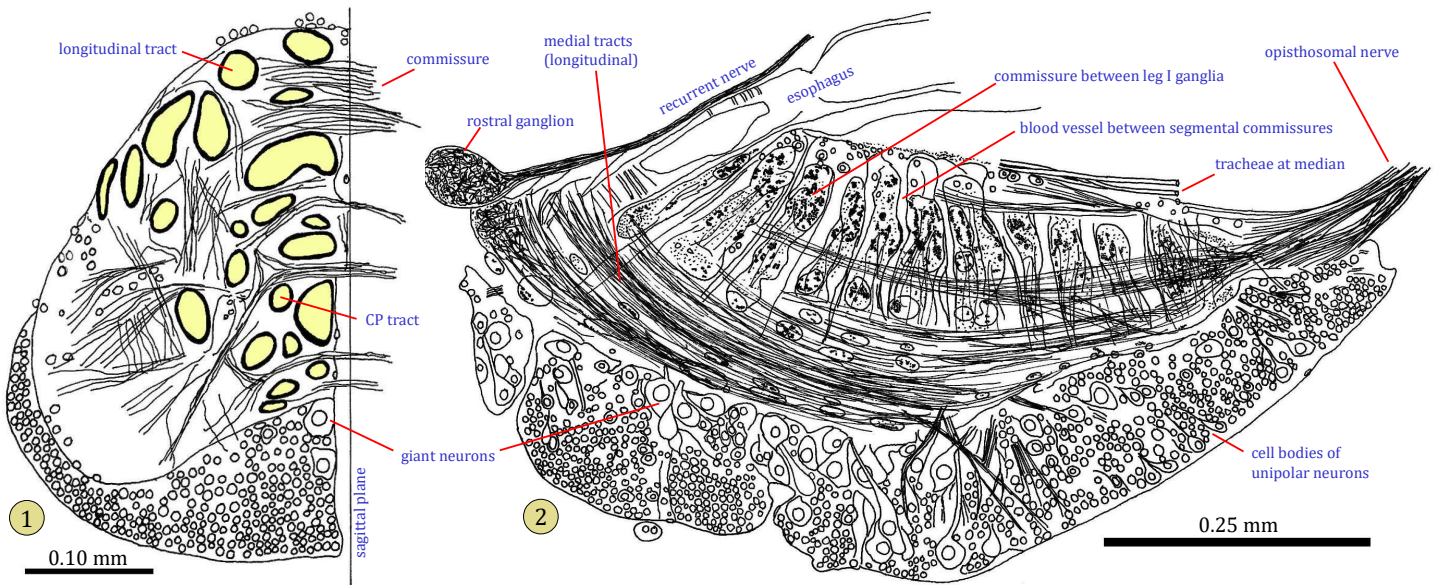


Figure 9. Sections through the CNS, stained with reduced silver impregnation to highlight nerve fibers. **1**, Half transverse section between the first and second legs of a sixth instar *Phidippus johnsoni*. Longitudinal tracts (in a plane perpendicular to the page) are highlighted in yellow. At multiple levels *commissures*, or transverse tracts cross the midline, connecting the right and left ganglia of each segment. The *CP tract* originates with the posterior end of a *corpus pendunculatus* and the ipsilateral lateral neuropile of the protocerebrum. **2**, Sagittal section through the fused subesophageal ganglia of a fifth instar *P. clarus*, showing medial longitudinal nerve tracts and segmental commissures separated by blood vessels. A recurrent nerve runs along the top of the esophagus, just behind the preoral rostral ganglion.

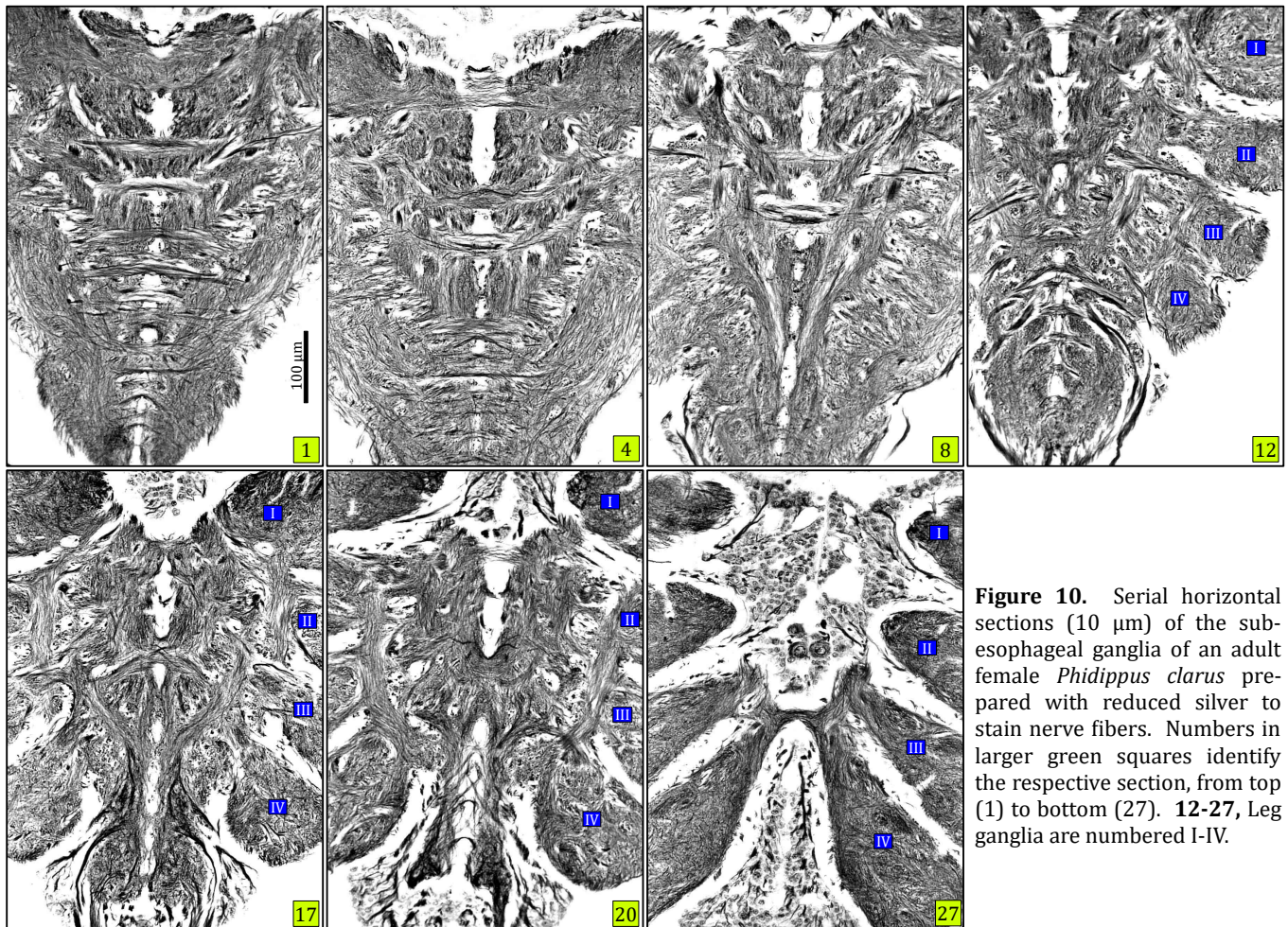


Figure 10. Serial horizontal sections (10 μm) of the subesophageal ganglia of an adult female *Phidippus clarus* prepared with reduced silver to stain nerve fibers. Numbers in larger green squares identify the respective section, from top (1) to bottom (27). **12-27**, Leg ganglia are numbered I-IV.

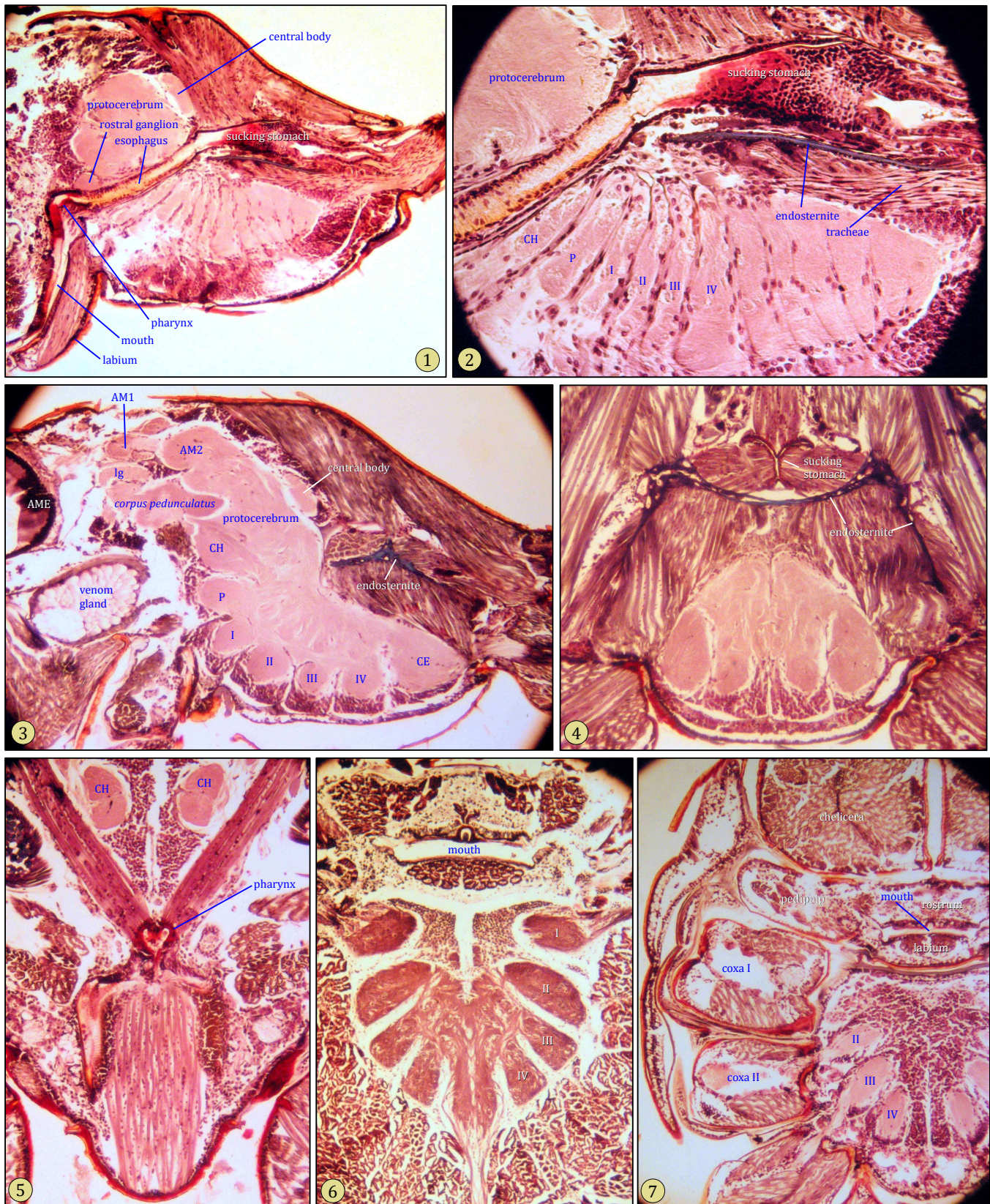


Figure 11. Stained 10 μm sections through the prosoma of *Phidippus* jumping spiders. **1-3**, Sagittal (1-2) and parasagittal sections of fifth instar *Phidippus clarus*. **4-5**, Transverse sections of fifth instar *P. johnsoni*. **6-7**, Horizontal sections of fifth instar *P. johnsoni* (6) and fifth instar *P. clarus* (7). Abbreviations: AME, AM1, AM2, anterior median eye and first, second neuropiles of that eye; CH, P, I, II, III, IV, ganglia of chelicera, pedipalp, and legs I-IV; coxa I, coxa II, coxa of respective leg segment; lg, *lame glomerulee*, or layer of glomerular synapses at the anterior end of each *corpus pedunculatus*.

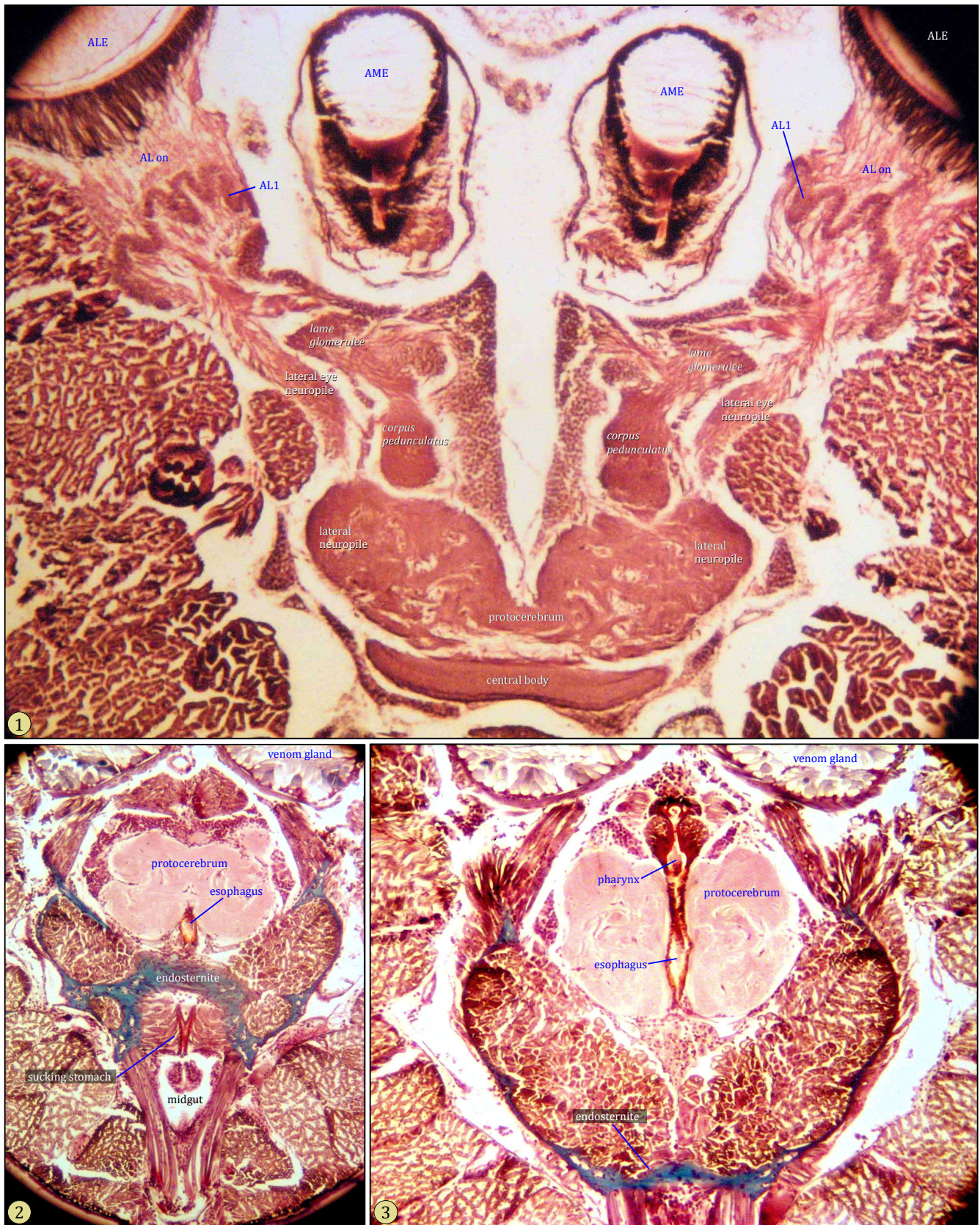


Figure 12. Stained 10 µm horizontal sections through the prosoma of sixth instar *Phidippus johnsoni*. **1**, Section at the level of the anterior lateral eyes and the central body. Sensory fibers of the anterior lateral eyes (optic nerve, AL on) synapse in a convoluted neuropile (AL1), connected to synapses of the *lame glomerulee* and the lateral eye neuropile by interneurons. **2-3**, Successively lower sections show how the neck of the CNS, surrounding the esophagus, is cradled by the endosternite (cartilage, stained blue), connected to powerful muscles.

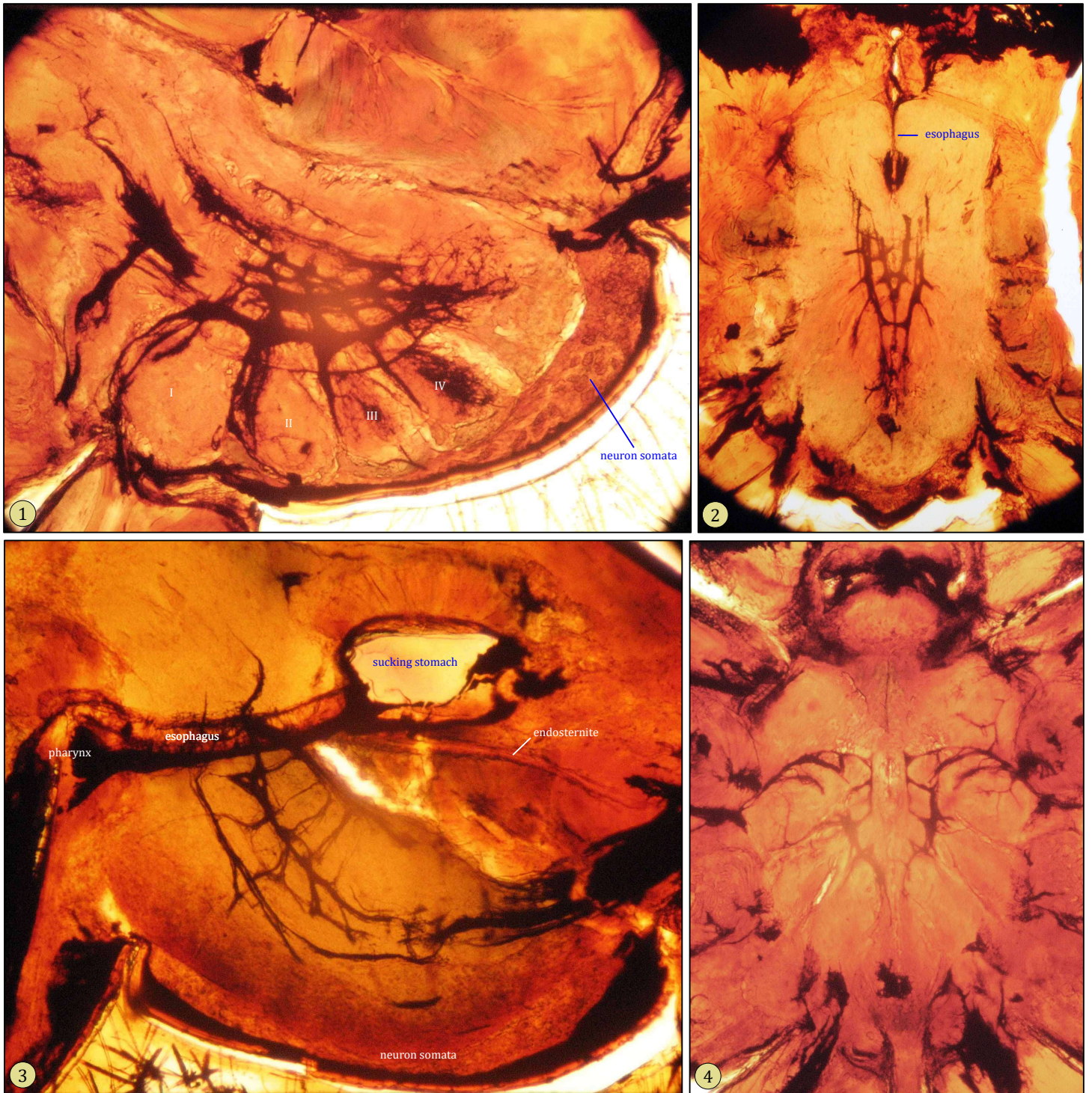


Figure 13. Thick (80 μm) sections of Golgi-Kopsch preparations of the prosoma of sixth instar *Phidippus johnsoni*. **1**, Parasagittal section. **2,4**, Horizontal sections. **3**, Sagittal (midline) section. Golgi-Kopsch preparations can selectively stain nerve fibers, but it is not possible to determine just what fibers will be stained, and the results can be misleading. Here some of the major fiber tracts in the subesophageal part of the CNS have been stained.

The eyes and visual centers

A current hypothesis of the connectivity of salticid eyes with discrete neuropiles of the protocerebrum (supraesophageal part of the CNS) is shown in Figures 14-15, based on studies of *Evarcha arcuata* (Clerck 1757), *Hasarius adansoni* (Audouin 1826), *Marpissa muscosa* (Clerck 1757), *Naphrys pulex* (Hentz 1846), *Salticus scenicus* (Clerck 1757), *Servaea vestita* (L. Koch 1879) and *Phidippus* spp.

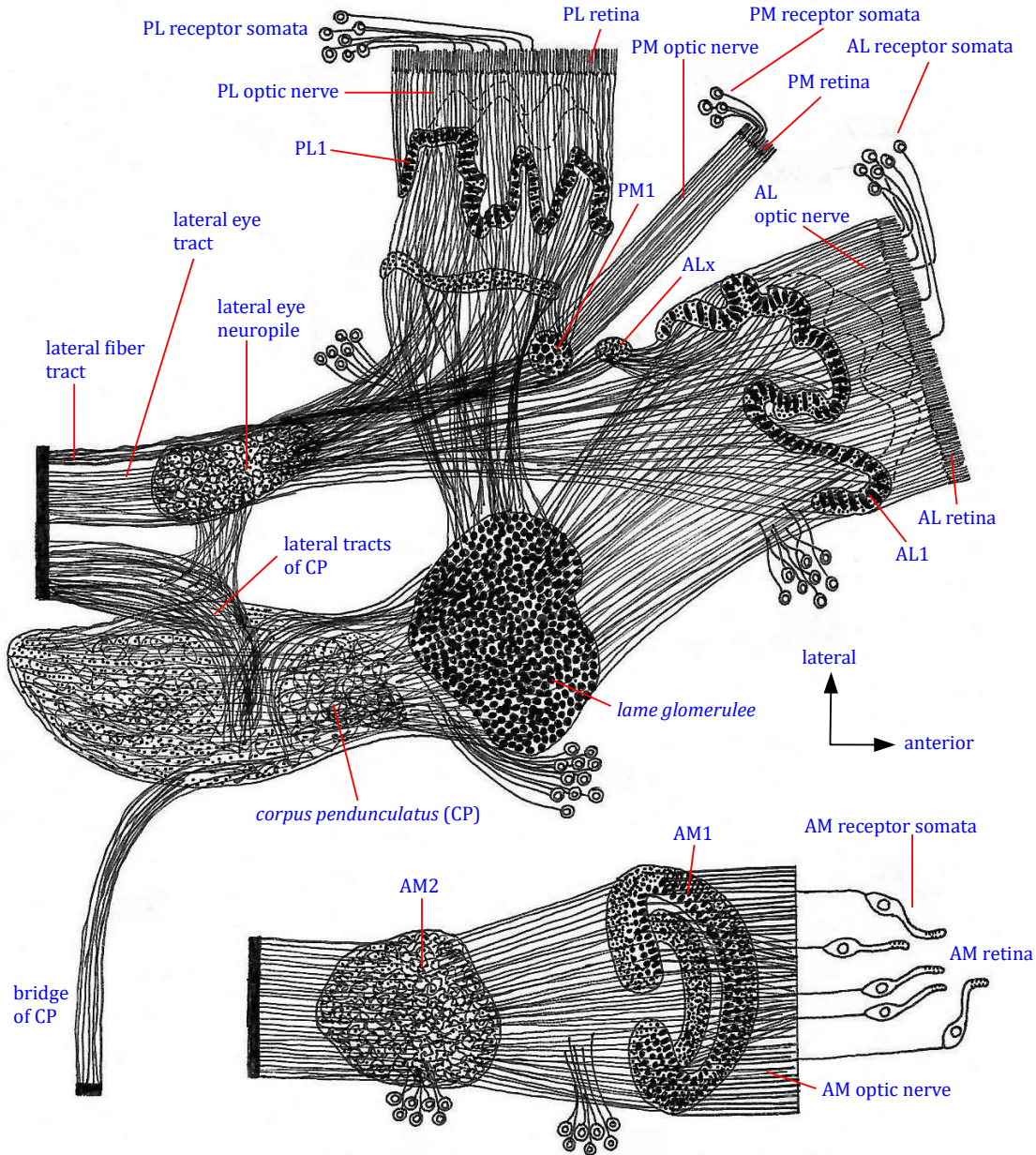


Figure 14. Semi-schematic diagram of primary visual centers in the CNS of *Phidippus* (after Hill 1975, 2006). Dorsal view of the left side, based on examination of serial silver and Masson Trichrome sections. The first link between information received by the lateral eyes and the anterior medial eyes is in the protocerebrum. The solid black bars indicate groups of fibers entering the protocerebrum. Fibers leading from the primary neuropiles of the lateral eyes (AL1 and PL1) lead to either the synaptic layer (*lame glomerulee*) of the *corpus pedunculatus* (pedunculate body), or to the *lateral eye neuropile* and *lateral eye tract*. Large, distinctive fibers of the primary neuropile of the posterior medial eyes (PM1) join similar fibers originating with a small neuropile (ALx) associated with the primary neuropile of the anterior lateral eye (AL1). These large fibers enter the protocerebrum as a distinctive tract (lft). Several important groups of neuron somata are shown. A *bridge* (fiber tract) connects the left and right corpora pedunculata. See Figure 15 for a more current view.

Anterior medial or primary eyes (AME). There are easily more published studies of the AME visual systems than exist for all other neurosensory capabilities of salticids, combined. This is for good reason. Although other spiders have scanning AME equipped with retinæ that can be moved behind the fixed corneal lens, and some even have layered receptors in these eyes (e.g. Thomisidae; Insausti et al. 2012), the large size and high resolution of these eyes in salticids is unique.

General features of the AME and associated visual centers are shown in Figures 16-22. Light must pass through the cuticular cornea, the corneal lens, the columnar matrix of the eye tube, the clear matrix of the eye tube, and the foveal matrix, before it can enter the distal receptor processes of the bipolar receptors at each layer of the fovea. The fovea of the AME contains all receptor layers. Layers I and II are boomerang-shaped, with more granular packing of receptors into dorsal and ventral arms. Proximally, each bipolar receptor sends a neurite (axon) to the first AME neuropile (AM1), where it synapses with neurites that also synapse in a relatively unstructured second AME neuropile (AM2). The first AME neuropile is highly structured, with two (outer and inner) lobes.

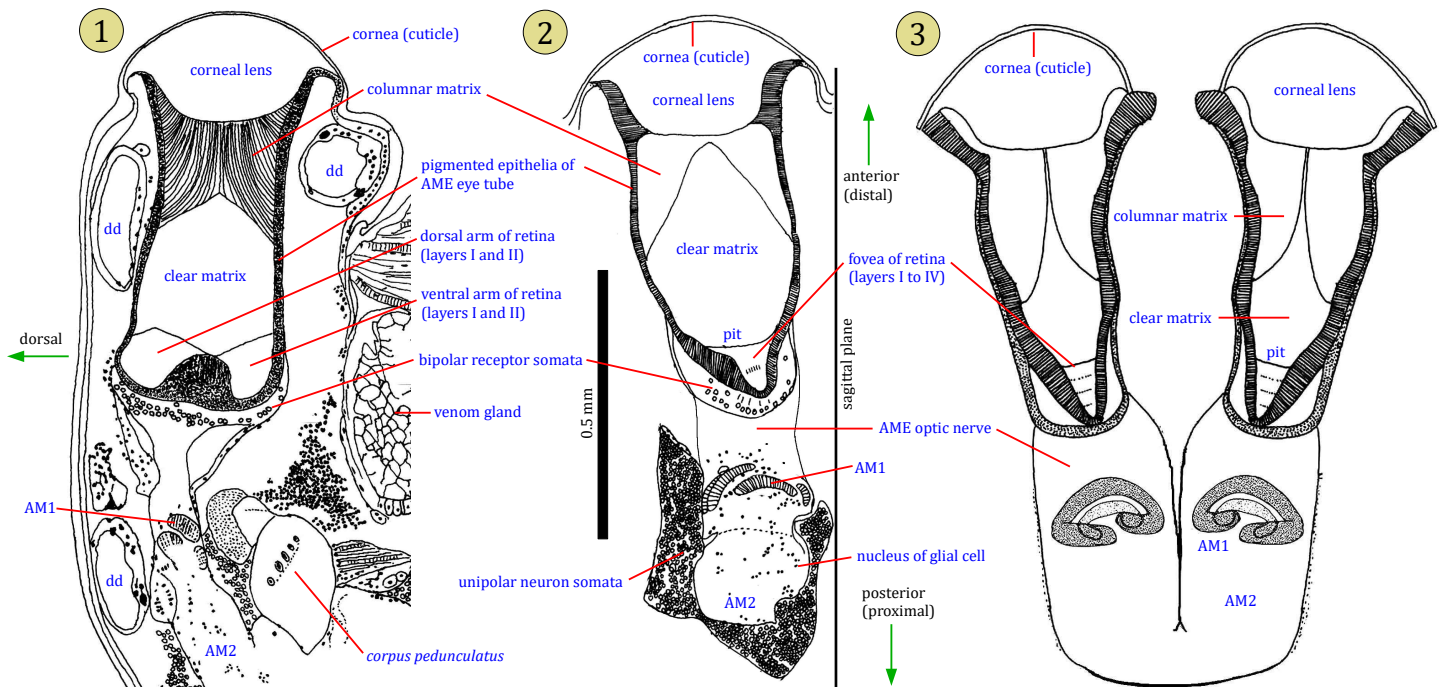


Figure 16. General structure of the AME and related visual centers. **1**, Camera lucida drawing of a parasagittal section of the anterior prosoma of a fifth instar *Phidippus clarus*. Since retinal layers I and II are dorso-ventrally elongated and boomerang-shaped, only the dorsal and ventral arms of these layers can be seen in this view. The *columnar matrix* that is shown here is quite visible in stained sections, but has not been mentioned in other studies. In older spiders, the midgut digestive diverticulae (dd) are much larger than this. **2**, Camera lucida drawing composited from several horizontal sections of the prosoma of a sixth instar *P. johnsoni*. In this view only the central, foveal part of the retina can be seen. Sections of the outer and inner lobes of the first AME neuropile (AME I) can be seen. **3**, Semi-schematic dorsal view with the AME of a fifth instar *P. clarus* presented in horizontal section, showing the relationship of the eyes to the reconstructed lobes of the AME I neuropile. As a convention with the AME and the other eyes, *distal* refers to a direction along the optical axis toward the cornea, and *proximal* is a direction away from the cornea, toward the retina and optic nerve. As noted by Land (1969a), each AME optic nerve rotates by $\sim 90^\circ$ between the eye and AME1, although the degree of this rotation varies when the eye-tube is rotated. Note that some shrinkage and distortion did occur as part of the preparation of these sections, which were stained with Masson Trichrome. After Hill (1975, 2006).

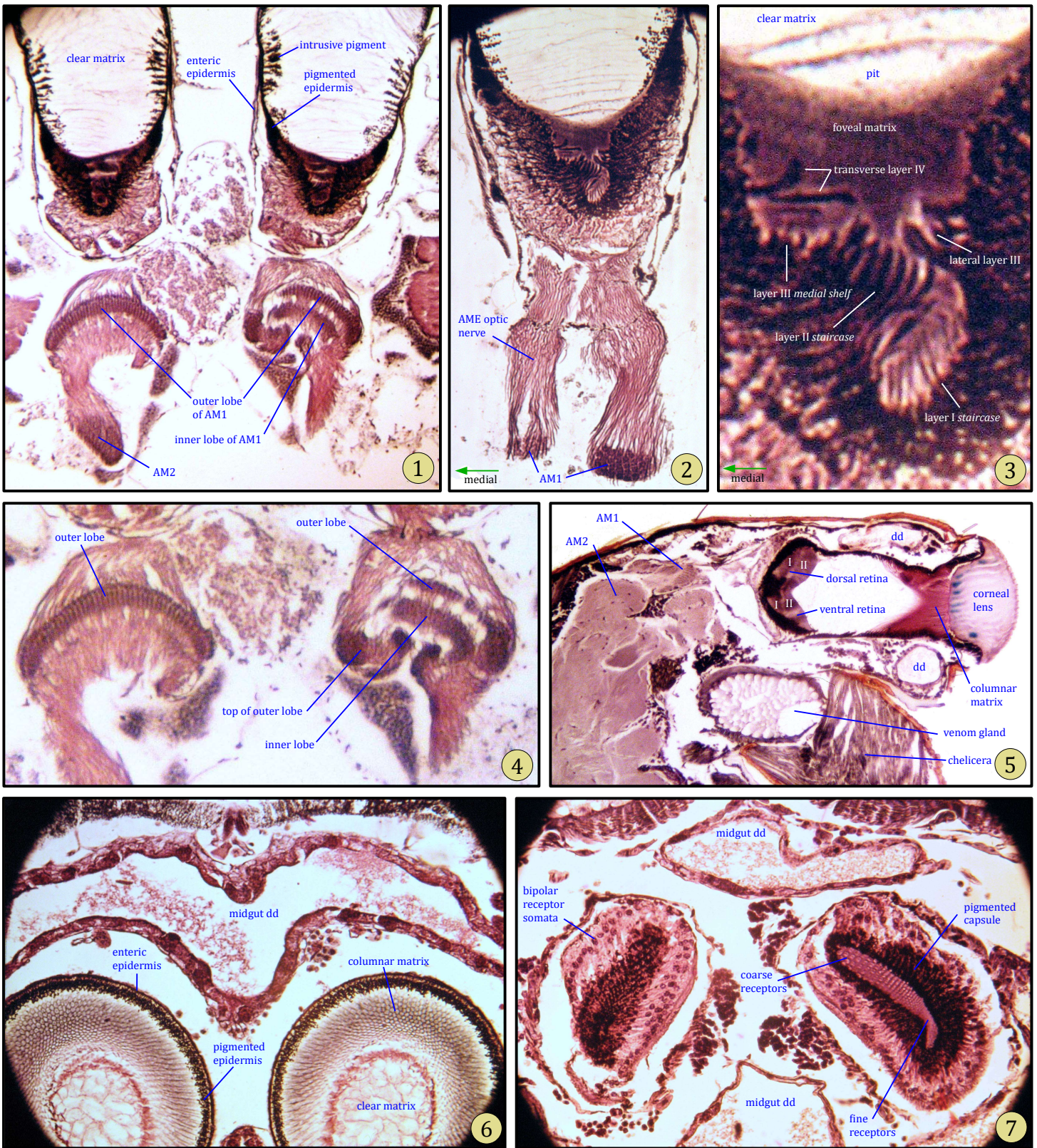


Figure 17. Stained sections through the AME and associated visual centers of *Phidippus*. **1**, Horizontal section through prosoma of an adult female *P. clarus*. **2**, Another horizontal section of the right AME and AME optic nerve of an adult female *P. clarus*. **3**, Detail from (2), showing receptor tiers in the fovea. **4**, Detail of AM1 in horizontal section, close to (1). **5**, Parasagittal section of prosoma of fifth instar male *P. clarus*, showing dorsal and ventral lobes of the AME retina. **6**, Transverse (frontal) section through prosoma of sixth instar *P. johnsoni*. **7**, Transverse section through prosoma of a sixth instar *P. johnsoni*, through the boomerang-shaped retinae of the AME.

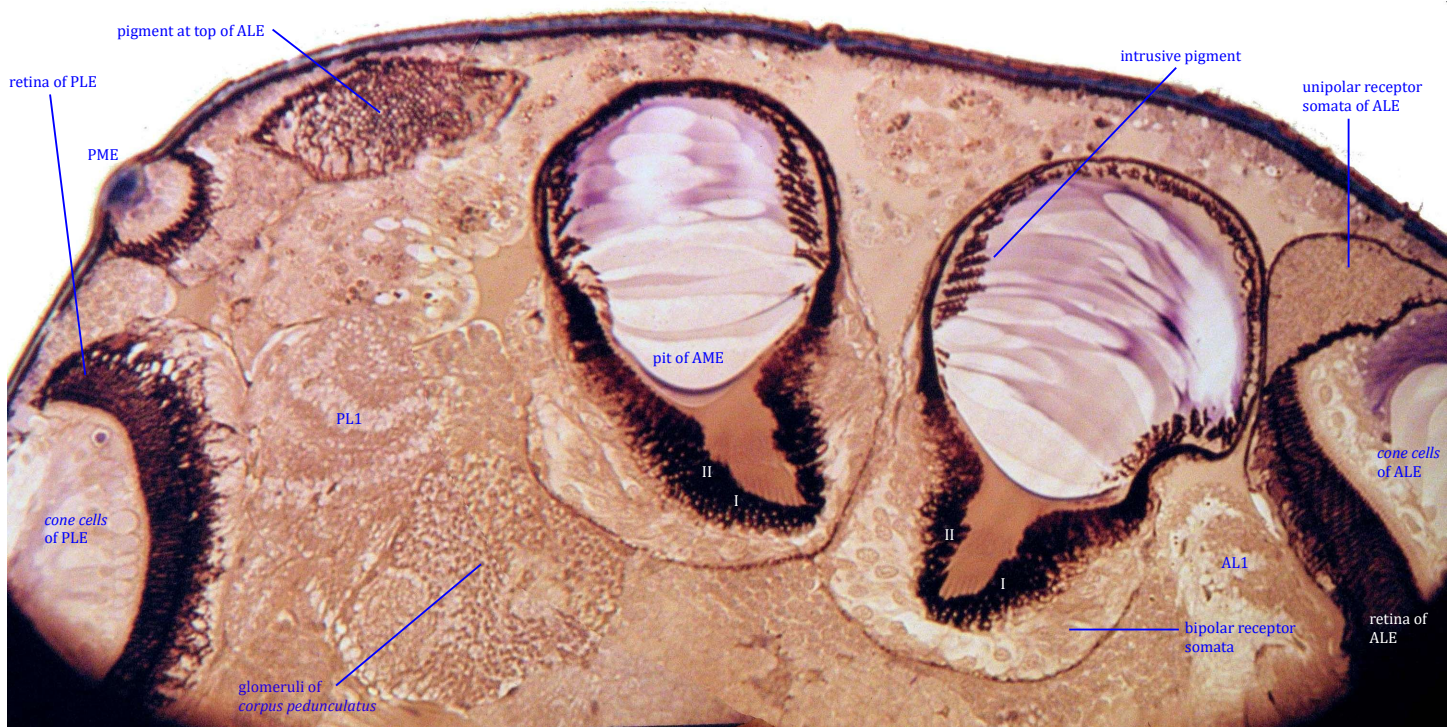


Figure 18. Oblique horizontal section through the anterior prosoma of a second instar *Phidippus johnsoni*. This was a 5 μ m Epon section stained with Toluidine Blue, and thus very little shrinkage of structures occurred. Note the smooth pit and *staircased* (placed in multiple focal planes) receptors of layers I and II in the foveae of the AME, at center. The *intrusive pigment* at the margins of each AME eye tube is aligned with thin, membraneous structures within the clear matrix. Receptor layer I is most distinct, and nothing can be seen of receptor layers III and IV in this view.

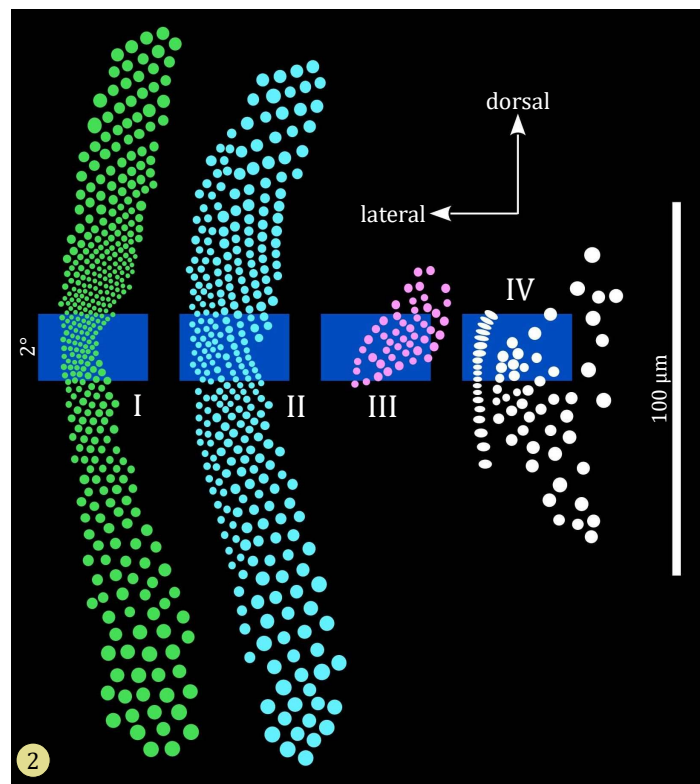
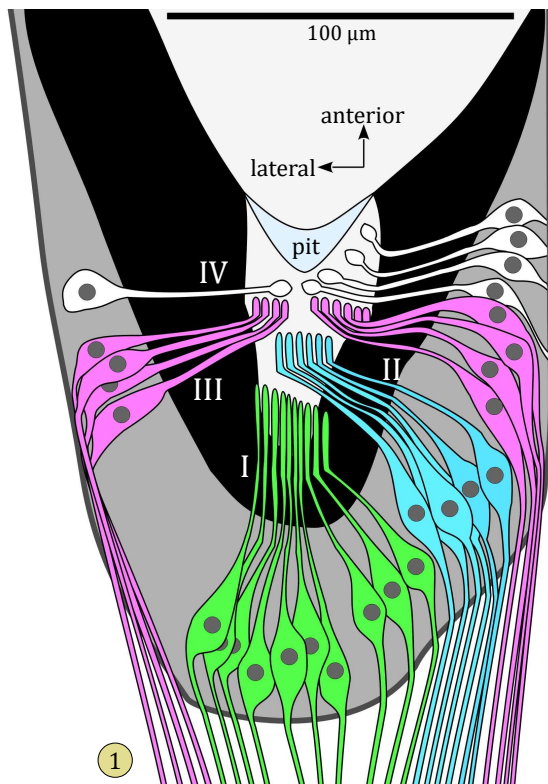


Figure 19. Arrangement of bipolar receptor neurons in the AME of *Pelegrina aeneola* (Curtis 1892), after Land 1969a, 1985b. **1**, Semi-schematic drawing of horizontal section through the proximal end of the AME. **2**, Plotted position of receptors for each layer (I-IV) of the retina (anterior projection). Blue rectangles occupy the same position in a parasagittal (axial) projection.

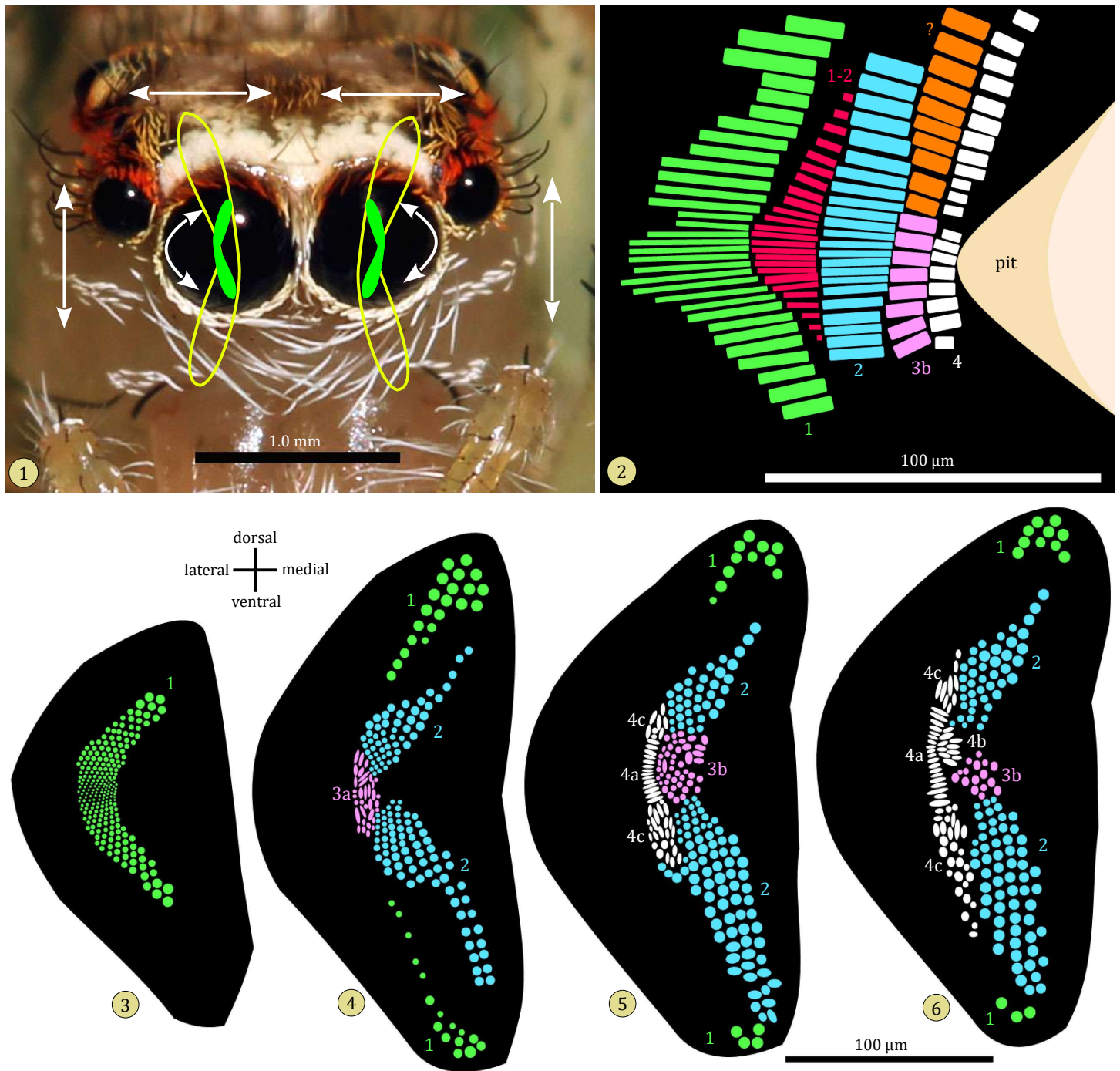


Figure 20. Arrangement of receptors in the tiered retina of the AME. **1**, Anterior view of an adult female *Colonus sylvanus* (Hentz 1846), depicting the boomerang shape of the AME retinae (in green), and the alignment of respective fields of vision (outlined in yellow). White arrows depict the six directions in which each AME can be moved, to include left-right, up-down, and clockwise-counterclockwise rotation. Each of these directions corresponds to the contraction of a set of oculomotor muscles that position the long AME eye tube within the prosoma. After Hill 2018a. **2**, Parasagittal diagram of the respective alignment of receptors in the four layers of the AME of *Servaea vestita*, near the center of the retina. The identity of the receptors shown in orange was not known. Red rectangles show the position of columns connecting layers I and 2. After Blest et al. 1981. **3-6**, Diagrams of serial (proximal to distal) transverse sections through the retina of *S. vestita*, showing a cross section of individual receptors by layer (after Blest et al. 1981; Blest 1988). Lateral receptors of layers III-IV include groups 3a, 4a and 4c. Medial receptors of these layers include group 3b and 4b. Based on the findings of Nagata, Arikawa & Kinoshita (2019; see Figure 22:5), the separation of layer III and IV receptors into these lateral and medial groups may have more anatomic or functional significance than their relative position (or layer) along the axis of the eye.

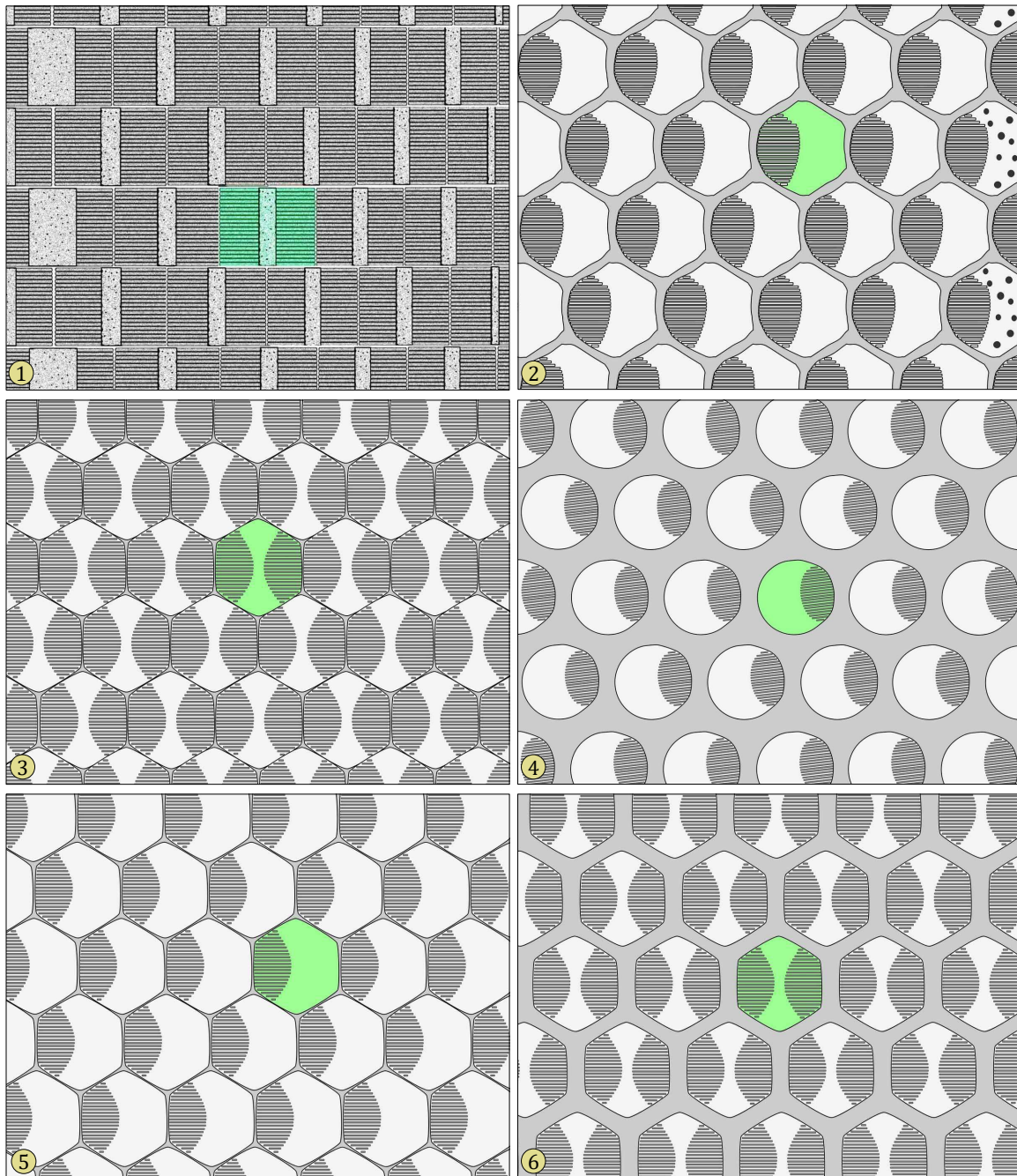


Figure 21. Schematic cross sections of the AME retina (layer I). All are packed in a space-filling hexagonal array, although the paired rhabdoms of *Goleba puella* (Simon 1885) are rectangular (1). One receptor cell is highlighted in green in each image. The diameter of each receptor varies, with the smallest receptors, more closely packed, near the center of the retina. Each receptor is surrounded by the projections of unpigmented glial cells. **1**, *Goleba puella*, after Blest, O'Carroll & Carter 1990. **2**, *Portia fimbriata* (Doleschall 1859), *Spartaeus spinimanus* (Thorell 1878), or immature *Servaea vestita*, after Blest & Price 1984; Blest & Sigmund 1984; Blest 1985b; Blest & Carter 1987, 1988. **3**, *Lyssomanes viridis* (Walckenaer 1837), *Cyrba algerina* (Lucas 1846), *Spartaeus spinimanus*, or *Yaginumanis sexdentatus* (Yaginuma 1967) after Blest & Sigmund 1984, 1985; Blest, O'Carroll & Carter 1990. **4**, *Colonus sylvanus* or immature *Servaea vestita*, after Blest & Carter 1987, 1988; Blest, O'Carroll & Carter 1990. **5**, *Phidippus*, *Cyrba algerina*, *?Jacksonoides kochi* (Simon 1900) or *Lyssomanes dissimilis* Banks 1929, after Eakin & Brandenburger 1971; Blest & Price 1984; Blest & Sigmund 1984; Blest, McIntyre & Carter 1988; Blest, O'Carroll & Carter 1990. **6**, *Phidippus johnsoni*, lateral, after Eakin & Brandenburger 1971. Note reduced packing and paired rhabdoms of these larger, lateral receptors. In some species the presence of one or two rhabdom groups in each cell depends on the plane of section.

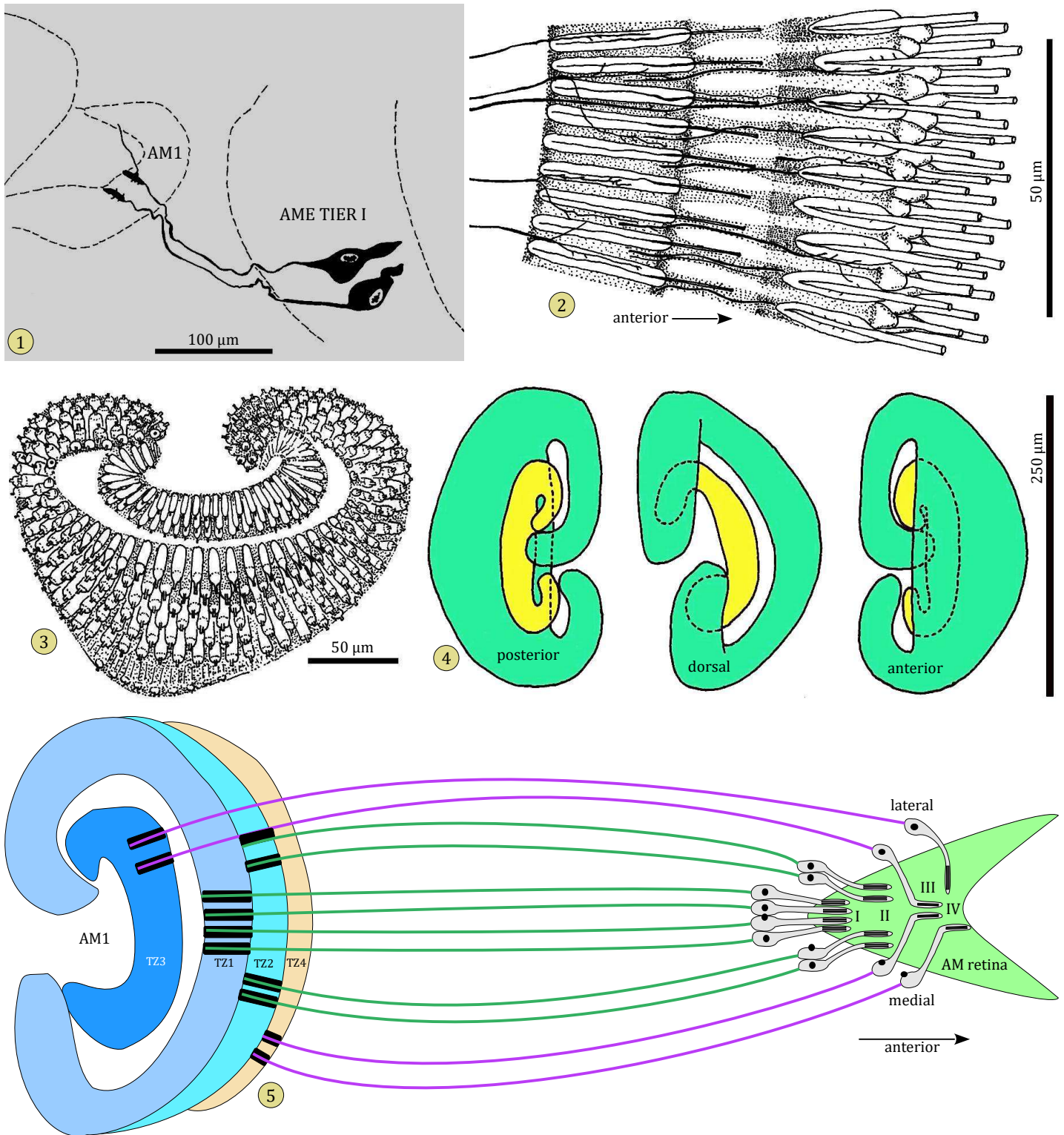


Figure 22. Relationship of tiered AME receptors to the first AME neuropile (AM1). **1**, Camera lucida drawing of a Golgi-Kopsch impregnation of two neurons of the left AME (sixth instar *Phidippus johnsoni*), suggesting that the relative position of receptors in the retina corresponds to the relative (retinotopic) position of corresponding, columnar terminals in the cortex of AM1. **2**, Semi-diagrammatic drawing of a section through the inner (at left) and outer (at right) lobes of a *Phidippus* AM2, showing a 1:1 correspondence between columnar terminals of the two layers (after Hill 1975, 2006; Oberdorfer 1977). **3**, Diagrammatic antero-dorsal view of the left AM1 of *Phidippus*. Fibers and terminals of the upper outer lobe are larger than those of the inner lobe and the lower part of the outer lobe. **4**, Three views of the inner (yellow) and outer (green) lobes of the AM1. **5**, Mapping of tiered AME receptors (I-IV) to respective terminal zones (TZ1-TZ4) of the AM1 of *Hasarius adansoni* (after Nagata, Arikawa & Kinoshita 2019). 1-4, after Hill (1975, 2006).

Muscles associated with movement of the AME. Although each cuticular cornea and corneal lens is fixed in position with the carapace of the salticid, these spiders can use six different non-striated muscles to move or to alter the shape of each eye (Figures 23-25, Tables 4-5; Scheuring 1914; Homann 1928; Kästner 1950; Land 1969b; Foelix 2011). Land (1969b) traced the separate innervation of each muscle by a single axon, with 6 axons comprising an oculomotor nerve associated with each eye, running under the respective first AME neuropile (AM1) into the protocerebrum, above the esophagus.

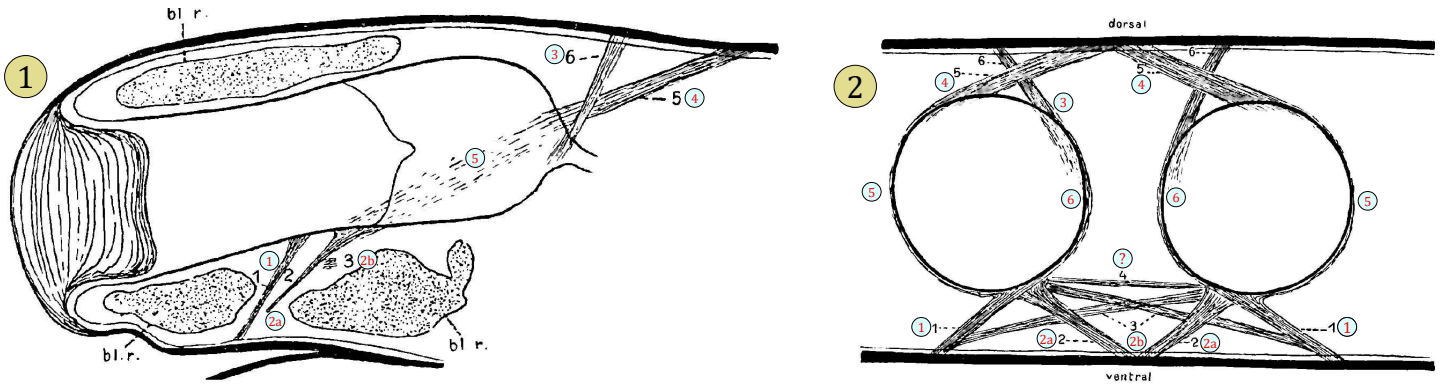


Figure 23. Scheuring's (1914) drawings of the extraocular muscles of *Salticus scenicus*. Corresponding muscle numbers assigned by Land (1969b) are shown in circles. **1,** Parasagittal section drawn from 10 serial sections (Fig. J2, p. 412). **2,** Frontal schematic view combining 30 serial sections (fig. J3, p. 413). The spaces that Scheuring called *Bluträume* (bl. r., or blood spaces) were probably midgut digestive diverticulae. Scheuring did not observe the two wide circular ocular muscles described by Land (1969b), and Land could not find Scheuring's muscle 4 in his study of *Pelegrina aeneola*. We need to reserve judgement about these discrepancies until the eye muscles of more salticids have been studied, as some differences in configuration may be found between species.

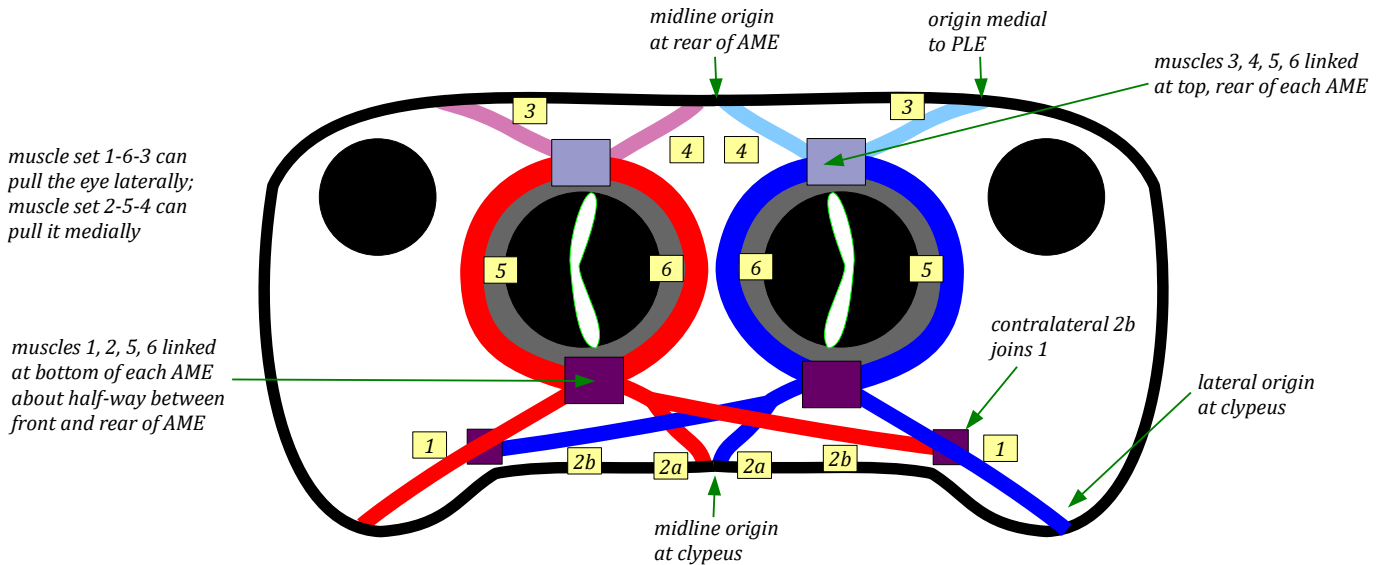


Figure 24. Schematic frontal view of the arrangement of muscles associated with the AME, after Land (1969b, *Pelegrina aeneola*). Land described how, in dissection, these appeared as two sets per eye (1-6-3 and 2-5-4). Muscles 1-4, originating on the carapace, are *extraocular* muscles. Note that the dorsal muscles (3, 4) originate toward the rear of the ocular quadrangle, and the ventral muscles (1, 2) originate at the clypeus. The wide but thin circular muscles (5 and 6) are *ocular* muscles. These encircle the eye tube obliquely on either side, joining the extraocular muscles where they originate at either the top or the bottom of the eye tube. Muscle 2 divides into two branches, one of which (2b) joins muscle 1 before a common lateral origination point on the clypeus.

Table 4. Eye muscles of salticids (after Land 1969b) compared with extraocular eye muscles of humans (Mission for Vision 2006). A major difference between the two lies in the fact that only the eye tube, not the lens, of the salticid AME is moved. thus any movement of the eye tube in one direction moves the field of view of that eye in the opposite direction. In salticids, each extraocular muscle is controlled by a single motor neurite (Land 1969b), whereas vertebrate eye muscles are innervated by nerves containing many neurites. Numbers assigned to salticid muscles are based on Land (1969b). Although there are six muscles in each case, their specific functions are not the same. Functions assigned here to the extraocular muscles of salticids are based on my models (Figure 25) based on Land's diagrams. Groups of muscles must act in concert to move each salticid eye tube to a specific position (Table 6), just as human eye muscles work in concert. Salticid muscles (5) and (6) are *ocular* muscles, as they are only attached to the eye. Salticid muscle (2) has both an ipsilateral origin (2a) and a contralateral connection to muscle (1) of the other eye, and can thus support movement of both eye tubes in parallel. There is no counterpart to this connectivity in vertebrate eyes.

human extraocular muscles		salticid extraocular <i>and</i> ocular muscles	
muscle name	function	muscle name	function (acting alone)
<i>Medial Rectus</i>	rotate eye inward in horizontal plane for medial view	1. <i>Inferior Lateral (extraocular)</i>	move proximal eye tube laterally and ventrally
<i>Lateral Rectus</i>	rotate eye outward in horizontal plane for lateral view	2. <i>Inferior Medial (extraocular)</i>	move proximal eye tube medially and ventrally
<i>Superior Rectus</i>	rotate eye upward in vertical plane for dorsal view, or inward in horizontal plane for medial view; rotate top of eye medially (<i>intorsion</i>)	3. <i>Superior Lateral (extraocular)</i>	move proximal eye tube laterally and dorsally
<i>Inferior Rectus</i>	rotate eye downward in vertical plane for ventral view, or inward in horizontal plane for medial view; rotate top of eye laterally (<i>extorsion</i>)	4. <i>Superior Medial (extraocular)</i>	move proximal eye tube medially and dorsally
<i>Superior Oblique</i>	rotate eye downward in vertical plane for ventral view, or outward in horizontal plane for lateral view; rotate top of eye medially (<i>intorsion</i>)	5. <i>Circular Lateral (ocular)</i>	shorten lateral length of eye tube; if the distal (anterior) eye tube is rigid relative to the proximal eye tube, this can contribute to lateral rotation of the top of the eye tube (<i>extorsion</i>)
<i>Inferior Oblique</i>	rotate eye upward in vertical plane for dorsal view, or outward in horizontal plane for lateral view; rotate top of eye laterally (<i>extorsion</i>)	6. <i>Circular Medial (ocular)</i>	shorten medial length of eye tube; if the distal (anterior) eye tube is rigid relative to the proximal eye tube, this can contribute to medial rotation of the top of the eye tube (<i>intorsion</i>)

To examine how combinations of the six muscles associated with each salticid AME could be expected to move the respective eye tube, I produced a model with rubber bands and a balloon (Figure 25, Table 5).

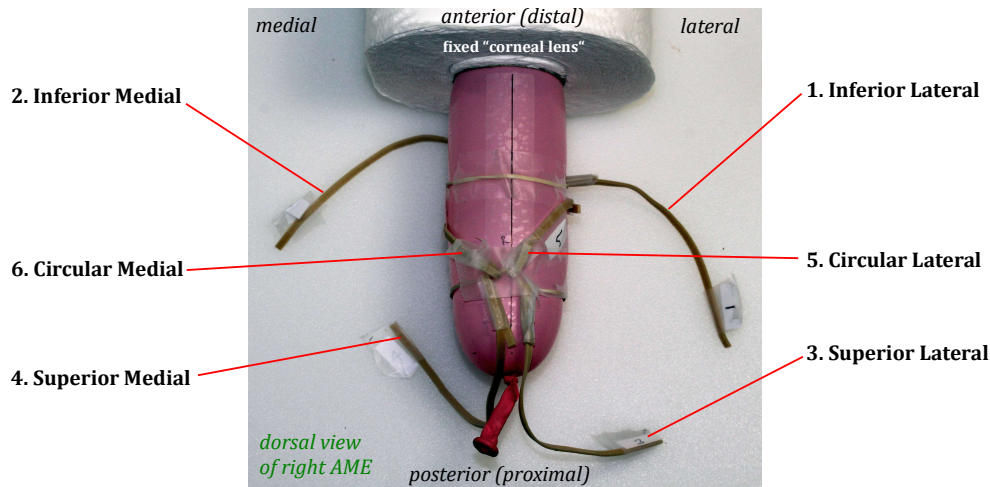


Figure 25. Simple apparatus built with a balloon to represent the eye tube of the right AME, a roll of paper to secure the anterior end of the tube, and attached rubber bands used to model the action of each of the four (1-4) extraocular muscles, as well as the two circular ocular muscles (5, 6). Muscle numbers correspond to those assigned by Land (1969b). By pulling on one or more rubber bands, the likely action of the respective muscles could be observed directly. The action of the circular muscles was more challenging to model, but I was able to simulate their contraction by pulling the ends against a loop in the middle of each band.

Table 5. Effect of contraction of some *ipsilateral* combinations of eye muscles, based on the model shown in Figure 25. Given the fact that I was modeling with a balloon, I did observe a slight elongation of the eye tube with contraction of both ocular muscles (5, 6). This has not been observed in living salticids.

combination	expected movement associated with contraction of these muscles
1, 2	move proximal eye tube ventrally
1, 3	move proximal eye tube laterally
1, 4	rotate top of eye tube medially (<i>intorsion</i>); may be supported by (6)
1, 5	move proximal eye tube laterally and ventrally (1), with lateral compression of the eye tube by (5)
1, 6	medial compression of the eye tube (6) <i>opposes</i> action of (1) to move the proximal eye tube laterally and ventrally
2, 3	rotate top of eye tube laterally (<i>extorsion</i>); may be supported by (5)
2, 4	move proximal eye tube medially
2, 5	lateral compression of the eye tube (5) <i>opposes</i> action of (2) to move the proximal eye tube medially and ventrally
2, 6	move proximal eye tube medially and ventrally (2), with medial compression of the eye tube by (6)
3, 4	move proximal eye tube dorsally
3, 5	move proximal eye tube laterally and dorsally (3), with lateral compression of the eye tube by (5)
3, 6	medial compression of the eye tube (6) <i>opposes</i> action of (3) to move the proximal eye tube laterally and dorsally
4, 5	lateral compression of the eye tube (5) <i>opposes</i> action of (4) to move the proximal eye tube medially and dorsally
4, 6	move proximal eye tube medially and ventrally (2), with medial compression of the eye tube by (6)
5, 6	pressure applied to sides of eye tube can increase intraocular pressure, elongating the eye slightly
2, 4, 6	medial compression of the eye tube (6) supports medial movement of the proximal eye tube by (2) and (4)
1, 3, 5	lateral compression of the eye tube (5) supports lateral movement of the proximal eye tube by (1) and (3)

Land (1969b) observed that, in dissection, there were two connected sets of muscle groups associated with the AME, (1, 6, 3) and (2, 5, 4). Land also thought that (5) and (6) were used to rotate the eye. In my models, both ocular muscles (5, 6) exerted *equal* torsion in either direction when they contracted, and thus could not rotate the eye tubes. However, if the distal (anterior) eye tube is rigid and serves as an origin relative to insertion on the proximal (posterior) eye tube, then these ocular muscles could contribute to rotation of the eye tubes. By shortening the medial side of the eye tube, (6) opposes (1) and (3). Similarly, (5) opposes (2) and (4), as shown in Table 6. Although (1, 6, 3) and (2, 5, 4) are good *structural* units, it appears that (2, 4, 6) and (1, 3, 5) are the major *functional* units associated with side to side movement of the AME.

A change in length of the eye tube has not been observed, but remains a possibility that could help to maintain the relative position of lens and retina, particularly when the eye is moved. This would represent an evolutionary parallel to the ability of vertebrates to accommodate by changing the shape of the lens. If the rear of each AME eye tube does in fact constitute a lens element (Williams & McIntyre 1980), then this would indeed change the shape of the salticid lens. At this point, we do know that the eye tube, in order to move and rotate, must be flexible, and it must change shape. If you twist it, it may get shorter. However we do not know the details of this process. Land (1969b) did not observe any change in length of the AME.

In salticids that are relatively transparent (Figures 26-27) it is possible to observe movement of the AME eye tubes directly. Land (1969b) also observed the parallel (conjugate) and independent (disjunctive) movements of the AME through the transparent dorsal prosoma of *Phanias harfordi* (Peckham & Peckham 1888). He reported a range of horizontal movement of the eye tube between about 20° laterally and 28° medially relative to the axis of the prosoma. Most of the movement of the two eye tubes that he observed was parallel or conjugate, even during torsional movements. He classified this activity into four categories. The first he called *spontaneous activity*, consisting of irregular lateral movements of highly variable extent and duration, primarily in a horizontal plane, and often asymmetric. The second type of movement, *saccades*, consisted of the rapid movement of both AME retinæ to bring about both foveae to converge on a small target in the visual field. He also described *tracking* movements of both retinæ, to

maintain this alignment with a small, moving target. This fourth category of movement, *scanning*, was like spontaneous activity in many respects, but was more regular and predictable, based on the properties of a specific target. Torsion cycles (alternating about 20-30° in either direction) were combined with regular, side to side horizontal movements during scanning (Figures 28-29).

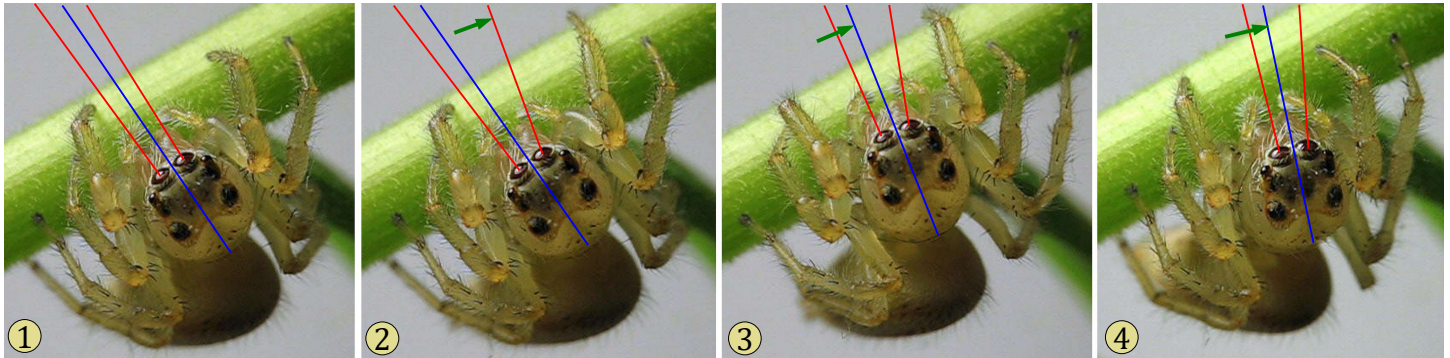


Figure 26. Four frames from a video of an adult female *Colonus sylvanus* in Greenville County, South Carolina. The transparency of the prosoma allowed a direct view of the movements of the AME. **1**, This spider faced a *Leucauge venusta* (Araneae: Tetragnathidae) suspended under a nearby grass blade. The axis of the prosoma (blue line) and the optical axes of the AME (red lines) faced the prey directly. **2**, The eye tube of the right AME moved to the left, shifting the axis of that eye to face the stem that would serve as an indirect route of access to that prey. **3-4**, The spider slowly turned to the right, lowering its profile in the prey direction (upper left), and faced that access route. Subsequently, this *Colonus* slowly climbed the nearby stem, then moved under the attached grass blade to approach its prey, which was then captured with an upside-down jump. Active movement of the two AME tends to be loosely coupled, but each eye can also be moved independently as shown in (2).

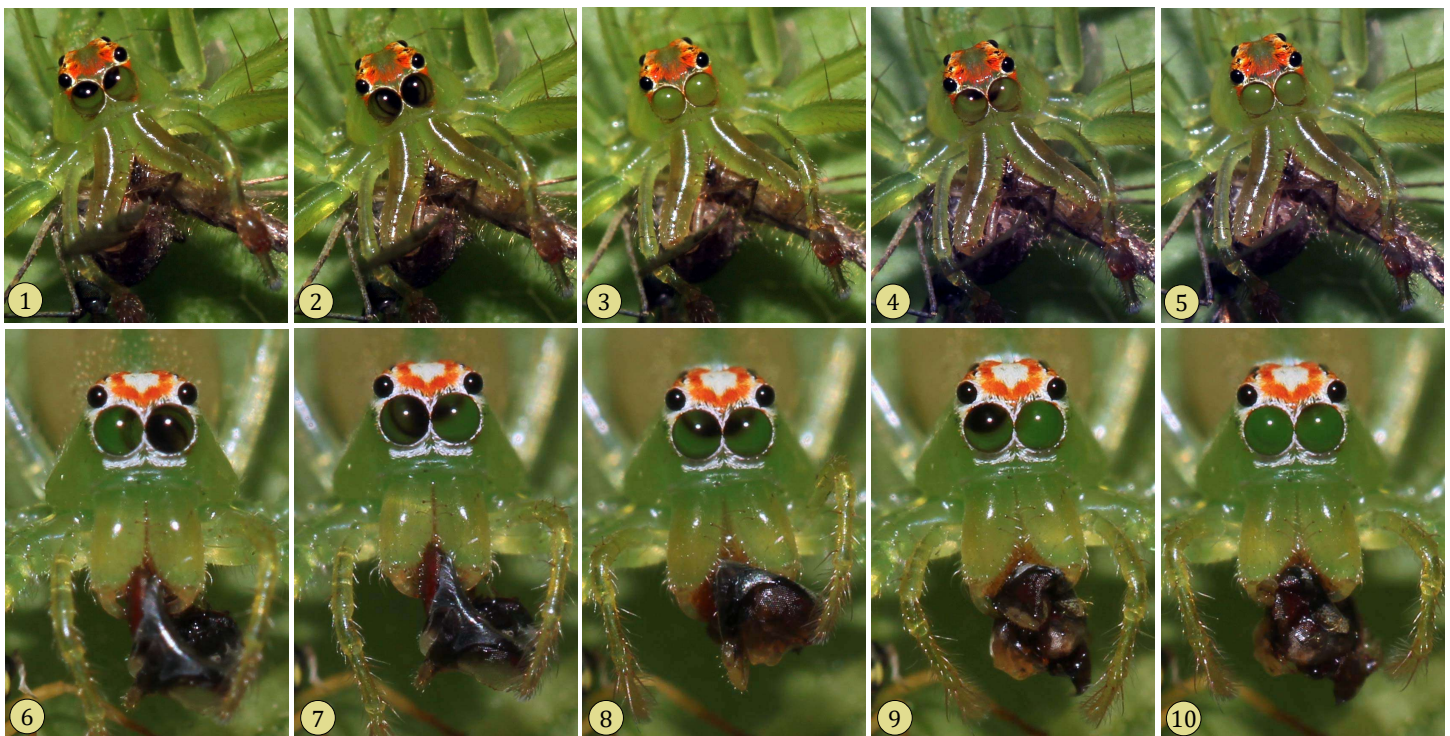


Figure 27. Movement of the AME eye tubes of adult male (1-5) and female (6-10) *Lyssomanes viridis* from Greenville County, South Carolina, as seen from the front. When these spiders are looking directly at the camera, the AME is completely black in appearance. These examples show both parallel and independent movement of the two AME.

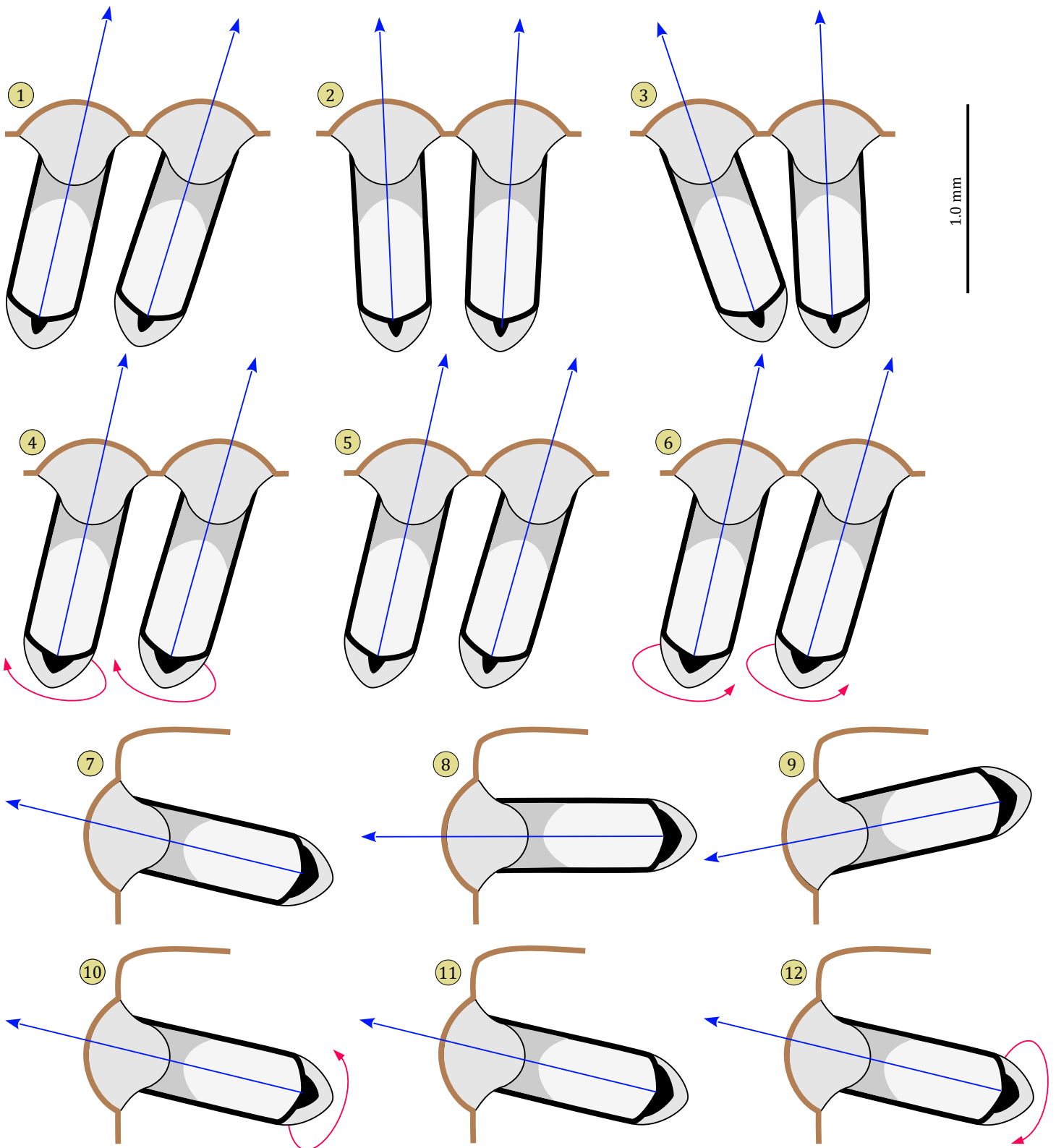


Figure 28. Schematic diagrams showing movement of the long tubes of the AME of *Phidippus johnsoni*, after Land (1969b), drawn to scale. Land found that his direct measurements of focal length of these eyes were close to calculations that included the negative curvature at the rear of the corneal lens. Radial symmetry of this lens suggests that its ability to focus is not impaired as the eye tube is rotated. **1-3**, Horizontal sections depicting a sequence of spontaneous activity, with independent movement of each eye tube. **4-6**, Horizontal sections depicting alternating rotation of the eye tubes, in either direction, when the spider is *scanning* an object. **7-9**, Parasagittal sections of one eye, showing up and down movement. **10-12**, Parasagittal sections of one eye, showing alternating torsion in either direction.

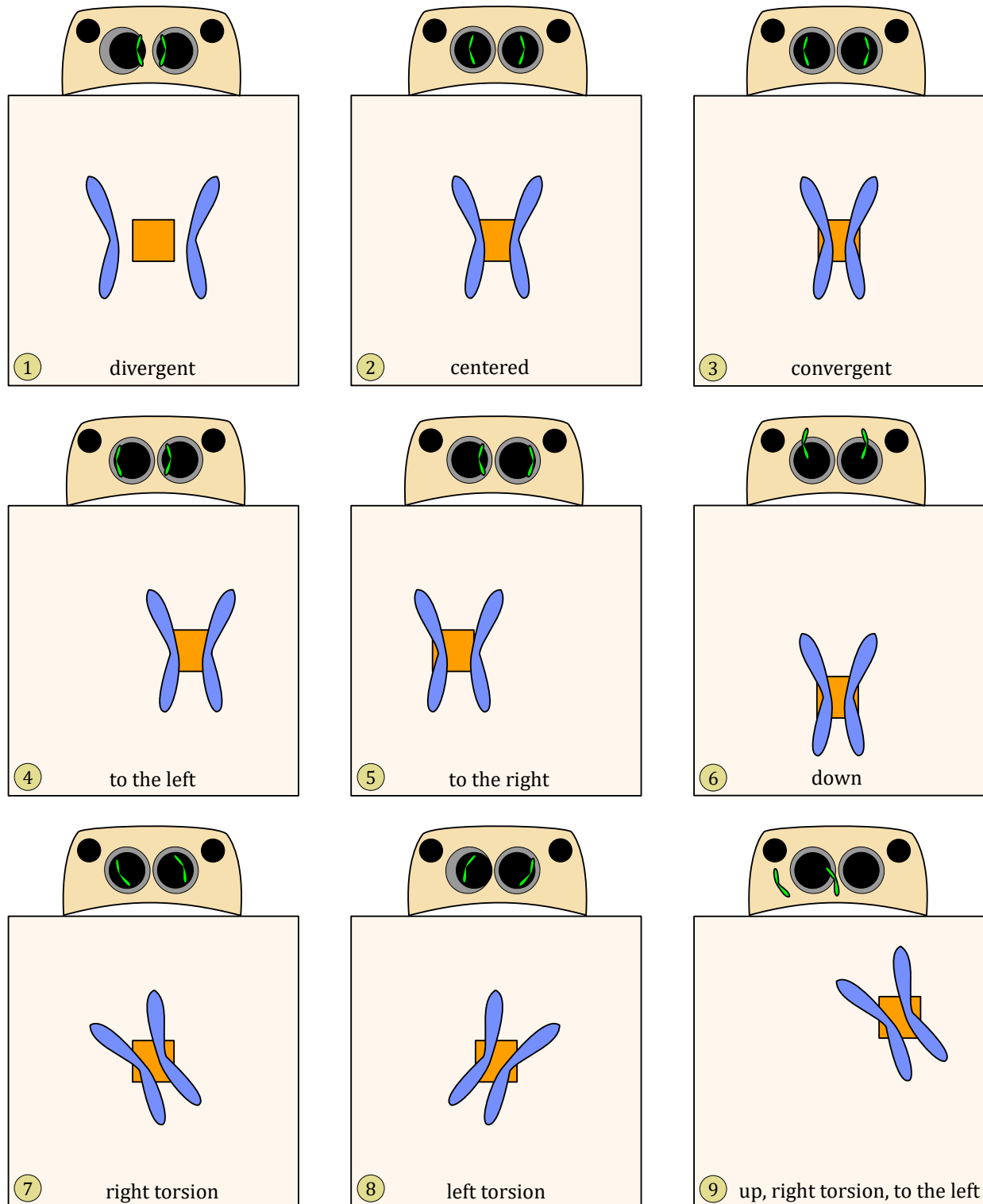


Figure 29. Schematic diagrams (1-9) depicting movement of the AME retinae as viewed from the front, after Land (1969b). At the top of each diagram the position of the retinae is shown (in green), as viewed from the front. Below each diagram, the corresponding visual field of the retinae is shown in blue outline. Land was only able to observe the upper layer of the retina through his ophthalmoscope, and the positions of the overall retinae shown here are inferred from anatomical studies. Land described four kinds of movement of these eyes: 1) *spontaneous activity*, or irregular and often independent movement of each eye in the absence of a visual stimulus, 2) *saccades*, or movement of both eyes to align their centers on a point stimulus (orange rectangle at center of these diagrams), 3) *tracking*, or following a moving target with aligned retinae, and 4) *scanning*, a combination of horizontal movement with intermittent torsion of the aligned eyes during the examination of a target. In *Pelegrina*, a distance of 10 μm in the plane of the retina corresponds to a visual field of ~ 1 degree (Land 1969a, 1969b).

Since these behaviors are highly variable with respect to their timing and duration, we can summarize as follows: Foveal fields of vision of the two AME can converge on a target, the eye tubes can also be moved to follow that target, and once a target is acquired it may be scanned by a combination of horizontal and torsional movements of the eye tubes, mostly in parallel. Finally, something like scanning (*spontaneous activity*), but less regular, can also be observed in the laboratory in the absence of specific visual targets.

The function of these eye movements was also considered by Land (1969b). Clearly the field of vision of the AME fovea is quite small, and it must be directed to a specific part of the visual field to collect detailed light patterns from it. This much helps to explain the role of *saccades* and *tracking*. Explanation of *scanning* movement, primarily horizontal and including torsion in both directions, is more challenging. This also clearly extends the visual field, to cover a much wider area, but the function of torsion must also be explained. Twisting the eye tube by as much as 30° *might* also change the length of that tube, affecting the focal plane. Salticids also often rotate the prosoma (ρ -turn; Figure 60) while examining an object (Hill 2010a), a behavior that may extend the angle covered by torsional movement of the retinae, at the same time that it alters the plane of horizontal scanning. This suggests that it may be useful for the salticid to collect light data in a particular direction across a border (or boundary between two areas of different coloration: hue, saturation, and lightness). Since no recordings have been made from multiple receptors when the eye tubes were moving, we presently have little information that can bear of the question of how this works.

One additional question related to the motion of the AME is simply: How does the CNS of the salticid know where the eye tube is pointing, or its torsion? We don't know of any related positional sensors associated with the AME, so the most plausible hypothesis is that, as with vertebrates (Bridgeman 1995; Lewis, Gaymard & Tamargo 1998), *efference copy* is the source of this information. This means simply that the same *efference* signals that drive the oculomotor activity would also convey the position of the AME to parts of the CNS that use this information. This is a problem that does not occur with the other eyes, all of which are fixed with respect to the prosoma.

Visual optics. There are two important considerations with respect to the design of eyes and cameras: The purpose of the system is to *restrict* the movement of photons as they move from the observed object to the retina or sensor, so that only those photons that originate from a *specific direction* have access to a *specific position* on an array of sensors. At the same time it is important to collect as many photons as are necessary to activate those sensors. The lens itself is a simple device that uses differences in refractive index, corresponding inversely to differences in the velocity and wavelength of light as it passes through different materials, to change the direction of incoming light so that more light can be collected from a single point source and directed toward a single receptor through *convergence*.

At this point I would like to briefly review the key aspects of human or vertebrate eye structure that affect its visual optics. This provides a useful background for discussion of the features of the salticid AME. As shown in Figure 30, refraction in the human eye is primarily associated with the cornea, supplemented by a proximal lens that can be stretched to change its optical properties, thus allowing the eye to *accommodate* or focus on objects at varying distances. When a viewed object is *in focus*, incoming light from each point on that object subtends as few sensory receptors as possible. Its passage is *more restricted*. As in salticids, a pit or fovea is associated with the part of the retina that has the highest resolution, in alignment with the optical axis of the lens system. In the vertebrate eye, however, receptor rhabdoms (rod and cone layer) are proximal to several layers of interneurons, including horizontal, amacrine, and ganglion cells. Distal interneurons, not proximal sensory cells, send encoded visual information back to the visual cortex of the brain through neurites that comprise the optic nerve.

Given the shape of the fovea, and the fact that the refractive index of the retina is greater than that of the vitreous chamber of the human eye, it has been proposed that this acts as a diverging lens to increase image size (Walls 1937; Locket 1992), as has been proposed for salticids (Williams & McIntyre 1980, Blest et al. 1981). In fact, even deeper foveas have been found in other vertebrates, including raptors (Locket 1992; Tucker 2000; Ross 2004). Walls' refraction hypothesis was challenged by Pumphrey (1948), who concluded that, due to diffraction effects that Walls had not considered, foveal refraction would actually *reduce* the quality of the resultant image. Pumphrey proposed that this refraction might nonetheless contribute to the ability to fixate on a moving object, as distortion of an image would be minimized when it was centered on the fovea. However, it now appears that foveal refraction is not that important in vertebrates. Recent studies (Franze et al. 2007, Labin & Ribak 2010), have shown that the Müller (glial) cells of the vertebrate retina serve as *light guides*, conveying photons through the entire thickness of the retina. We will return to this point later in our discussion of the retina of the salticid AME.

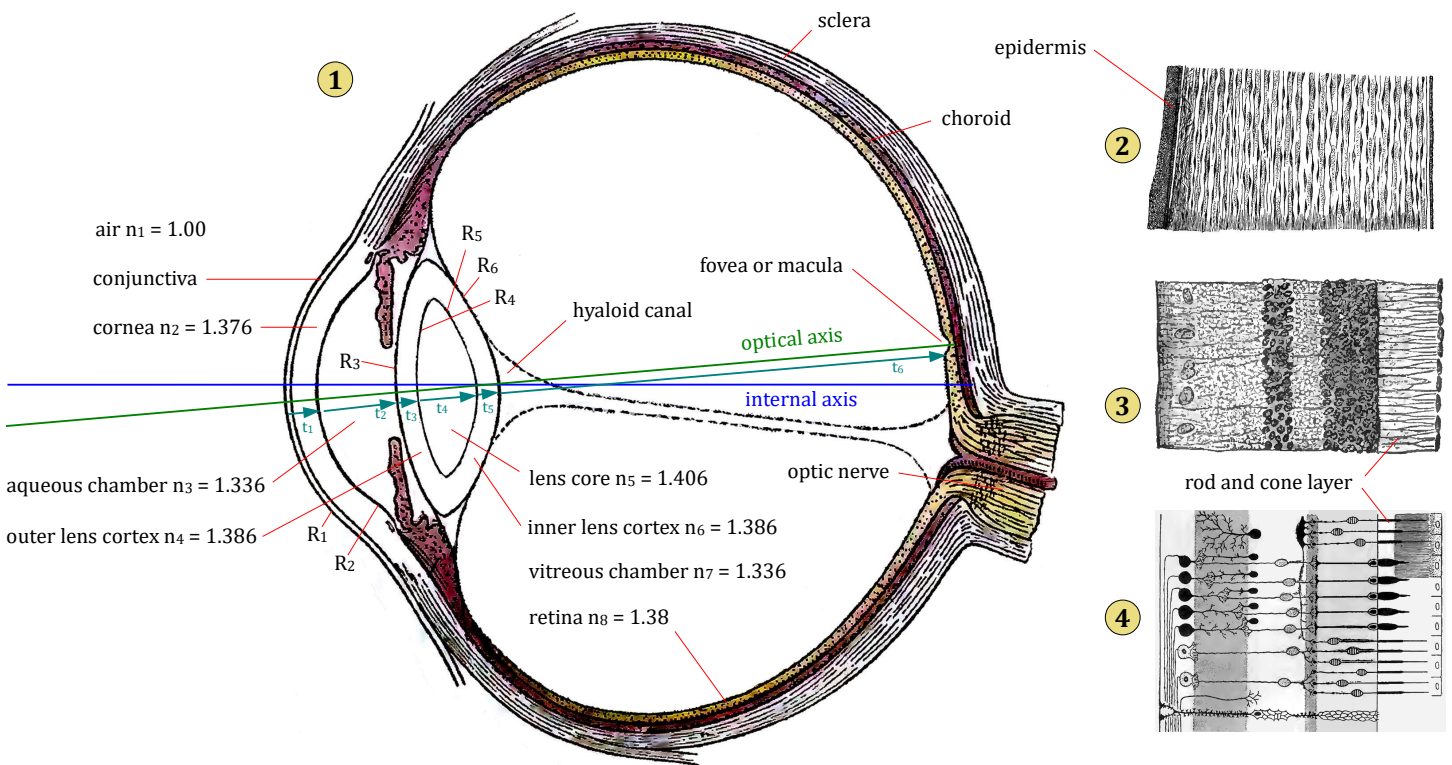


Figure 30. Model of the human eye. **1**, The properties (n , refractive index; R , radius; t , thickness) of a series of structures along the optical axis determine how the eye collects and focuses light on the retina. Intraocular muscles can stretch the lens, thus changing the values of R_3 , R_4 , t_3 and t_5 , resulting in a change in focal length. This allows the eye to focus light from objects at variable distance (accommodation). **2**, Section through stratified cornea. **3-4**, Histological (**3**) and schematic (**4**) sections through the retina, showing the proximal position of rods and cones, just distal to a basal pigmented layer. Cells to the left in (**4**) are interneurons. After Gray & Lewis (4, with credit to Cajal) 1918; Charman 1991; Gross et al. 2008; Katz & Kruger 2009.

Visual optics of the AME. In theory, the optics of the AME can be calculated from the geometry of component structures, as long as the *index of refraction* of each component material is known. This approach assumes, however that each material has a consistent index of refraction. This is a risky assumption, as biological materials may readily produce gradients in refractive index. For example, Williams & McIntyre (1980) reported that a graded refractive index in the corneal lens of a number of salticid species corrected for spherical aberration. Thus, published mathematical models of AME optics (Land 1969a; Williams & McIntyre 1980; Blest et al. 1981) have only been approximations, contingent on key assumptions related to quantities that could not be measured directly. In each of these studies, direct ophthalmoscopic measurements were ultimately used to refine or to complete a mathematical model of optics, to achieve the level of accuracy required to estimate image positions within retinal layers.

Published studies have relied greatly on standard *thick lens* (or *lensmaker's*) equations, and several of these do not include all measurements or calculations. To improve on the value of these models going forward, I have converted the published models that rely heavily on abstractions like *nodal point*, *primary plane*, and *front focal length* to a mathematically equivalent, but much simpler, *vergence* model. Vergence is a measure of the curvature of a wavefront, defined simply as (n/r) , where n is the refractive index of the medium, and r (– if *diverging* and + if *converging*) is the distance that the wavefront has moved from its source through that medium. Like the *power* of a lens surface, vergence is measured in *diopters* (1 diopter, $D = 1/m$). The simplicity of this approach becomes apparent when one works with thick lenses (where lens thickness, t , is significant), or with multiple lenses in a series. Equivalent to the graphic *ray-tracing* technique, one can follow convergence calculations directly from the object to the image. When a refractive boundary is crossed, the *optical power* of refraction is simply added to the convergence value in front of that boundary. Then, as light passes through a material of known refractive index, convergence changes in accordance with a simple formula, as a function of refractive index and distance. This approach not only *greatly simplifies* the subject of visual optics, but it is also much more intuitive and less prone to error.

Based on examination of sections under the microscope, a more detailed model of AME optics might include a good number of serial refractive surfaces, from the convex front of the cornea (converging) to the concave (diverging) *pit* in front of the retina (Figure 31:1). Following Homann (1928, 1950, 1952), Land (1969a) suspended a corneal lens in a drop of Ringer's solution to directly observe its magnification and thereby calculate its refractive index. He then incorporated this value into his models of AME optics (Figure 31:2 and Table 6), which were based on refraction by a single lens (the corneal lens) with two refractive surfaces. Williams & McIntyre (1980), followed by Blest *et al.* (1981), also using direct observation through a dissected corneal lens to estimate its refractive index, expanded on Land's model with the addition of a third refractive surface, the concave boundary between the pit and the foveal matrix of the retina (Figure 31:3 and Table 6). All of these models pertain only to the foveal receptors at the center of the boomerang-shaped AME, where the highest receptor density is found.

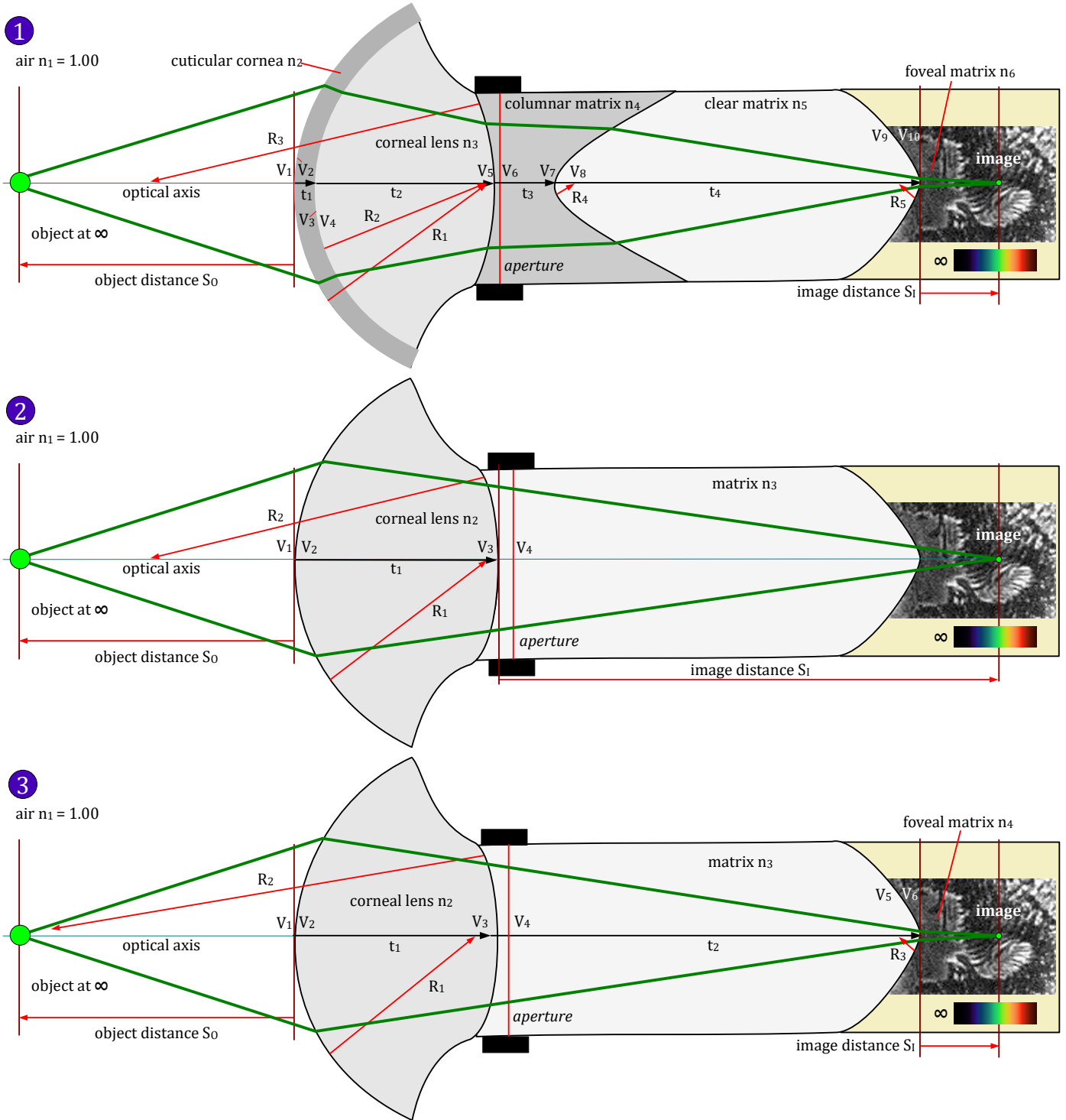


Figure 31. Optical models of the salticid AME in schematic parasagittal section. **1**, A more detailed model might account for differences between the cornea and the corneal lens, as well as variation in the matrix of the eye tube, based on materials that look different in stained sections that may have different refractive indices (n). Published attempts to model AME optics have all grouped n_2 with n_3 and n_4 with n_5 . **2**, Land's early (1969a) study grouped n_4, n_5 , and n_6 , assuming that they all had the same refractive index equivalent to *spider Ringer's* ($n = 1.335$). Land only modeled a single lens element, with two refracting surfaces. **3**, Later models (Williams & McIntyre 1980; Blest *et al.* 1981) included a second lens element behind the first, with a diverging concave surface (radius R_3) at the foveal pit. As shown by the spectrum at the lower right of each diagram, unless the AME compensates for *chromatic aberration*, the plane of focus of the AME will be determined by the spectral hue of light emitted by the object, as well as its distance. Chromatic aberration (or *dispersion*) results from the fact that the index of refraction of a material tends to be greater for shorter wavelengths. As a convention, vectors that point to the left here are negative in value, to the right positive. Symbols: n , refractive index of material; R , radius of refractive surface; t , thickness of lens element; V , position in front of or behind refractive surface where vergence is calculated (Table 6).

Table 6. Published models of the salticid AME. Calculations shown here are based on *vergence* corresponding to positions identified in Figure 31. This simplified approach is mathematically equivalent to the thick lens optics equations that have been published. Land's models did not recognize a third refractive surface associated with the foveal pit. Only his modified *Phidippus johnsoni* model is shown here. Williams & McIntyre did not publish all of the relevant calculations, and some of their measurements (highlighted in red) have been estimated to agree with all of the results that they did publish (e.g., f_1 of corneal lens = -1273 μm , f_2 = 1701 μm). With a small and powerful diverging lens, the angular subtense of receptors (bottom of chart) for Williams & McIntyre's model was particularly sensitive to distance, and only produced a virtual image for objects 2.0 cm in front of the lens. Since the system magnification (M_s) is negative, the resultant image was inverted in each case. All of these studies ultimately relied more on direct measurement of the plane of focus than on these optical models.

variable (see Figure 31)		Land 1969a	Land 1969a	Williams & McIntyre 1980	Blest et al. 1981
		<i>Phidippus johnsoni</i>	<i>Pelegrina aeneola</i>	<i>Portia fimbriata</i>	<i>Servaea vestita</i>
λ	reference wavelength	~500-550 nm	~500-550 nm	~520 nm	523 nm
S_0	object distance in front of first refractive surface	∞	∞	∞	∞
n_1	refractive index of material in front of first surface (air)	1.00	1.00	1.00	1.00
n_2	refractive index of material behind first surface	1.37	1.41	1.40	1.40
n_3	refractive index of material behind third surface	1.335	1.335	1.336	1.337
n_4	refractive index of material behind fourth surface			1.40	1.40
R_1	radius of first refractive surface	344 μm	217 μm	509.2 μm	315 μm
R_2	radius of second refractive surface	-179 μm	-525 μm	∞ (flat)	∞ (flat)
R_3	radius of third refractive surface			-5 μm (center)	-8 μm (center)
t_1	thickness of first lens element along optical axis	435 μm	236 μm	400 μm	375 μm
t_2	thickness of second lens element along optical axis			1282.4 μm	661 μm
V_1	initial vergence in front of first refractive surface = n_1/S_0	0 D	0 D	0 D	0 D
P_1	optical power of first refractive surface = $(n_2-n_1)/R_1$	1076 D	1889 D	786 D	1270 D
V_2	vergence behind first refractive surface = $V_1 + P_1$	1076 D	1889 D	786 D	1270 D
V_3	vergence in front of second refractive surface = $n_2V_2/(n_2-t_1V_2)$	1633 D	2763 D	1013 D	1924 D
P_2	optical power of second refractive surface = $(n_3-n_2)/R_2$	196 D	143 D	0 D	0 D
V_4	vergence behind second refractive surface = $V_3 + P_2$	1829 D	2906 D	1013 d	1924 D
S_1	image distance behind second refractive surface (BFL) = n_3/C_4	730 μm	459 μm		
V_5	vergence in front of third refractive surface = $n_3V_4/(n_3-t_2V_4)$			36487 D	39599 D
P_3	optical power of third refractive surface = $(n_4-n_3)/R_3$			-12800 D	-7875 D
V_6	vergence behind third refractive surface = $V_5 + P_3$			23687 D	31724 D
S_1	image distance behind third refractive surface (BFL) = n_4/V_6			59 μm	44 μm
M_3	linear magnification at third refractive interface = V_5/V_6			1.54	1.25
M_s	system magnification for ($S_0 = 10.0$ cm) = $(V_1/V_2)(V_3/V_4)(V_5/V_6)$	-0.0084	-0.0051	-0.0294	-0.0106
X_A	object angular size/image size for $S_0 = \infty$	8.28 minutes/ μm	13.66 minutes/ μm	3.51 minutes/ μm	6.99 minutes/ μm
X_{A10}	object angular size/image size for $S_0 = 10.0$ cm	8.22 minutes/ μm	13.60 minutes/ μm	2.34 minutes/ μm	6.51 minutes/ μm
X_{A5}	object angular size/image size for $S_0 = 5.0$ cm	8.15 minutes/ μm	13.53 minutes/ μm	no retinal image	6.03 minutes/ μm
X_{A2}	object angular size/image size for $S_0 = 2.0$ cm	7.96 minutes/ μm	13.53 minutes/ μm	no retinal image	4.59 minutes/ μm

Image plane and chromatic aberration. Largely based on direct observation of the top of (distal) retinal layer IV with an ophthalmoscope rather than on optical models, the focal position (image plane) of green light as a function of object distance has been estimated for several salticids (Figure 32). Chromatic aberration, a result of the fact that the refractive index of a material can vary considerably as a function of wavelength, has also been estimated. Land (1969a) based his estimates on the chromatic aberration of water. Blest *et al.* (1981) measured chromatic aberration of the isolated corneal lens (with cuticular cornea) directly, finding a significantly higher level of aberration (about 5% at $\lambda = 400$ nm compared to 523 nm) than Land estimated. Does the intact AME correct for chromatic aberration? It is possible that lens elements proximal to the converging corneal lens, or a diverging pit lens do this to the extent that chromatic aberration is not a problem, but we do not know at this point.

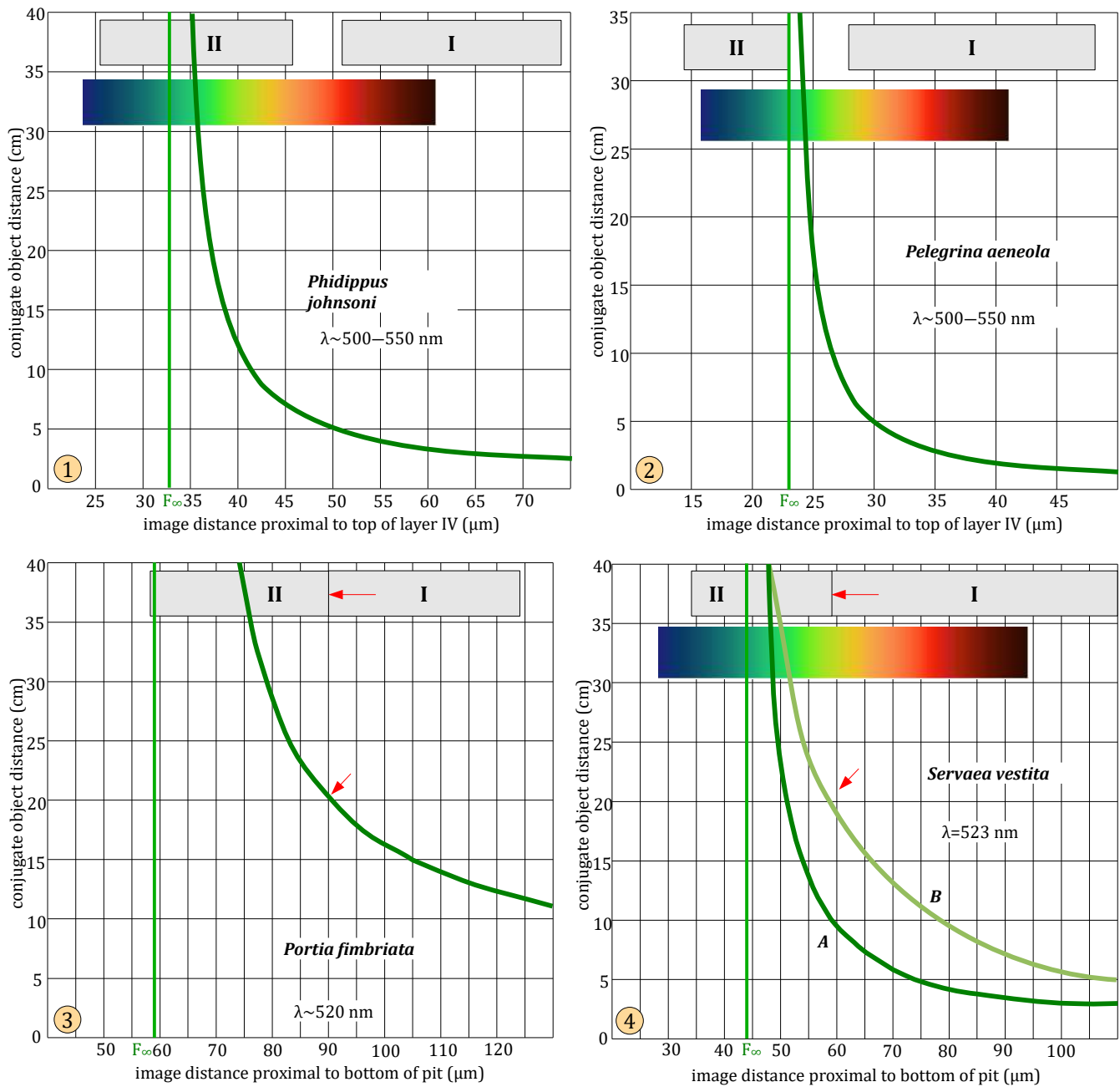


Figure 32. Relationship of image (focal) plane in the AME retina to the conjugate object distance. In each case, the curve shown in dark green was calculated for the stated wavelength according to models described in Figure 31 and Table 6. **1**, Land's (1969a) modified model for *Phidippus johnsoni*. Land recognized the presence of a gap between retinal layers I and II (extent indicated at top), but not the staircased position of layer I receptors that brought them up to the level of the most proximal layer II receptors, as described in subsequent studies. A spectrum illustrates the extent of chromatic aberration estimated by Land, based on the chromatic aberration of water. As an object moves closer to the lens, the focal plane moves proximally, away from the lens. F_∞ indicates the focal plane of an object at infinity. If chromatic aberration is not countered then shorter wavelengths have a more distal focus. **2**, Land's model for *Pelegrina aeneola*. **3**, Model for *Portia fimbriata* based on Williams & McIntyre 1980. Williams & McIntyre thought that focus of green light from an object at a distance of 20 cm at the top of layer I receptors (red arrows) was reasonable given the behavior of *Portia*, but as a result of the high power of the diverging pit lens that they proposed, this model does not allow green light at less than 10 cm in distance to focus within the confines of the retina. **4**, Model for *Servaea vestita* based on Blest *et al.* 1981. In this study, optimal focus for an object at 20 cm distance at the top of layer I (red arrows) was also assumed, giving a curve (B) quite different from that calculated from the optical model that was published (B). The spectrum for chromatic aberration shown here is conjectural, based on their discussion. Blest *et al.* measured the chromatic aberration (5% at $\lambda = 400$ nm compared to 523 nm standard) of the isolated corneal lens directly.

In lens design, a distal *converging* lens can be paired (in a *couplet*) with a proximal *diverging* lens to reduce chromatic aberration to an acceptable level (Figure 33). The concave AME pit lens appears to have a significantly higher proximal refractive index (retinal matrix $n \sim 1.40$ compared to $n \sim 1.34$ in the pit; Williams & McIntyre 1980), so it should reduce chromatic aberration. This would certainly simplify the information produced by the layered retina of the salticid AME. In nature, light sources (objects) are certainly not monochromatic (as some discussions of chromatic aberration might lead us to believe!), and thus chromatic aberration would put light from a real object into sharpest focus at many different layers. One of the proposed functions for retinal tiering is related to the hypothesis that this allows light of different wavelengths to be focused at different levels of the retina (Land 1969a; Williams & McIntyre 1980; Blest et al. 1981). This has been thought to correlate with the presence of different receptor types (based on the λ sensitivity of each type) in each level. Since chromatic aberration has only been measured directly for the isolated corneal lens of the AME (Blest *et al.* 1981), we cannot make any firm conclusions at this point regarding the chromatic aberration of the *entire* lens system.

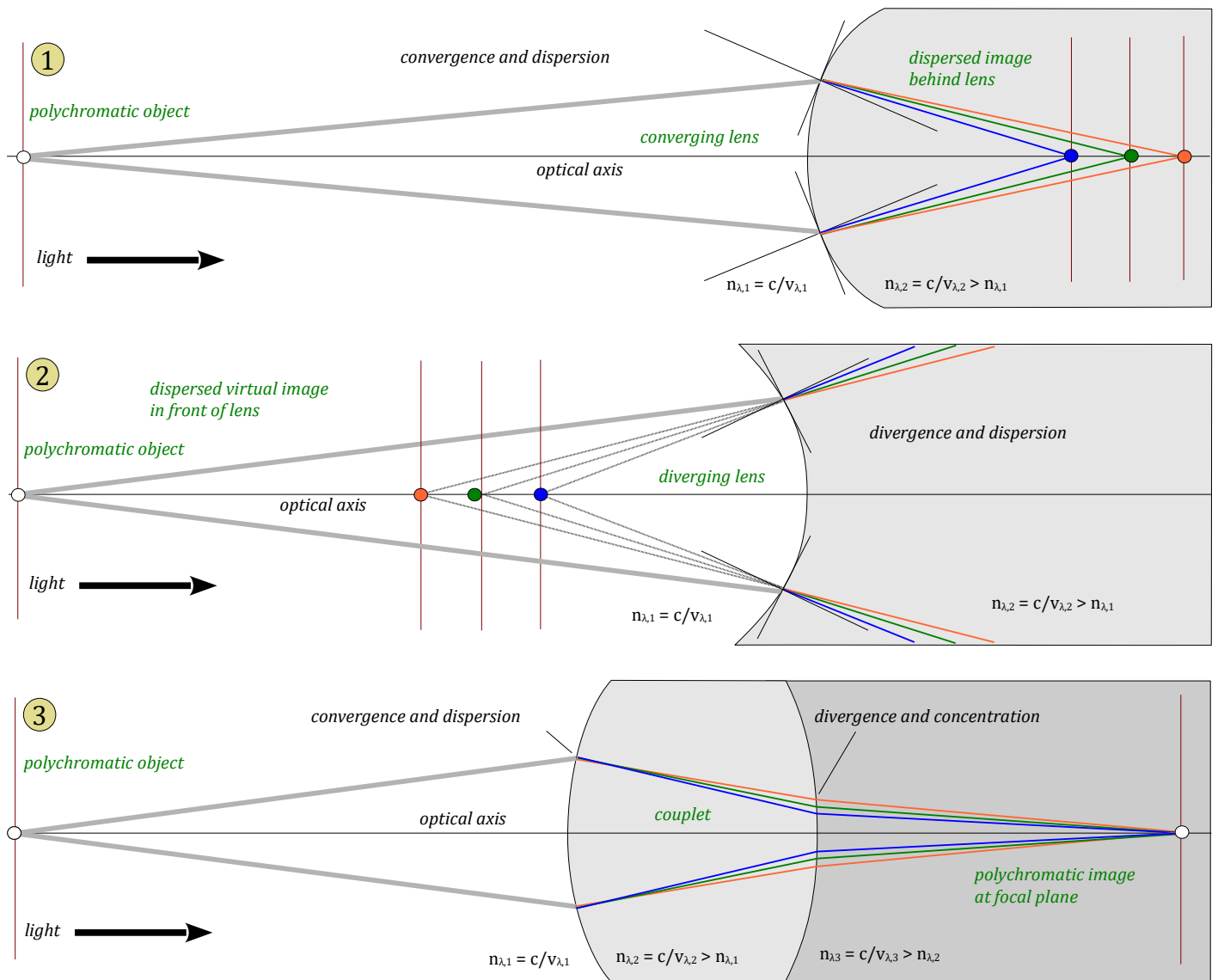


Figure 33. Compensation for chromatic dispersion by a converging lens element with a divergent lens element. Note that since the velocity of light with a shorter wavelength (blue) is slower ($n > 1$) as it moves through a material, it has a higher index of refraction (n) and hence its path changes more at each interface, going from left to right. This results in chromatic dispersion (chromatic aberration) at both converging (1) and diverging (2) lens elements. However, if a converging and diverging lens element are matched in a *couplet* (3) chromatic aberration can be reduced to an acceptable level.

Small diverging lens at the fovea? Williams & McIntyre (1980) first proposed that magnification due to refraction by a small but powerful diverging lens (pit) or *telephoto component* at the front of the retina played a key role in increasing both the effective focal length in some, *but not all*, salticids, and the resultant magnification of an image (Figure 31, Table 6). They cited the then-current hypothesis that the foveae of falconiform birds and other vertebrates functioned in the same manner, as a powerful diverging lens (Walls 1942; Snyder & Miller 1978). As noted in my review of the human eye, recent studies (Franze et al. 2007; Labin & Ribak 2010) have shown that the Müller cells of the vertebrate retina serve as wave (or light) guides, challenging the earlier views of a small foveal lens. One of the peculiarities of the salticid retina lies in the fact that distal receptor layers are directly in front of proximal layers, and the layer that should have the highest resolution is actually *behind* three other layers. The receptor processes of each of these intervening layers may themselves behave as wave guides, further confusing our understanding of the passage of light back to the closely packed receptors of layer I. Even if light is *in focus* at layer I, after all, it must still pass first through either glia (supportive cells) or receptors of layers II-IV, where it must either be absorbed or transmitted, and possibly, refracted. As noted by Eakin & Brandenburger (1971), the receptor processes of layer II are aligned in parallel with the receptor processes of layer I below them, and receptors in both layers are *surrounded by thin sheetlike extensions of the supportive cells* but not pigmented glia. They also described the level between layers I and II, also noted by Land (1969a), as a *stratum of extensions of supportive cells*. The detailed structure and refractive index of both neuroglia (supportive cells) and receptors must be taken into account if we are to understand the transmission of light through the retina of the salticid AME. The concerns of Pumphrey (1948) regarding degradation of the image as a result of *diffraction* (tendency of light waves to spread out after passing through a small opening) at a small foveal lens must also be addressed. Discussions of diffraction limits of the salticid AME (Land 1969a, Williams & McIntyre 1980, Blest *et al.* 1981; see below) have only considered the aperture associated with the much larger corneal lens, and not the small size of a foveal lens.

Does spherical aberration or diffraction limit AME resolution? *Spherical aberration* is the loss of focus or sharpness of an image due to the fact that the calculated focal point of a spherical lens assumes a small angle of incidence, that is, that light from an object is refracted near the optical axis. Because of this geometric constraint, incoming 'rays' that are not near the optical axis of a spherical lens will not converge on the calculated focal point. A lens can be *corrected* for spherical aberration in several ways, including reduction of the aperture so that only rays close to the optical axis are refracted, or by a change in the shape of the lens so that it is not completely spherical. The resolution of corrected lenses is generally limited by diffraction. *Diffraction*, like spherical aberration, also causes a loss of image resolution, a result of the fact that light waves converging on a small aperture tend to bend around the edges of that aperture. A smaller aperture results in a larger depth of field, but at the expense of a loss of image quality due to diffraction. Land (1969a) used ray tracing to estimate spherical aberration, and suggested that this might be a limiting factor that could be matched to AME receptor spacing. However Land found that receptors could be spaced much more closely if diffraction were the only consideration, so he did not consider diffraction to be the limiting factor. However, when Williams & McIntyre (1980) later examined the corneal lens of *Portia fimbriata* and several other salticids with interference microscopy, they found that spherical aberration was actually corrected by a graded refractive index, and concluded that diffraction was the limiting factor for the salticid AME. Blest *et al.* (1981) also modeled spherical aberration with ray tracing through a single convex surface of the corneal lens of *Servaea vestita*, and found a much lower level of aberration than did Land. They also concluded that diffraction was the factor that limited AME resolution.

Spatial cut-off frequency is a measure of the maximum linear density of waves or grid-lines that can be resolved, based on diffraction limitations of an optical system. Calculations related to both the corneal lens and pit lens of the salticid AME are presented here (Table 7).

Table 7. Theoretical limits of resolution resulting from diffraction in an ideal AME. The spatial cut-off frequency represents the greatest density of light/dark cycles (grid lines) that could be resolved, if no other properties of the system reduced contrast. The standard equations used here are based on Land (1969a) and Goodman (1968). Closer spacing of receptors than that shown at the bottom of this chart would not improve resolution. At this *limiting* value, however, optics of the eye would have to be 'perfect' and even then the separation (or contrast difference) between grid lines and intervening spaces would be just barely perceptible. The studies presented here only considered diffraction associated with the corneal lens. Additional diffraction associated with the pit lens could increase the minimal useful receptor separation to higher levels than are shown here. *Minimal useful receptor spacing* does not double the number of lines that can be resolved, but provides a receptor for each peak (or line), and a separate receptor for each valley (or space). I have included two models of pit lens refraction here, based on the assumption that this lens behaves like a small aperture not far from the focal plane.

reference	Land 1969a		Williams & McIntyre 1980		Blest <i>et al.</i> 1981	
species	<i>Phidippus johnsoni</i>		<i>Pelegrina aeneola</i>		<i>Portia fimbriata</i>	
system	corneal lens	corneal lens	corneal lens	pit lens	corneal lens	pit lens
λ = wavelength in air	500 nm	500 nm	520 nm	520 nm	523 nm	523 nm
n = refractive index of transmitting material	1.335	1.335	1.336	1.400	1.337	1.400
λ_n = wavelength in transmitting material = λ/n	371.43 nm	374.53 nm	389.22 nm	371.43 nm	391.17 nm	373.57 nm
R = radius of wavefront at image	767 μ m	512 μ m	1273 μ m	59 μ m	787.5 μ m	44 μ m
a = effective diameter of aperture	260 μ m	200 μ m	350 μ m	10 μ m	200 μ m	16 μ m
f/# = focal ratio or f-stop = R/a	2.95	2.56	3.64	5.90	3.94	2.75
S_d = spatial cut-off period = $(\lambda_n)(f/\#)$	1.10 μ m	0.96 μ m	1.42 μ m	2.19 μ m	1.54 μ m	1.03 μ m
f_d = spatial cut-off frequency = $1/S_d$	0.91 cycles/ μ m	1.04 cycles/ μ m	0.71 cycles/ μ m	0.46 cycles/ μ m	0.65 cycles/ μ m	0.97 cycles/ μ m
minimum useful receptor separation = $S_d/2$	0.55 μ m	0.48 μ m	0.71 μ m	1.10 μ m	0.77 μ m	0.51 μ m

Depth of field. With a layered retina, depth of field is clearly an important consideration. The sharpness of an image degrades on either side of the focal plane, but an estimate of what constitutes acceptable degradation (or separation of converging light) can allow us to estimate how far we can move from this plane in either direction and still remain *in focus*. The relationship of aperture size to *depth of focus* and *depth of field* is explained in Figure 34.

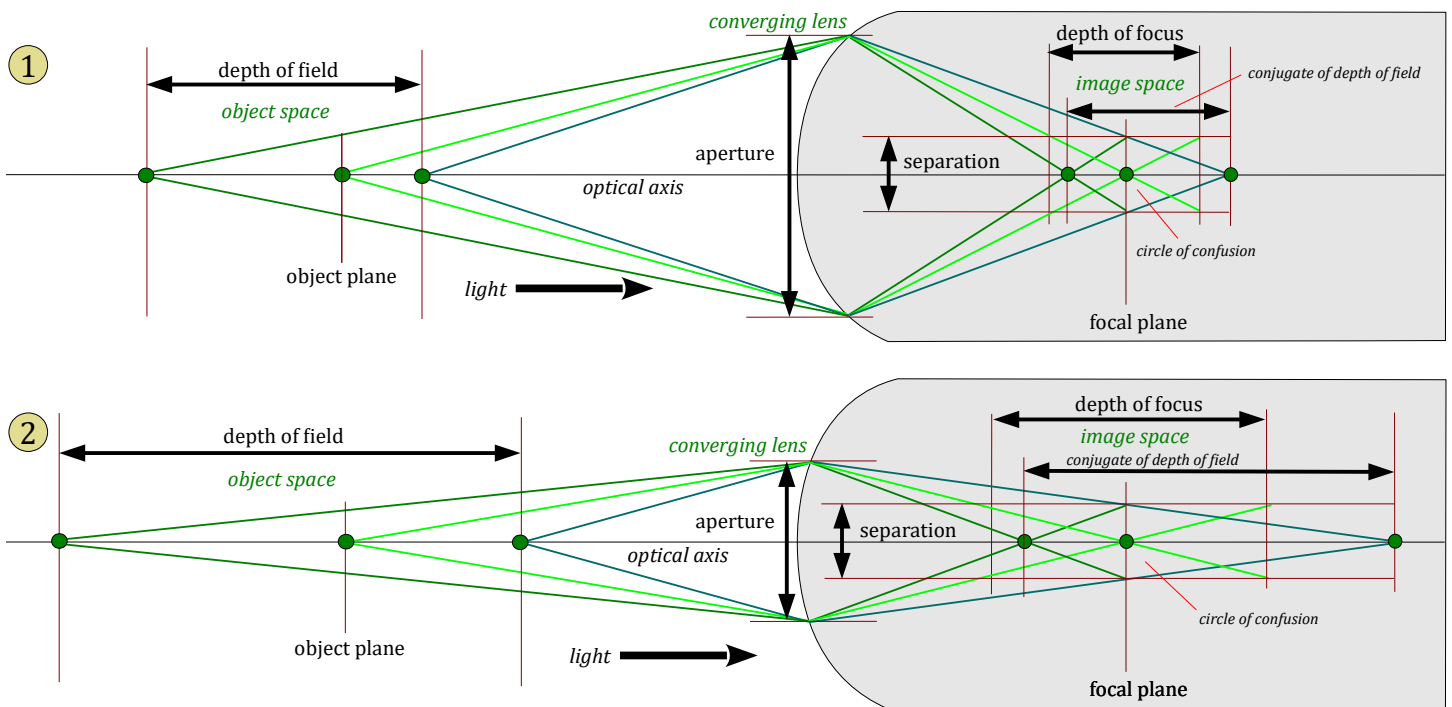


Figure 34. Relationship of aperture size to depth of focus and depth of field. **1,** We begin by deciding on an acceptable criterion for the *separation* of incoming light rays in the image space. Then, for a given object the the focal plane is determined by the distance of that object, and the power and refractive index of the lens. For an object, the *depth of focus* corresponds to the paraxial range of image space over which the separation of light rays from that object meets our criterion. For a focal plane within the retina, the *depth of field* corresponds to the range of positions in object space from which the separation of light rays meets our criterion. **2,** When we reduce the diameter of the aperture, both depth of focus and depth of field increase. Sometimes the depth of focus is defined as the *conjugate of depth of field*.

Published estimates of AME depth of focus and depth of field are shown in Table 8. These should be compared to the graphs shown in Figure 32. One of the complexities related to determination of depth of field of individual receptor layers lies in uncertainty about exactly where light enters these receptors. For example, focus at the top of a layer I receptor would not be useful if the intervening layer II receptors and associated glial processes displayed significant wave guide properties, as in humans (Labin & Ribak 2010), or any of the optical activity (including photon capture by rhabdoms) that their structure suggests. As noted above, chromatic aberration would greatly complicate this situation. The current hypothesis is that there are multiple focus planes in the AME retina, and that images (or at least some wavelengths in each image) are blurred in some layers when they are focused in others.

Table 8. Theoretical depth of focus and depth of field of the AME. Calculation of geometric depth of focus follows the definition shown in Figure 30. Physical depth of focus is limited by the amount of defocus required to produce a $\pm \lambda/4$ wavefront error. Land (1964a) used receptor separation for (s), considered the physical depth of focus to be a more legitimate estimate, and treated depth of focus numbers as conjugates of depth of field. Formulas shown here are based on Land's work, and the other publications referenced here did not include calculations. Calculated depth of focus numbers for Williams & McIntyre (1980) are based on data that they did include in their publication, applied to Land's formulas. All of these values are based on estimates included in respective models, and need verification.

reference	Land 1969a		Williams & McIntyre 1980	Blest <i>et al.</i> 1981
species	<i>Phidippus johnsoni</i>	<i>Pelegrina aeneola</i>	<i>Portia fimbriata</i>	<i>Servaea vestita</i>
system	corneal lens	corneal lens	corneal lens	corneal lens
λ = wavelength in air	500 nm	500 nm	520 nm	523 nm
n = refractive index in image space	1.335	1.335	1.336	1.337
R = radius of wavefront at image	767 μm	512 μm	1273 μm	787.5 μm
a = effective diameter of aperture	260 μm	200 μm	350 μm	200 μm
f/# = focal ratio or f-stop = R/a	2.95	2.56	3.64	3.94
s = diameter of <i>circle of confusion</i> (blur circle)	2.0 nm	1.7 nm	1.4 nm	?
Δf_g = geometric depth of focus = $\pm s(f/\#)$	$\pm 5.90 \mu\text{m}$	$\pm 4.35 \mu\text{m}$	$\pm 5.09 \mu\text{m}$	$\pm 10 \mu\text{m}$ (green) or $\pm 3 \mu\text{m}$ (UV) ?
Δf_p = physical depth of focus = $\pm (8\lambda/\pi n)(f/\#)^2$	$\pm 8.30 \mu\text{m}$	$\pm 6.25 \mu\text{m}$	$\pm 13.11 \mu\text{m}$	
depth of field for layer I	4.7 cm – ∞	2.8 cm – ∞	9 cm – ∞ (green)	3 cm – ∞ (green)
depth of field for layer II				$\sim \infty - \infty$? (green)
depth of field for layer III				5 cm – 10 cm (UV)
depth of field for layer IV				10 cm – 20 cm (UV)
notes	calculations included in publication		calculations not published	calculations not published

Photoreceptors of the AME. A series of studies support the view that there are at least two different kinds of photoreceptor (bipolar *retinula* cells) in the salticid AME, a green-peak (~ 540 nm) receptor in the proximal layers I and II, and a UV-peak (~ 360 nm) receptor in the distal layers III and IV (Figure 35; Table 9; DeVoe & Zvargulis 1967; DeVoe 1975; Yamashita & Tateda 1976; Blest *et al.* 1981; Sivertsen 1989; Nagata *et al.* 2012; Terakita & Nagata 2014). DeVoe found receptors with both UV and green peaks, but this has not been corroborated in subsequent studies. Peaslee & Wilson (1989) observed movement of the AME in response to illumination of the retina of *Maevia inclemens* (Walckenaer 1837), and detected sensitivity in the range of 340-680 nm, with UV and green maxima, to agree with the findings of earlier studies. Similar receptor classes (Rh3 or Rh3/Rh4 peaking in UV, Rh1 and Rh2 or Rh2a peaking in the visible spectrum), as well as the nonvisual *peropsin*, have also been found in the AME of various salticids, based on studies of the distribution of opsins (proteins that become light sensitive after they bind with 11-cis-retinal to form rhodopsins) in the AME of *Habronattus ustulatus* (Griswold 1979), *Hasarius adansoni* and *Plexippus paykulli* (Audouin 1826) (Koyanagi *et al.* 2008; Kashiyama *et al.* 2009; Nagata *et al.* 2010, Morehouse *et al.* 2017b). The AME of the euophryine *Saitis barbipes* (Simon 1868) have both green-peak and UV-peak receptors, but may also have a third, blue-peak (~ 450 nm) receptor (Glenszczyk *et al.* 2022). Recent reports of *four* different color receptors in the eyes of peacock spiders (*Maratus Karsch* 1878b; Morehouse *et al.* 2017a; Shepeleva 2022) have not been substantiated.

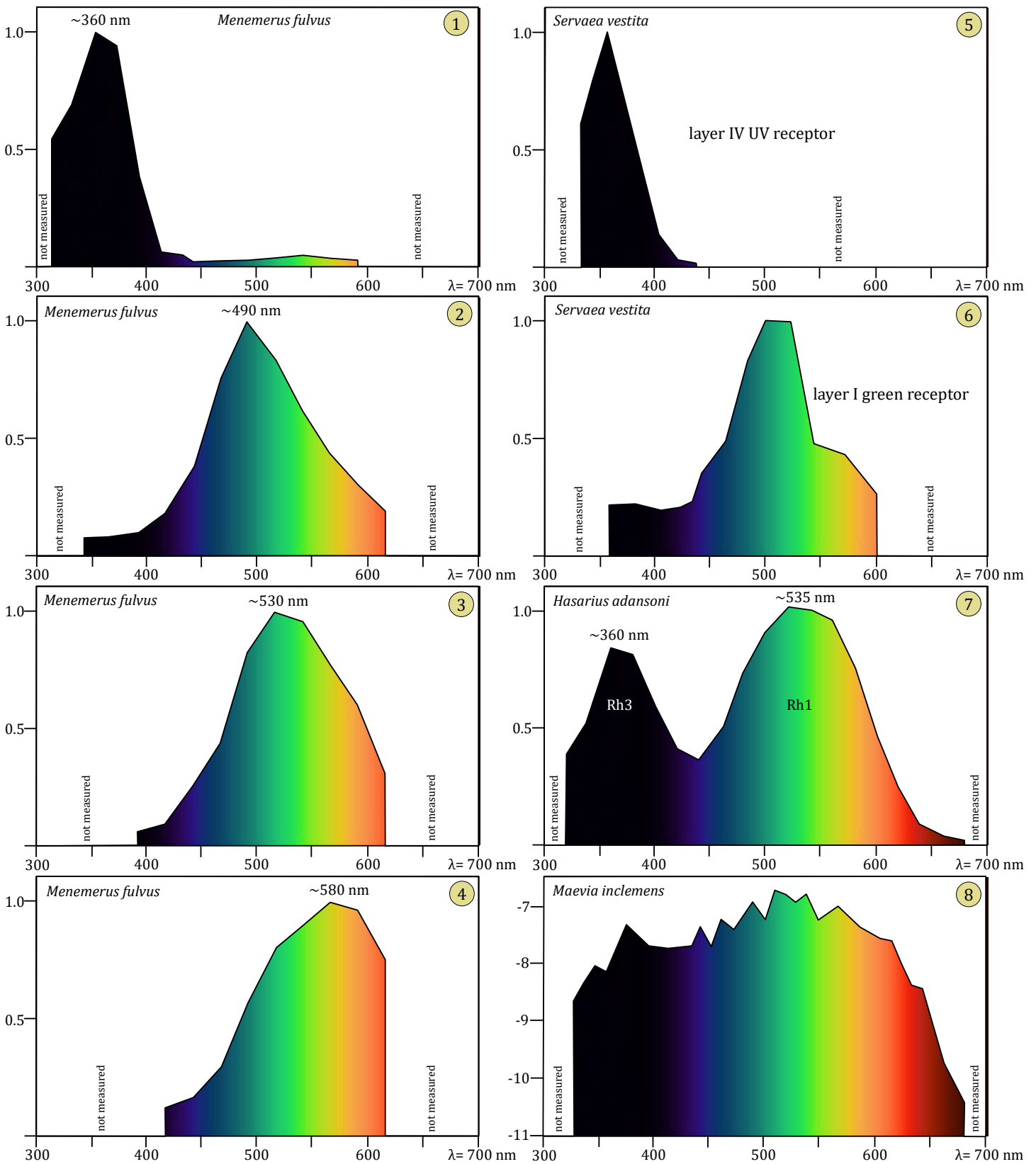


Figure 35. Relative spectral sensitivity (0.05-1.0) of photoreceptors in the AME of salticid spiders. **1-4**, Four receptor cells of *Menemerus fulvus* (L. Koch 1878), based on ERG (electroretinograms) of preparations subjected to a monochromatic light source, after Yamashita & Tateda 1976. **5-6**, UV (5) and green-peak (6) receptors identified in an ERG study of marked cells of *Servaea vestita*, after Blest et al. 1981. **7**, ERG of *Hasarius adansoni*, showing two peaks corresponding to a UV rhodopsin (Rh3) and a green-peak rhodopsin (Rh1), after Nagata et al. 2012. **8**, Log quantal spectral sensitivity of *Maevia inclemens*, based on observation of resultant eye movements under general infrared (>720 nm) illumination, after Peaslee & Wilson 1989.

Table 9. Receptor types associated with the AME of salticid spiders.

λ in nm		peak color	layer	opsin	species	method	references
peak	range						
~530	410–650	green	?	?	<i>Phidippus regius</i>	cell	DeVoe & Zvargulis 1967, DeVoe 1975
~370	350–460	near UV	?	?	C. L. Koch 1846	cell	DeVoe 1975
~360	320–410	near UV	?	?	<i>Menemerus fulvus</i>	cell	Yamashita & Tateda 1976
~490	390–620	blue-green	?	?		cell	Yamashita & Tateda 1976
~530	410–610	green	?	?		cell	Yamashita & Tateda 1976
~580	410–610	orange	?	?		cell	Yamashita & Tateda 1976
~360	330–410	near UV	IV	?		<i>Servaea vestita</i>	marked cell
~500	410–575	blue-green	II	?	marked cell		Blest et al. 1981
~540	400–600	yellow-green	II	?	marked cell		Blest et al. 1981
?	340–490	?	?	?	<i>Maevia inclemens</i>	saccades	Peaslee & Wilson 1989 (inferred from adaptation)
~535	410–700	green	?	?		saccades	Peaslee & Wilson 1989
?	480–640	?	?	?	<i>Phidippus</i> spp.	interneuron activity	Sivertsen 1989
?	?	near UV	?	Rh3	<i>Plexippus paykulli</i>	RNA	Koyanagi et al. 2008
?	?	blue	?	Rh2		RNA	Koyanagi et al. 2008
?	?	green	?	Rh1		RNA	Koyanagi et al. 2008
~360	320–420	near UV	III or IV	Rh3	<i>Hasarius adansonii</i>	RNA, IF, ERG	Koyanagi et al. 2008, Nagata et al. 2012
?	?	blue	?	?		RNA	Koyanagi et al. 2008
~535	450–650	green	I or II	Rh1		RNA, IF, ERG	Koyanagi et al. 2008, Nagata et al. 2012
?	?	near UV	?	Rh4		RNA	Nagata et al. 2012

Other studies have found similar UV and green maxima in the AME of the lycosid *Hogna* (DeVoe, Small & Zvargulis 1969; DeVoe 1972) and the thomisid *Misumena* (Defrize et al. 2011). Three classes of retinula (receptor) cell have been identified with intracellular recordings from the AME of the araneid *Argiope*: 360 nm peak UV, 480-500 nm peak blue, and 540 nm green (Yamashita & Tateda 1978; Yamashita 1985). Opsin gene sequencing supports the hypothesis that the origin of these receptor classes found in the Araneae precedes the separation of Chelicerata from Pancrustacea (Pichaud, Briscoe & Desplan 1999; Koyanagi et al. 2008; Morehouse et al. 2017b).

Recently a relatively thick (~10-15 μm from front to back) cluster of pigment granules has been described near the center of the AME retina of five species of *Habronattus* F. O. Pickard-Cambridge 1901, between layers I and II (Zurek et al. 2015; Morehouse et al. 2017b). This pigment selectively transmits red light (>600 nm) and filters out almost all light at or near the peak sensitivity (500-600 nm) of the green receptors associated with layers I and II of the retina. Except for the transmission of red light, this pigment is almost as effective as the surrounding black pigment granules in blocking the passage of scattered light. It has been hypothesized (Zurek et al. 2015) that this acts as a red filter in front of some of the layer I receptors, in effect providing a third class of spectral receptor as well as, coupled with the UV-peak and green-peak receptors, trichromatic vision. However, spectral sensitivity of the layer I receptors proximal to this pigment has only been estimated (Zurek et al. 2015, fig. 1), not measured directly, and the pathway of incoming light through this pigment to specific receptors has not been documented. The possible role of light guides in transmission to this deep part of the retina must be considered. Almost-complete blocking of light to part of the highest-resolution receptor array of the AME would be a high price to pay for trichromatic vision, given that the UV sensitivity is possible with a much smaller group of distal receptors. Intervening pigment granules in this cluster would not support image resolution by the underlying receptors of layer I, and thus the proximal plane of focus for red light might not be an important factor in the placement of a red filter.

The front eyes of salticids are often colored in a manner that suggests diffraction by either the surface or by layers of the corneal cuticle, with a possible role in glare reduction (Figure 36). Foelix & Erb (2011) found parallel ridges on the eyes of *Phidippus regius* that might account for diffraction. These colors are most evident when these spiders are viewed under diffuse lighting. A study of 128 species of salticids (Hu et al. 2012; Figure 37) showed that the corneal lens of the salticid AME transmitted light within the full range of these sensors, but also found some variation in UV transmission that could have relevance with respect to microhabitat.



Figure 36. Front eyes of four salticids from Oklahoma. **1**, Male *Phidippus otiosus* (Hentz 1846). **2**, Male *P. mystaceus* (Hentz 1846). **3**, Male *Maevia inclemens*. **4**, Male *Zygoballus rufipes* Peckham & Peckham 1885. Diffraction at the surface of the cornea is most evident with diffuse illumination or natural lighting. Photographs ©Thomas Shahan, used and modified under a [CC BY 2.0](https://creativecommons.org/licenses/by/2.0/) license.

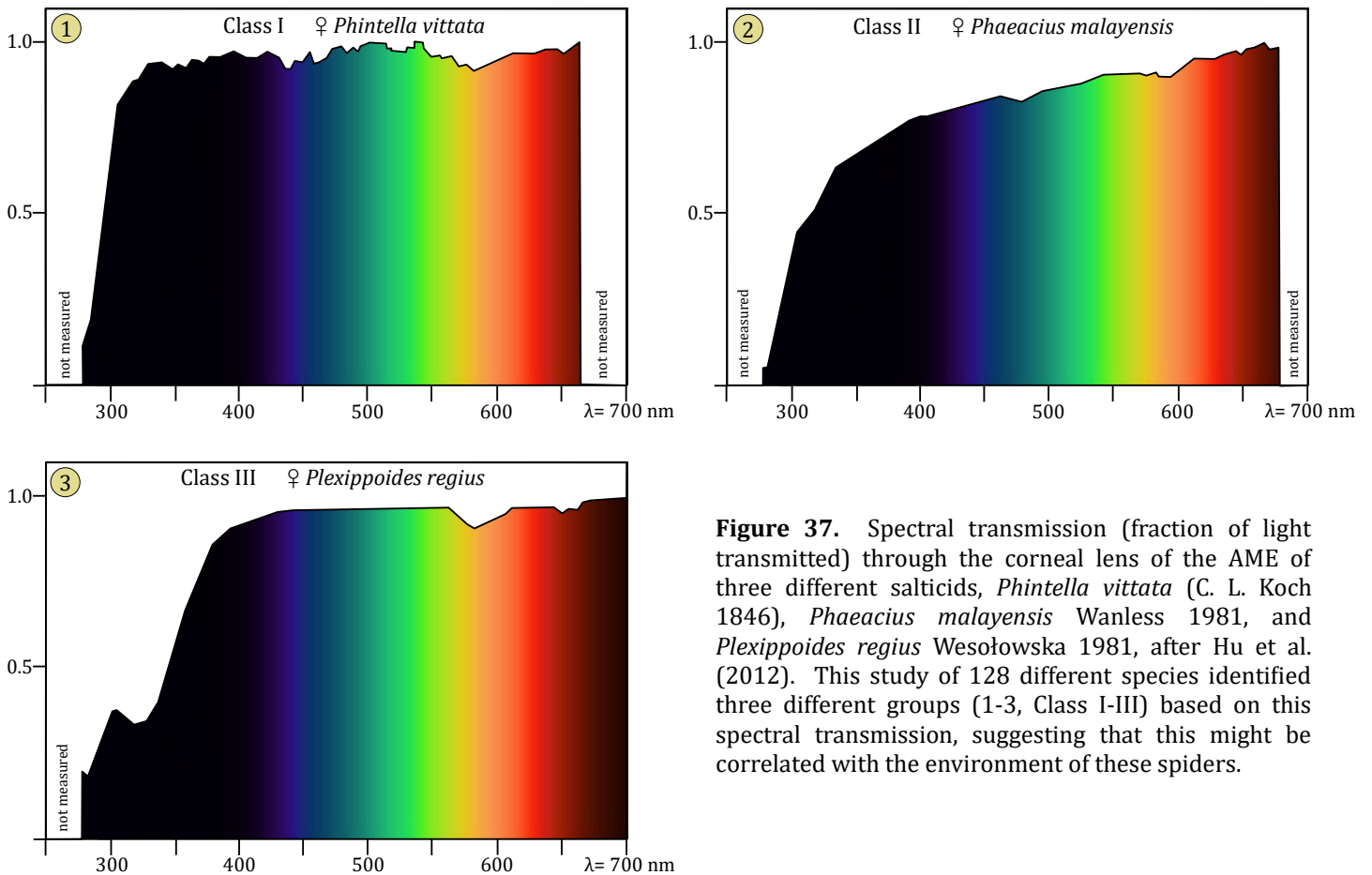


Figure 37. Spectral transmission (fraction of light transmitted) through the corneal lens of the AME of three different salticids, *Phintella vittata* (C. L. Koch 1846), *Phaeacius malayensis* Wanless 1981, and *Plexippoides regius* Wesolowska 1981, after Hu et al. (2012). This study of 128 different species identified three different groups (1-3, Class I-III) based on this spectral transmission, suggesting that this might be correlated with the environment of these spiders.

Color vision. Given that many salticids appear to have only two spectral classes of photoreceptor (S, or UV-peak, and M, or green-peak) questions related to the use of color by these often very colorful spiders have received considerable interest (e.g., Kästner 1950; Nakamura & Yamashita 2000; Zurek et al. 2015; Glenszyck et al. 2022). To understand the neurology behind the *perception* of color, it is useful to examine our own subjective experience of this phenomenon, and related research.

Humans differ from most mammals in that we have evolved a third spectral class of color receptor or *cone*, associated with what we call *trichromaticity* (Figure 38). In addition to our three classes of cones (S, M and L), our rods also have the potential to contribute to our perception of color, with a peak sensitivity (~498 nm) that is intermediate between the S and M cones. In addition, the ganglion cells at the front of our retina contain photosensitive melanopsin, with a peak-sensitivity between the S cones and the rods. A great deal of spectral data could be collected by our eyes, yet much of the processing of receptor activity appears to follow the theme of data extraction and simplification.

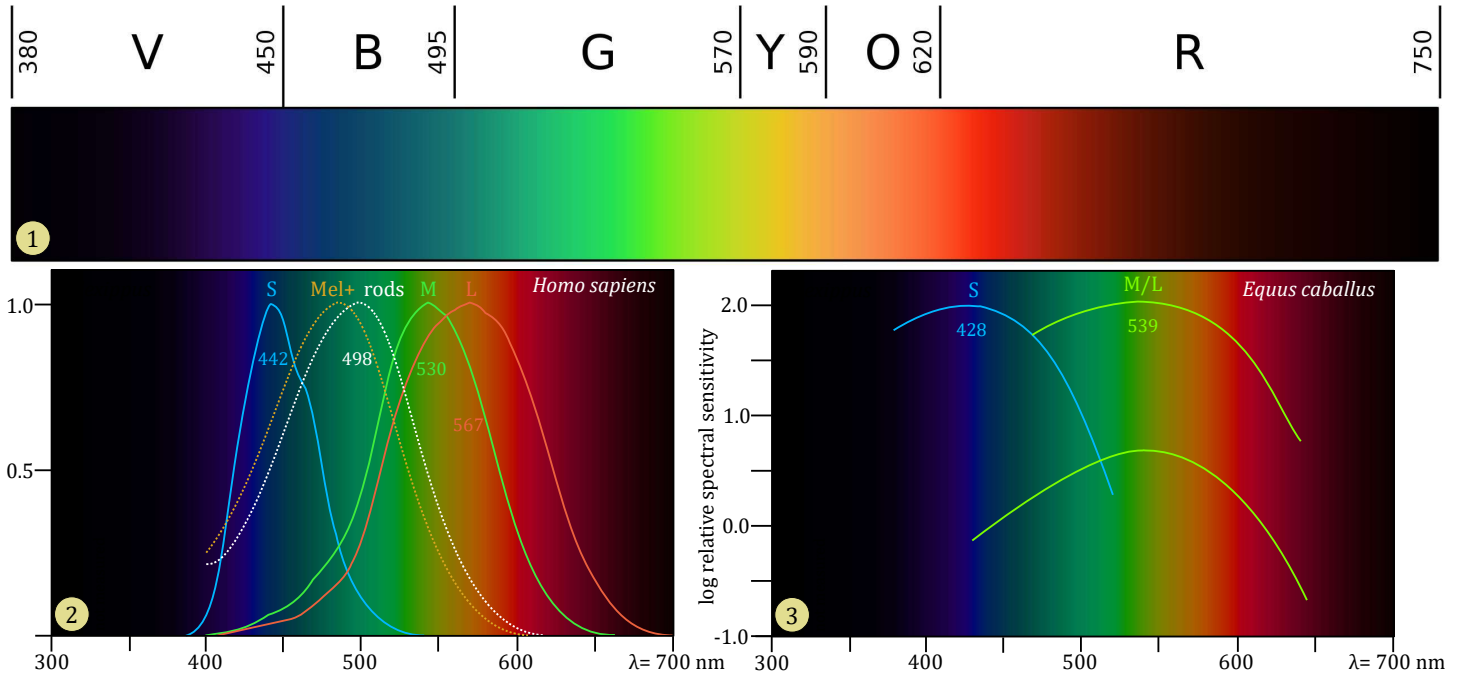


Figure 38. Our familiar spectrum. **1**, Calibrated spectrum. The range of each color (V-R) in the top line varies by individual. **2**, Relative spectral sensitivity of our three cones (S-opsin, M-opsin, L-opsin), rods (Rhodopsin), and ganglion cells (Mel+, Melanopsin) (after Patterson, Neitz & Neitz 2021). **3**, Log relative spectral sensitivity of the two spectral classes of cone of a horse, based on electroretinogram flicker photometry (after Carroll et al. 2001). The lower M/L curve was obtained by suppression of the M/L peak to improve recording of the S peak. Background colors shown here reflect the corresponding human spectrum, and should not be taken as an interpretation of the *perceptual color space* of the horse, a *dichromat*.

The actual *perception* of color, or spectral hue, can only be understood at present on a subjective basis. The data collected by only two spectral classes of receptor (*dichromaticity*) could be translated into many different color (*chromatic*) spaces, depending on how it is processed (Figure 39).

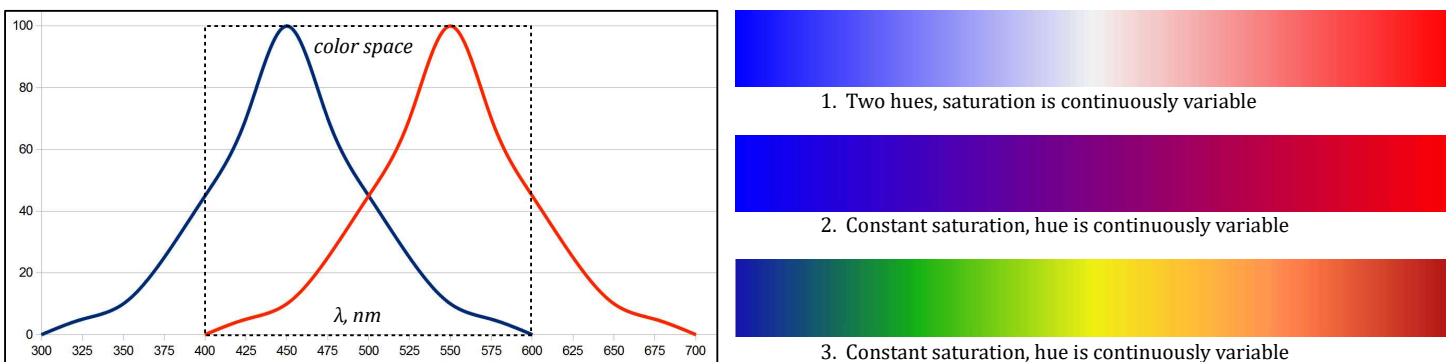


Figure 39. The overlap between a single pair of wavelength-sensitive receptors (at left) could translate into a virtually unlimited number of one-dimensional *color (chromatic) spaces* (examples 1-3, at right). At least in part this is due to the way that receptor activity is regulated and processed. Example (1) has an *achromatic neutral point* (white), at center.

In practice, determination of perceived *color space* for a dichromat is a challenge, but there is support for the view that this represents a continuous color spectrum (Figure 39, examples 1 and 2) and it is *not* interrupted by a *neutral point* (Figure 39, example 3) in the horse *Equus caballus* L. (Roth, Baleknius & Kelber 2007). Even for trichromatic humans, there is considerable variation in the wavelength that people will identify as a *true color* (blue, green, yellow or red; Kuehni 2004).

Much research has been directed toward elucidation of the neurological process behind color vision in mammals, and in primates like our own species in particular. Whereas only the bipolar (AME) or unipolar (secondary eyes) receptors pass through the salticid retina, in vertebrates the activity of receptors is modified by many different interneurons comprising four different classes (Figure 40).

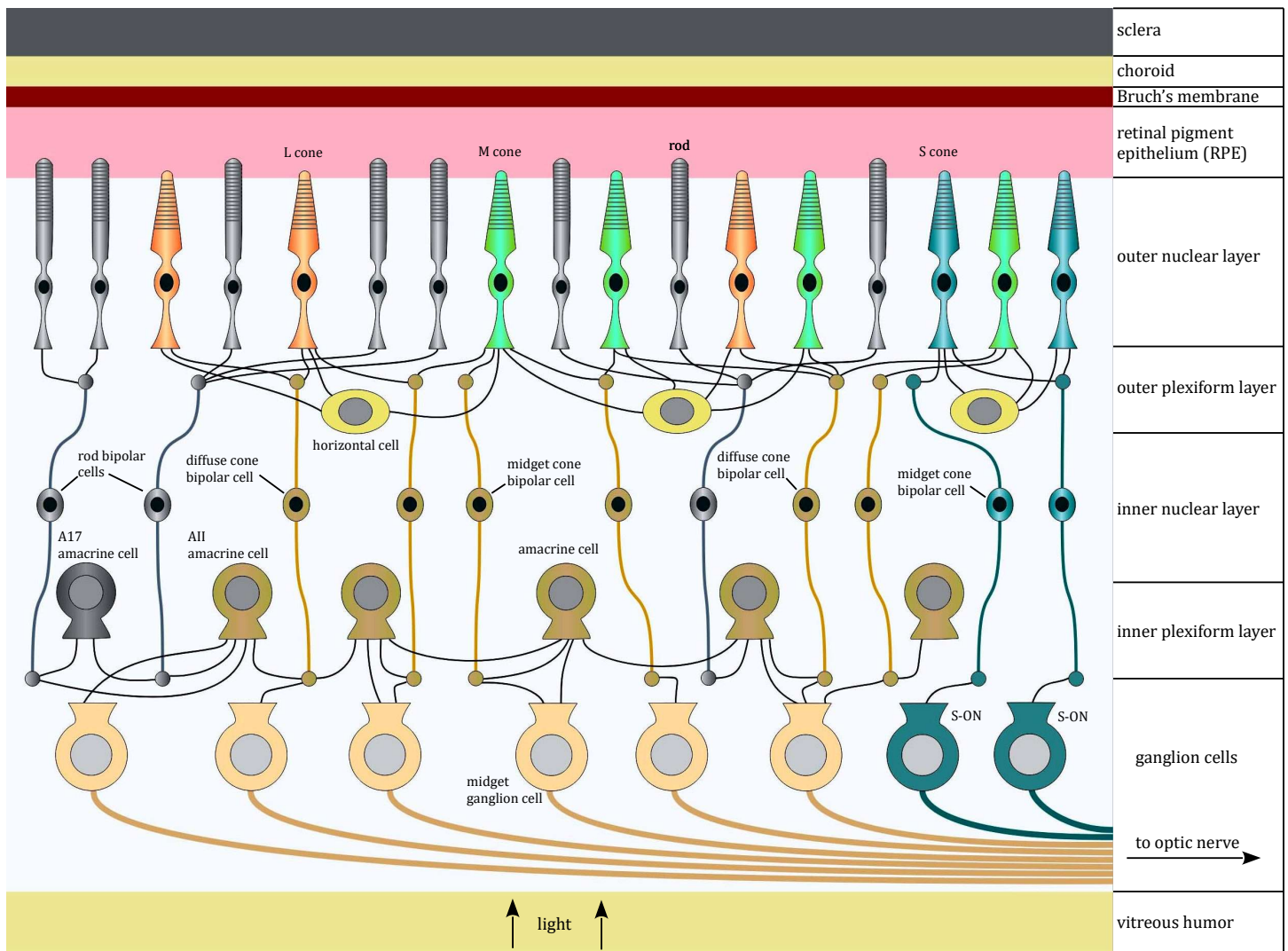


Figure 40. Schematic view of receptors (cones and rods, at the top) and interneurons in the retina of a trichromatic primate (after Masland 2001, 2011; Surrige, Osorio & Mundy 2003; Solomon & Lennie 2007; Winkler 2010; Field et al. 2010; Nakano et al. 2014; Behrens et al. 2016; Toreson & Dacey 2019; Johnson & Winlow 2019; Patterson, Neitz & Neitz 2021). Receptors interact with both ON (active when receptor is depolarized by light and withholds glutamate) and OFF bipolar cells (activated by glutamate), which then interact with ganglion cells, the axons of which comprise the optic nerve. A variety of horizontal cells collect input from surrounding receptors and modify the behavior of bipolar cells (Chaya et al 2017). There are many different kinds of amacrine cells, with many special functions (Masland 2011; Chen & Li 2013; Yan et al. 2020). These modify the output from bipolar cells to the ganglion cells. The A17 amacrine cell only communicates between rods. The AII amacrine cell relays the activity of rod bipolar cells to ganglion cells. Many bipolar and ganglion cells are dedicated to single cones, and these groups of cells are called a *midget system*. Note that light must pass through all layers of the vertebrate retina before it reaches the receptor cells. Passage of light through the retina is assisted by large Müller cells, neuroglia that act as wave guides.

Two frequently-cited models for the color process of humans are *trichromatic theory* (Young 1802; Wu 2010) and *opponent process or color-opponent theory* (Hering 1964; Shapely & Hawken 2002; Solomon & Lennie 2007; Schmidt, Neitz & Neitz 2014; Thoreson & Dacey 2019). Recent versions of trichromatic theory suggest that signals sent to the brain over the optic nerve contain the signals corresponding to each of the three spectral classes of cones (S, M, L), much like RGB (red, green, blue) encoding in modern information systems. Opponent process theories are usually based on the idea that signals from these cones are compared within the retina, and the color information that is passed to the brain is the result of this comparison (Figure 41).

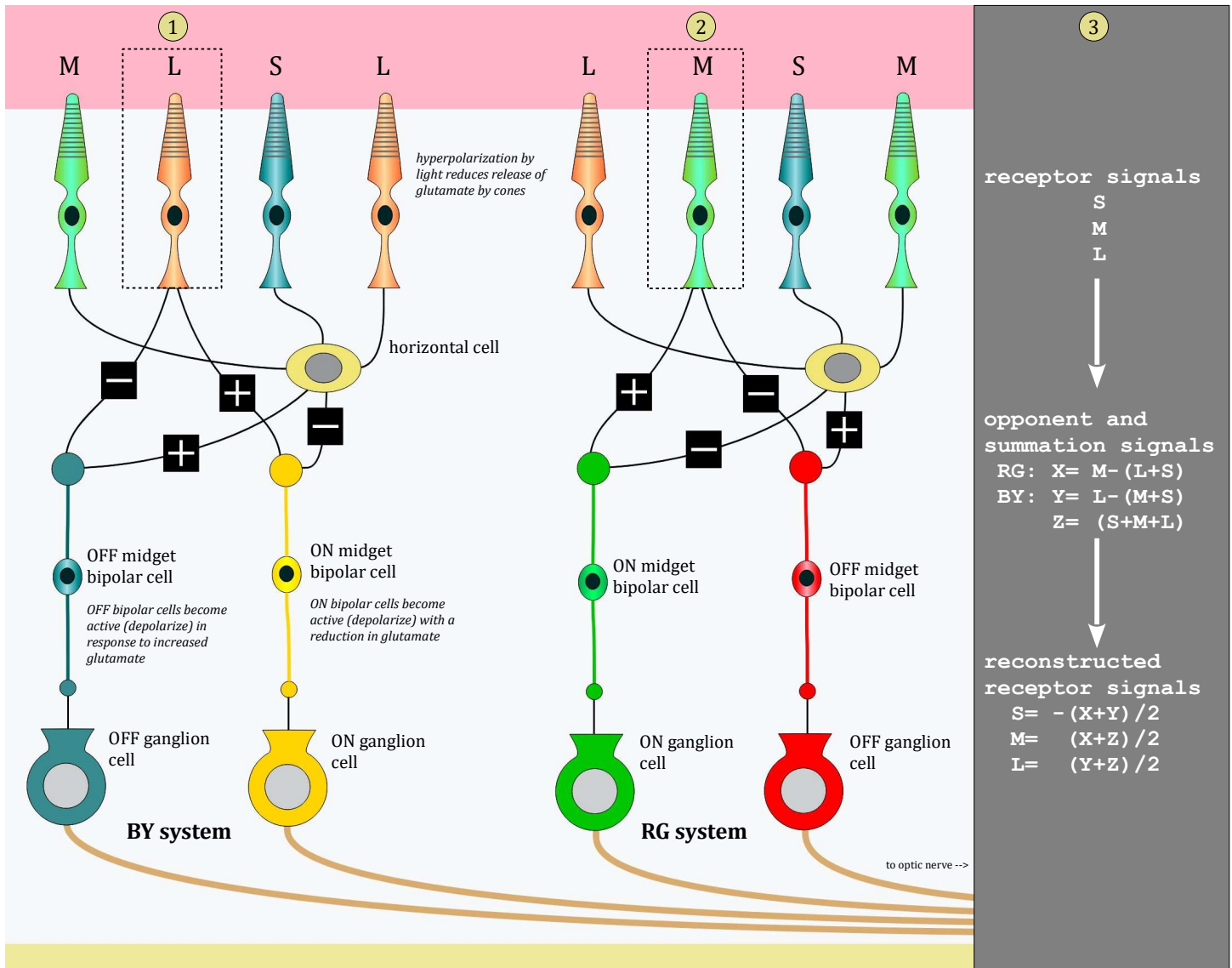


Figure 41. Retinal opponent process theory of human color vision, after Schmidt, Neitz & Neitz 2014. This is a variation on the *standard model of color vision and opponent color process* (Pridmore 2013). **1**, In the blue-yellow (BY) system, hyperpolarization of an L-cone (outlined) by light leads it to reduce its output of glutamate, activating an ON bipolar cell that produces a "yellow" signal, as it deactivates an OFF bipolar cell that would otherwise produce a "blue" signal. These actions are opposed by horizontal cells that collect output of surrounding cones of all three types (S, M, L). **2**, In the red-green (RG) system, hyperpolarization of an M-cone (outlined) by light leads it to reduce its output of glutamate, activating an ON bipolar cell that produces a "green" signal, as it deactivates an OFF bipolar cell that would otherwise produce a "red" signal. These actions are opposed by horizontal cells that collect output of surrounding cones of all three types (S, M, L). **3**, Although opponent color processing might explain certain psychoperceptual phenomena, addition of a total activity or illuminance signal (Z) to two opposition signals (X, Y) would provide all of the information required for the cerebral cortex to reconstruct each of the original signals (S, M, L). However, these signals do not correspond to our perceptions of *true color*.

Since the terminals of the AME receptors appear to map on a 1:1 basis with the synaptic capsules of AM1, and no retinal interactions of these receptors are known (Land 1969a; Hill 1975, 2006; Oberdorfer 1975), we need to look to the connectivity and physiology of the downstream neuropiles (AM2, AM3) to determine what kind of color processing might be relevant for salticids. Oberdorfer (1975) described the encapsulated triad synapses of AM1, arranged in a space-filling hexagonal array that resembles the arrangement of the receptor segments in each layer of the retina. Nagata, Arikawa & Kinoshita 2019, in their mapping of AME receptor layers to AM1 zones (Figure 22:5), described the presence of lateral processes between AM1 terminals of lateral layer II-IV UV-peak receptors (TZ3) and layer I receptors (TZ1), interneurons connecting terminals of layer I with terminals of layer II, interneurons branching within a single terminal zone, and interneurons with branches throughout the AM1 neuropile. We presently do not know enough to draw any conclusions about the role of these structures in color processing.

Retinal tiering. Since the pioneering work of Michael F. Land (1969a), the role of retinal tiering of the AME with respect to the vision of salticid spiders has represented one of the most challenging and worthwhile questions addressed by salticid biologists (Table 10).

Table 10. Some hypotheses related to the function of retinal tiering in the salticid AME.

#	hypothetical function	references	notes/issues
1	increase ability of eye to capture light	Land 1969a; Cerveira, Jackson & Nelson 2019	Combination of in-focus and out-of-focus images would degrade the available information. Might explain behavior in dim light.
2	accommodation for focus of objects at variable distance	Land 1969a, 1985b; Blest et al. 1981; Yamashita 1985	No other method for accommodation is known, but rotation of eyes or use of lateral portions of the retina might also change the distance of the retina from the corneal lens.
3	support simultaneous focus on receptors with different spectral sensitivity by placing these in different layers (correct chromatic aberration)	Land 1969a, 1985b; Blest et al. 1981; Yamashita 1985; Peaslee & Wilson 1989	Only one receptor type (green-peak) has been found in layers I and II, but placement of UV receptors in layers III and IV is consistent. But a single layer might be sufficient for focus from infinity to 2.8 cm in distance (Land 1969a).
4	e-vector (polarization) detection by exposed layer IV	Land 1969a; Dacke et al. 2001	No behavioral evidence that salticids can use polarization of sky light (the e-vector) to determine map direction (Land 1969a; Hill 1978, 1979, 2010a)
5	estimate distance through monocular comparison of focus at layers I and II (<i>depth of focus cues</i>)	Sivertsen 1989; Nagata et al. 2012; Terakita & Nagata 2014; Nolte 2015; Nolte et al. 2017	Spectral hue could also alter focal length of the eye, confusing color with distance. Computer models can model the proposed mechanism if light is collected from the entire thickness of each layer of the retina (Nolte 2015; Nolte et al. 2017).
6	increase receptor density and effective resolution using wave guides to layer I	(this paper)	Evaluation requires more detailed study of fine structure at the cellular level. Statistical sampling has not been considered in previous studies.
7	high resolution in both dim (with layer II) and bright (with layer I) light	(this paper)	If screened by photopigments of layer II, layer I might operate better in bright light.
8	resolve spectral hue through comparison of focus at layers I and II	(this paper)	Degree of focus could specify hue within the range of the green-peak receptors, from blue to red.
9	resolve spectral hue through selective reduction of spectral sensitivity of layer I relative to layer II	(this paper)	If layer II serves as an effective waveguide for light en route to layer I, or otherwise affects the passage of light to layer I receptors in a wavelength-specific manner, then a comparison of activity between layer I and layer II receptors could provide detailed resolution of color across a wide spectrum (Figure 42).

The hypothetical functions listed in Table 10 are not exclusive. There is good support for the hypothesis that a *single* AME can be used to establish the distance of an object. Land (1969a) was the first to describe the relationship of object distance to focal plane in the tiered retina. Later Sivertsen (1989) identified some interneurons *behind* the central body that exhibited *size-constancy* (firing based on absolute size, rather than the angle subtended by, an object) in response to objects visible to a single AME, and proposed that this was sufficient to determine the distance of an object. Sivertsen also found cells with angular-constancy, and positional (directional) constancy. More recently, Nagata et al. (2012) presented essentially the same hypothesis (*image defocus*) in their study of *Hasarius adansonii*, based on a difference in focus between green-peak receptors layers I and II of the retina. However, limited behavioral evidence presented by Nagata et al. was not convincing and more extensive experimentation of this kind is needed. They reported a slight improvement in the accuracy of short-range (0.7-3.7 cm distance) jumps to capture small prey under monochromatic (~520 nm) green light, when compared to

jumps illuminated by monochromatic (~630 nm) red light, with some of the jumps under red light short of the target by a fraction of a cm. For many salticids, these jumps would be very short, of the kind that they may even be able to complete accurately in darkness (see Taylor, Jackson & Robertson 1998). But in the absence of the binocular vision provided by the ALE, there are several other known methods by which a salticid, like ourselves, could estimate distance, to include perspective relative to other objects in the visual field, and previous familiarity with the absolute size of the object. I have observed that salticids routinely fed on small flies in the laboratory often jump far short of the target when first presented with a larger fly at a distance that subtends a similar angle. This anecdotal observation deserves more study.

To increase spectral resolution at the long-end of the spectrum (Table 10, hypothesis 9), it may not be necessary for a salticid to have a pigmented filter that selectively blocks some of the AME layer I receptors, as has been proposed for *Habronattus* (Zurek et al. 2015; Morehouse et al. 2017b). Since layer II blocks the visibility of layer I for an observer (Land 1969a), it is also quite possible that alignment of receptors in layers I and II allows the shorter layer II receptors to selectively reduce the passage of the wavelengths near the green-peak to which they are most sensitive, effectively altering the spectral sensitivity of the longer layer I receptors (Figure 42). Comparison of activity in corresponding layer I and layer II receptors (Figure 42:4), combined with the activity of the UV-peak receptors of layers III and IV, would then allow the salticid to resolve colors across a wide spectrum.

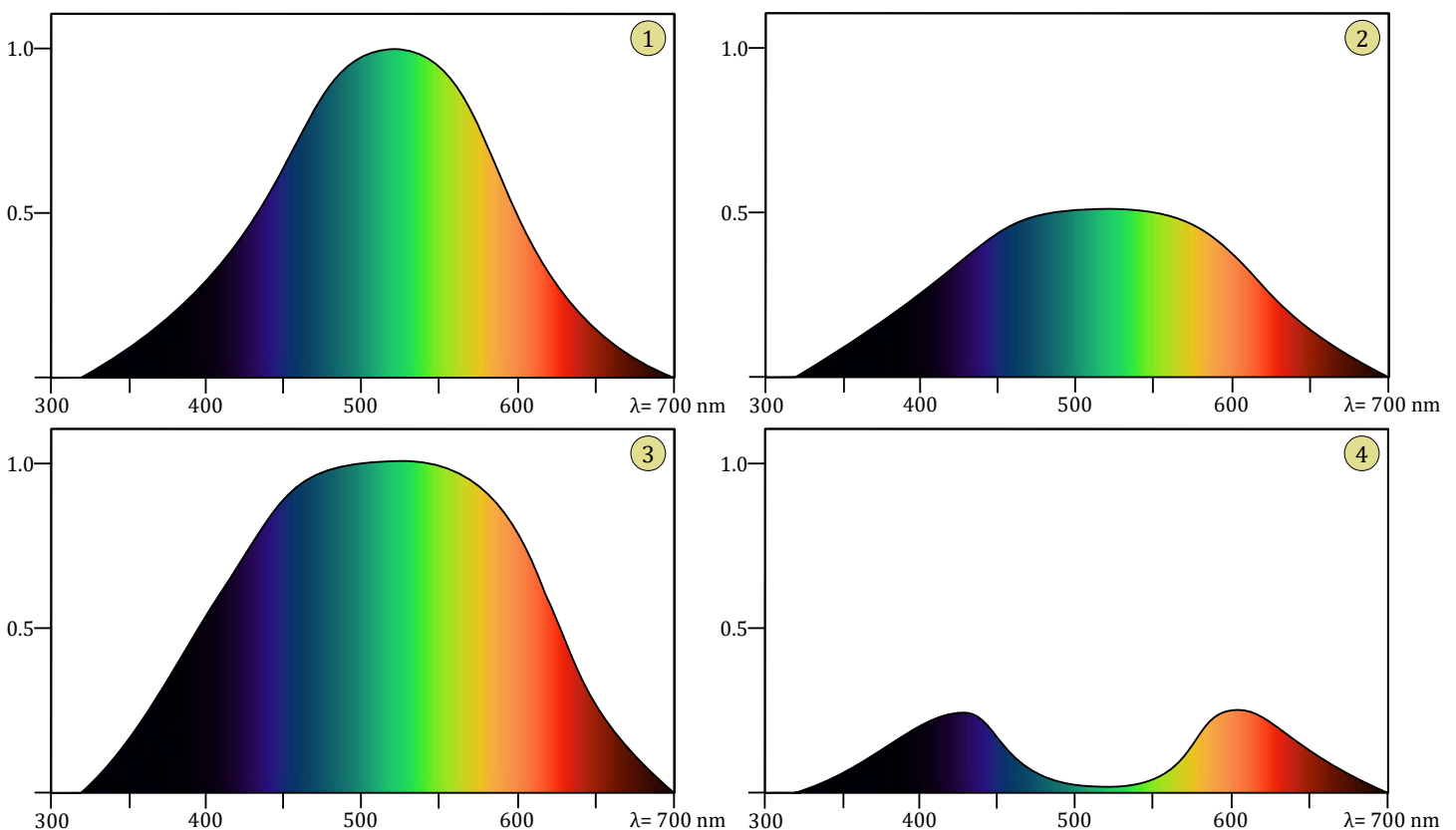


Figure 42. Resolution of spectral hue through two tiers of receptors with the same measured spectral sensitivity (Table 10, hypothesis #9). **1**, Relative spectral sensitivity (hypothetical) of a single receptor at each tier. **2**, Reduced spectral sensitivity of the underlying (layer I) tier after selective removal of 50 percent of the incoming light in proportion to the spectral sensitivity of the overlying (layer II) tier. This assumes that the wavelengths to which overlying receptors are most sensitive are filtered to a proportionately greater extent by those receptors. **3**, Resultant relative spectral sensitivity of the underlying receptors, reflecting the selective removal of light near the green peak. **4**, Difference between (1) and (2), providing a basis for the neurological resolution of color in both the S (blue) and L (red) ends of the spectrum. Ambiguity between the S and L signals could be resolved through an additional comparison with S (or near UV-peak) receptors in overlying layers III and IV, where that part of the spectrum is relatively unfiltered.

The AME are *scanners* with a narrow visual field. This implies several things. Any part of an object that is viewed can be scanned with multiple parts of the retina (Figure 43). Given that layers I and II occupy more than a single plane of focus, many of the functions associated with retinal tiering could also be associated with comparison of information collected from different parts of the retina. For example, functional hypothesis #8 (Table 10) could relate to a greater sensitivity of the larger peripheral receptors (associated with dorsal and ventral extensions of the retinae), particularly since the aperture of the eye is fixed.

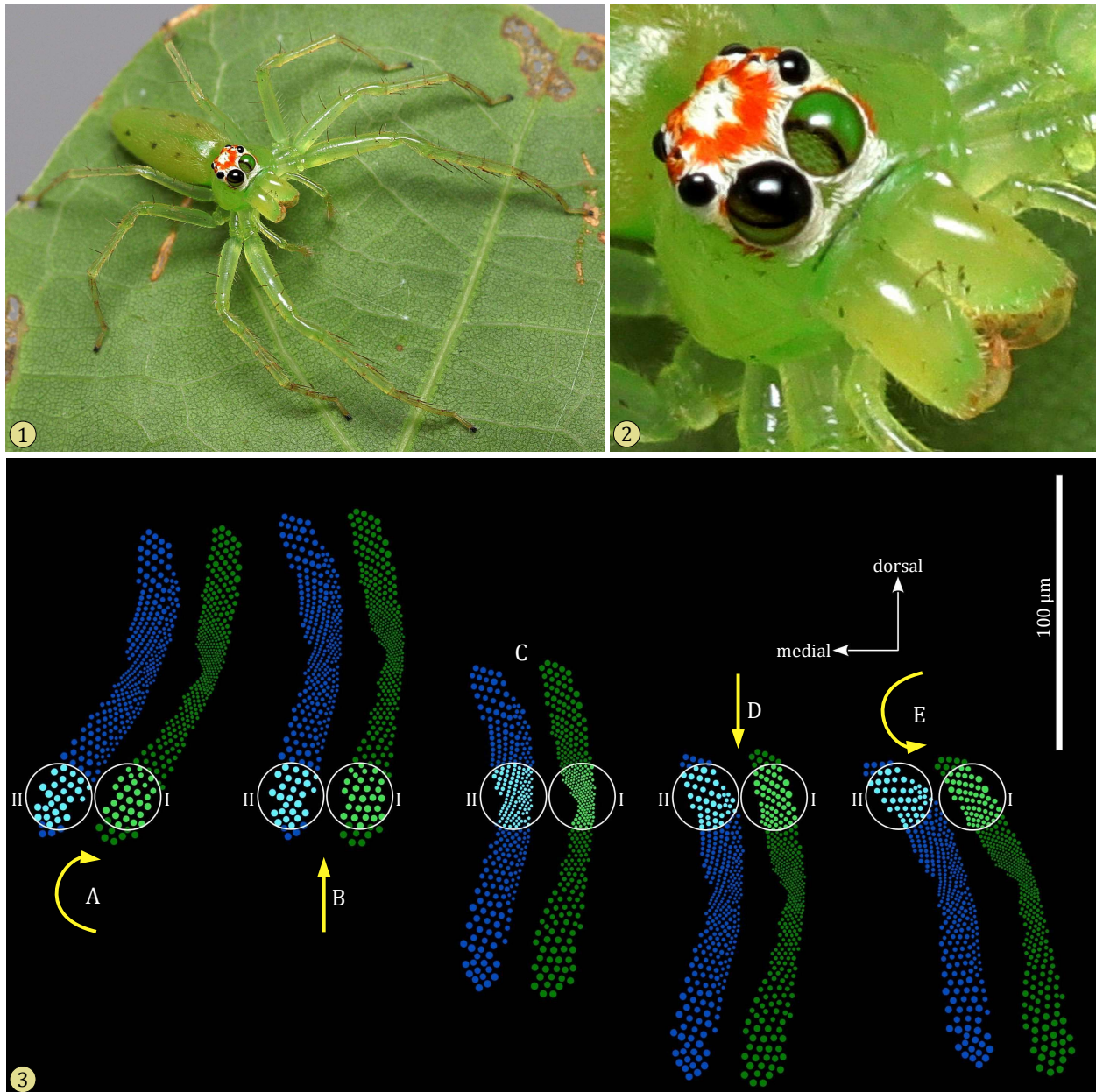


Figure 43. Different AME receptors can be used to evaluate the same object. **1**, Adult female *Lyssomanes viridis* from South Carolina. **2**, Detail from (1), showing focus on large, peripheral layer II receptors of the left AME. **3**, Various scanning positions of the retina of the left AME of a *Pelegrina aeneola* (anterior view, after Land 1969a). Layers I (green) and II (blue) are shown separately, although in an actual view they would overlap and only layer II is visible with an ophthalmoscope. From a centered position (C), retinae can be moved up or down to scan an object (circle) with arrays of larger, peripheral receptors (B, D), or rotated (A, E) to alter the scanning pattern.

Resolution of detail by the AME. The psychoperceptual experiments used to evaluate visual acuity (cycles per degree, or CPD) in mammals have not been conducted with salticids. For purposes of comparison we measure the angular separation of their receptors, multiplying this number by a factor of 2 to estimate the CPD. For a more meaningful comparison we can then consider how many lines they can resolve at the near point (NP) of their accommodation, which is much closer than that of larger animals. This has generally been estimated at about 2-3 cm (e.g., Blest, McIntyre & Carter 1988). Here, considering M. F. Land's (1969a) observation that *the image will be only slightly out of focus at much shorter distances*, I have used 1.5 cm for the NP of three salticid species. The result (Table 11, Figure 44) reveals that salticids can see a great deal of detail.

Table 11. Estimated visual acuity for various animals. For the salticids shown here (*Phiale*, *Phidippus*, *Portia*), estimates refer to layer I of the AME, at the fovea. Values calculated from numbers provided in the reference column are shown in parentheses. NP= near point of accommodation.

animal	visual acuity		accommodation		resolution at NP ~(NP)sin(1/CPD) mm	lines/mm at NP	references
	receptors/°	cycles/° (CPD)	D (diopters)	near point (NP) cm			
<i>Haliaeetus leucocephalus</i>		140-142 (141)	6.8	15	0.019	54	Reymond 1985; Glasser et al. 1997; Caves & Johnsen 2017; Martin 2017
<i>Bubo</i> sp.		17	2	50	0.513	2	Fite 1973; Martin & Gordon 1975; Glasser et al. 1997; Martin 2017
<i>Canis lupus</i>		8	2-3 (2.5)	40	0.873	1	Miller & Murphy 1995; Miller 2001
<i>Panthera leo</i> (photopic)		13.02	2.5	(40)	0.536	2	Bloom & Berkley 1977; Melin et al. 2016
<i>Homo sapiens</i>		60	10	10	0.029	34	Melin et al. 2016; Hashimi et al. 2019
<i>Phiale guttata</i> (C. L. Koch 1846)	26.09	(13.05)		(1.5)	0.020	50	Blest 1985
<i>Phidippus johnsoni</i>	7.5	(3.75)		(1.5)	0.070	14	Blest, McIntyre & Carter 1988
<i>Portia fimbriata</i>	24.69	(12.35)		(1.5)	0.021	47	Williams & McIntyre 1980; Blest & Price 1984

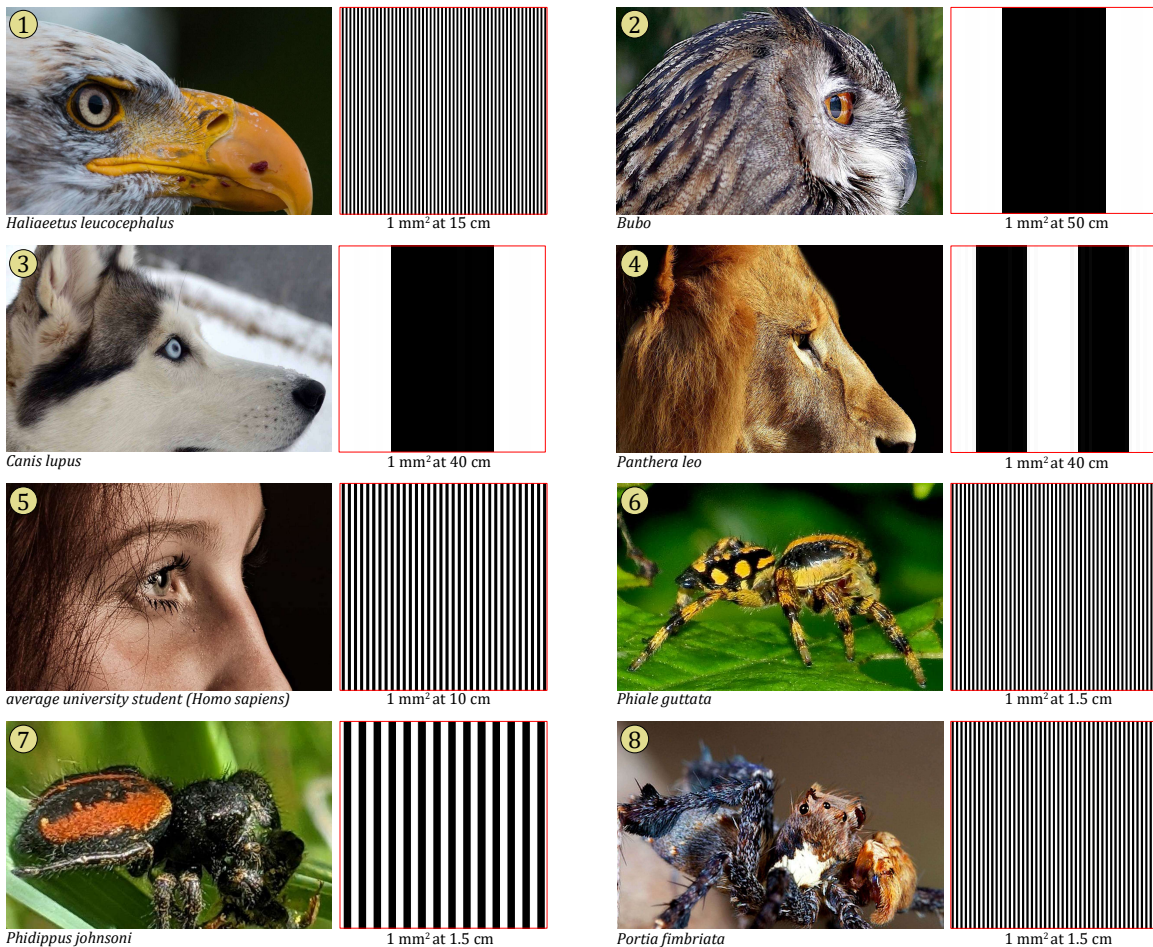


Figure 44. Visual acuity (black+white lines per mm²) of some animals at their near point of accommodation, based on estimates shown in Table 11. Photo credits (both edited): 6, ©Sarab Seth, used under a [CC BY-NC 4.0](https://creativecommons.org/licenses/by-nc/4.0/) license; 8, ©Jürgen Otto, used with permission.

Higher visual acuity is associated with diurnality (Veilleux & Kirk 2014), and the nocturnal animals shown here (Figure 44: 2-4) have relatively low acuity, even under daylight (photopic) conditions. Salticids have been viewed as *eight-legged cats* (Harland & Jackson 2000) but, as shown here, they are quite unlike those nocturnal predators with respect to their reliance on detailed imaging in daylight.

The estimate of visual acuity shown here for *Phidippus johnsoni* is probably low, as the orientation of receptors of layer I suggests much more divergence and corresponding magnification at the foveal pit (Blest, McIntyre & Carter 1988). In addition, the upper and lower extensions of the AME retina of salticines (e.g., *Phiale*, *Phidippus*), unlike those of spartaeines (e.g., *Portia*), are deeply furrowed or convexiculate, suggesting an adaptation for more divergence and higher visual acuity for these parts of the retina (Blest 1985). The estimated 2:1 relationship between the count of receptors and the count of units (lines) may not be accurate, as we know nothing about the related processing of information in the AM1 and AM2 ganglia. When certain objects are observed, statistical sampling across multiple rows of receptors through downstream processing could result in *hyperacuity* (Figure 59; Westheimer 1981, 2010; Geisler 1984; Poggio, Fahle & Edelman 1992), up to an order of magnitude greater than one might expect.

Visual illusions can give us much insight into our own processing of visual information, but they can be very difficult to interpret. They are much more than the entertainment that they provide to us. The challenge with respect to our study of salticid vision lies in finding illusions that work with these spiders in predictable ways. If we do find these, then we can try to elucidate the reasons that they work. We will need to know much more about the salticid retina, but even more about the kind of processing that takes place with the interneurons that synapse with the receptors, and the interneurons that, in turn, synapse with those interneurons. Simple optical illusions like those shown in Figure 45 have already been used in the study of both the honeybee *Apis mellifera* (Davey, Srinivasan & Maddess 1998; Howard et. al 2017) and the fruit fly *Drosophila melanogaster* (Tuthill, Chiappe & Reiser 2011). Illusions that work on our own species may not work on other species in the same manner (Becker, Prasad-Shreckengast & Byosiere 2021). But we should also be able to find visual illusions that fail with humans but are quite effective with certain kinds of jumping spiders, for example illusions (still or animated) that relate to prominent visual features of the salticid courtship display (e.g., Figure 49:1).

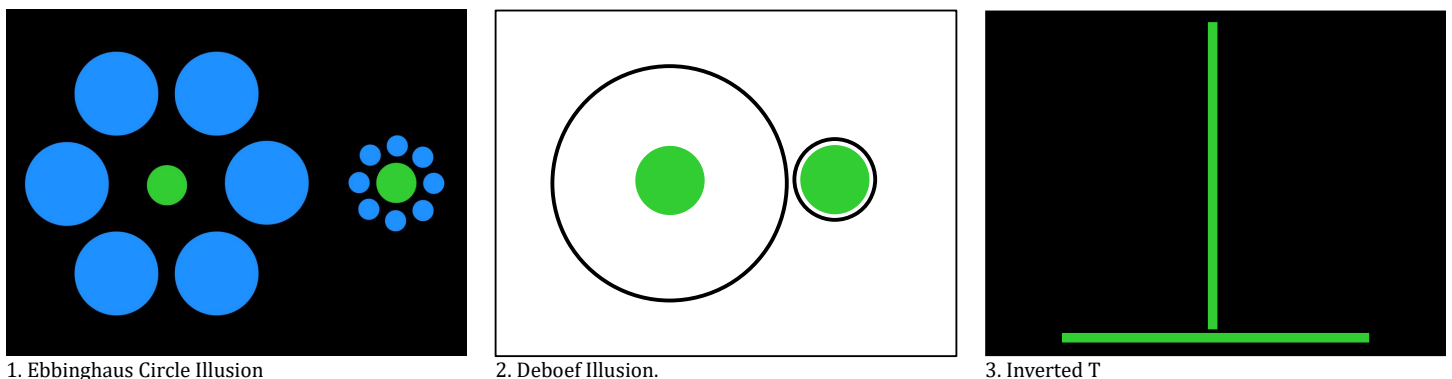


Figure 45. Simple visual illusions that could be used in the study of arthropods. **1-2**, In each case the green circle to the right appears larger (Howard et al. 2017). **3**, The vertical line appears longer than the horizontal line (Mikellidou & Thompson 2013).

There are many other interesting optical illusions that might, in some form, be applied to the study of jumping spiders (Figure 46). These illusions are still the subjects of active study, in some cases suggesting a role for some of the many cell types of the vertebrate retina. If nothing else, examination of these illusions informs us that visual perception goes far beyond the operation of a *camera* that collects

pixilated images. Processing of data collected by visual receptors includes many kinds of feature extraction and recognition, and we presently know very little about these functions in the Salticidae. In addition, since these spiders are highly dependent on vision that is rapidly evolving, we can expect to find many structures or functions that are present in some genera and species, but absent in others.

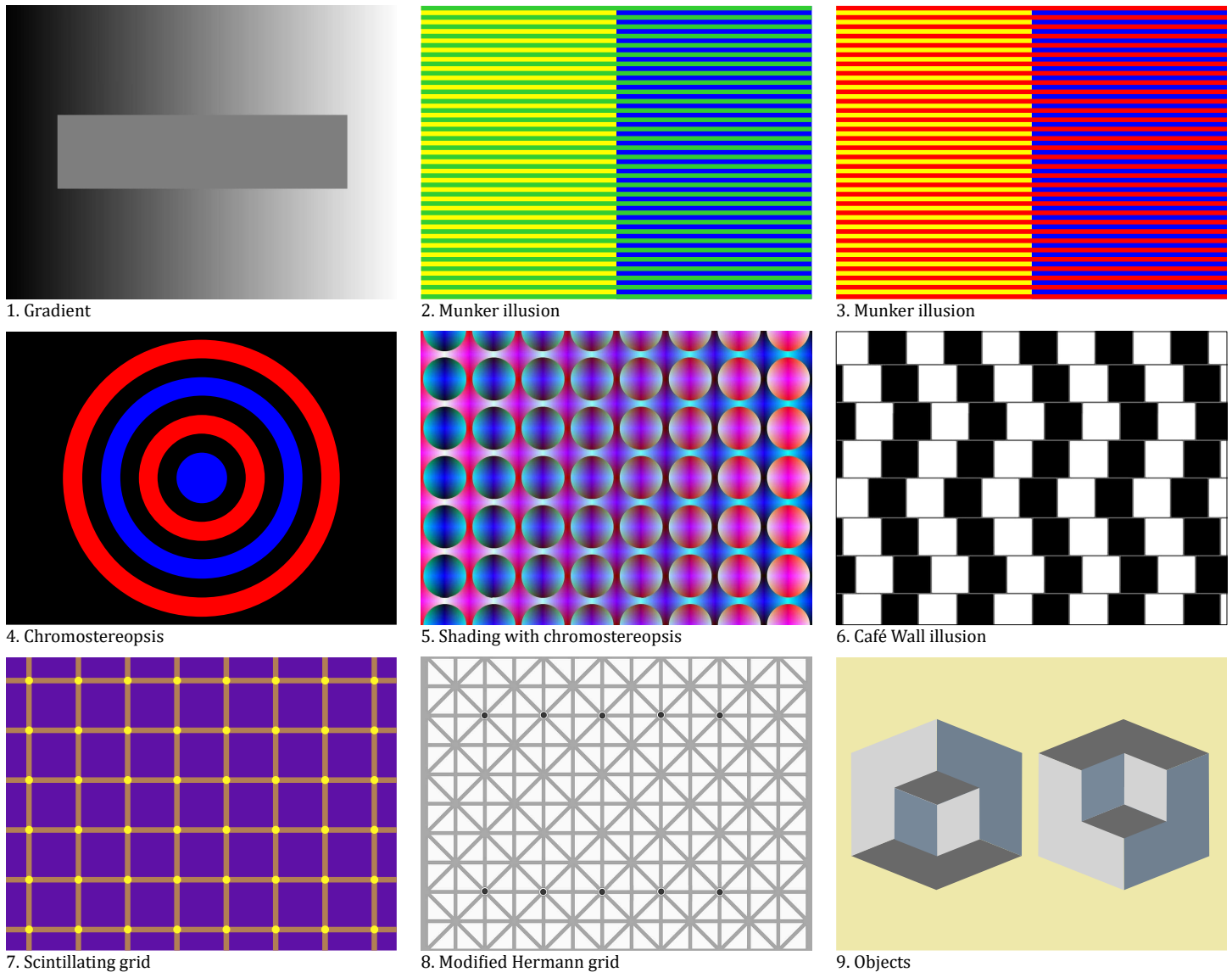


Figure 46. More visual illusions. **1**, The inner rectangle has a constant color, but contrast with the surrounding gradient alters our perception of this (McCourt 1982). **2-3**, There are only four primary colors in these two images (blue, green, yellow and red), but perceived color changes according to background (Einthoven 1885; Monnier & Shevell 2003). **4**, What is closer, the red or the blue? Chromostereopsis is the perception of depth as a result of color. The planes of focus for red and blue light differ, but you will not see depth here if you close one eye. Many people do not see depth in any case (Faubert 1994). **5**, Shading or chiaroscuro has long been used to create the illusion of depth in a painting. With both eyes open, this example also illustrates chromostereopsis. **6**, Try to see the horizontal lines here (Gregory & Heard 1979). **7**, This is a variation on the Hermann grid, with the addition of yellow dots. If you try to see them, those small black dots disappear (Schrauf, Lingelbach & Wist 1997). **8**, This variation actually has two rows of black dots, but if you look at one row of these dots, the other row disappears (Ninio & Stevens 2000). **9**, What do you see here? Either drawing could represent one of three things: a smaller cube in a corner, a larger cube with a missing corner, or a smaller cube floating in front of a larger cube. What you think here is what you see, but you will probably switch to a different interpretation after a few seconds (Stong 1974). See Bach (2022) for more illusions, including many that include animation.

Secondary or anterior lateral (ALE), posterior lateral (PLE) and posterior medial (PME) eyes. As shown in Figures 14-15, the *wiring* of the secondary eyes differs greatly from that of the AME. These three pairs of eyes provide a wide field of view to the salticid (Figures 2, 51) but, unlike the narrow-field AME, the view of each secondary eye is fixed with respect to the position of the carapace. The relative size, position and spacing of the secondary eyes is very useful to the salticid taxonomist. In the great majority of salticids, the PME are significantly reduced in size, but they are nonetheless present and wired (to the best of our knowledge) in all species. These eyes have evolved in several different directions in the Salticidae. The secondary eyes provide important peripheral vision to the sides and to the front of the spider (Figure 47). The ALE, positioned to complement the resolution of the AME with a fixed, binocular field of vision to the front, can vary greatly in both size and placement (Figures 48-49). Except for reduction of visual field in salticids with large PME (Figures 50, 51:6), we see little variation in the placement and size of the PLE.

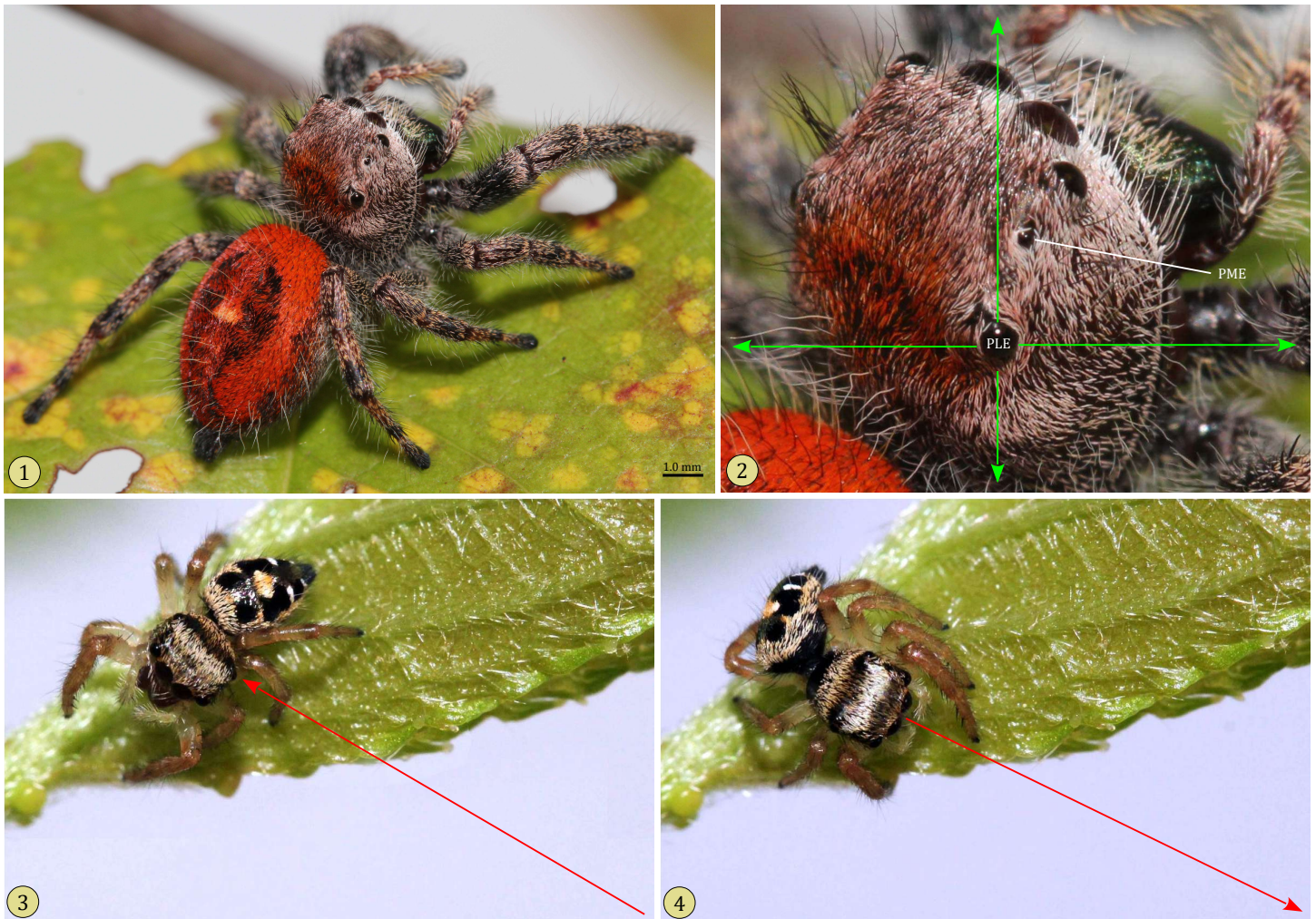


Figure 47. Placement of the posterior lateral eyes (PLE) gives the salticid a wide field of view not accessible to the four front eyes. **1**, Adult female *Phidippus princeps* (Peckham & Peckham 1883) from Georgia, looking up from a leaf. **2**, Detail from (1), showing the wide field of vision of a PLE. In most salticids the PME are very small as shown here, but their view is not blocked by numerous setae that cover the carapace. **3-4**, *Facing turn* by an immature *P. princeps* from South Carolina. Motion detected by the left PLE (3) resulted in a rapid turn (4) to face the moving object. These turns are very accurate with respect to integrated horizontal and vertical components of redirection, and no visual feedback from the object of attention is required during each turn (Land 1971, 1972; Hill 1978, 2010a; Bennett & Lewis 1979).

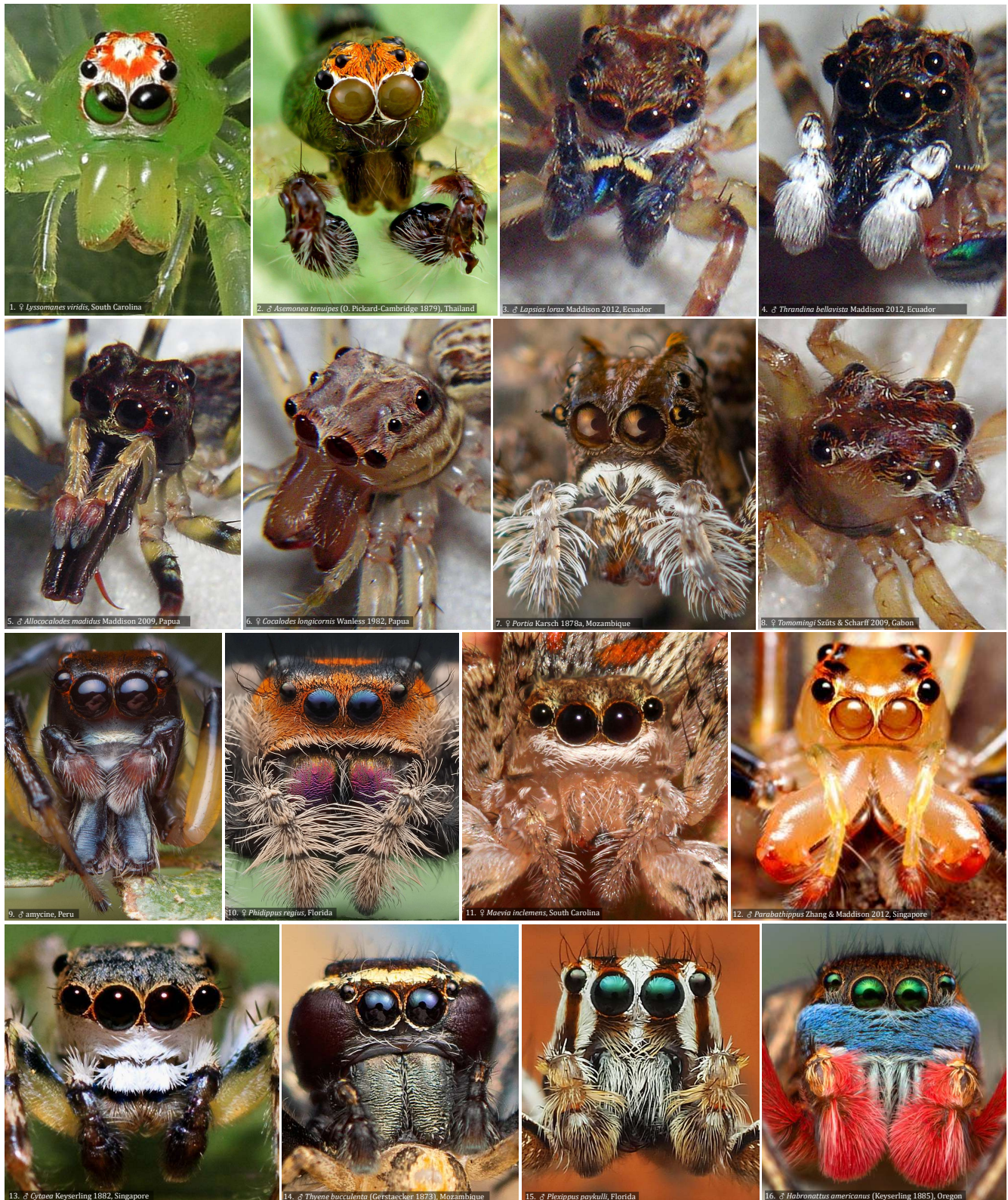


Figure 48. Variation in the size and position of eyes in the Salticidae. **1**, Reduction of the PME and repositioning of the ALE to a higher position can be seen in lyssomanines. **2-6**, Asemoneines (**2**) and most but not all spartaeines (**3-7**) have relatively large PME. **7**, Each PME of a hisponine is situated above the respective ALE, on a lateral extension of the carapace. **9-16**, All salticines have greatly reduced PME, but size and placement of the ALE varies greatly in this large group. Compare the large ALE of *Cytaea* (**13**) to the small ALE of *Thyene* (**14**). Photo credits (all images modified): **2**, ©Asher Lwin, used with permission; **3-6,8**, ©Wayne P. Maddison, used under a [CC-BY 3.0](https://creativecommons.org/licenses/by/3.0/) license; **7,9,14**, ©Thomas Shahan, used under a [CC BY 2.0](https://creativecommons.org/licenses/by/2.0/) license; **12**, ©Gio Diaz, **16**, ©Thomas Shahan, and **13**, ©Aaron Morales, used under a [CC BY-NC 2.0](https://creativecommons.org/licenses/by-nc/2.0/) license; **1,10-11,15**, in the public domain.



Figure 49. Large and small ALE in different Australian salticids. **1,** The ALE of peacock spiders, like this euophryine (*Maratus bubo* Otto & Hill 2016) from Western Australia, are quite large relative to the AME. The cornea of both the ALE and AME of these spiders can reflect a brilliant blue or green color. **2,** All of the lateral eyes of this small (~3 mm) baviine (*Copocrossa* Simon 1901) from Queensland are minute, as the AME take up most of the width of the narrow carapace. Photographs ©Jürgen Otto, used with permission.

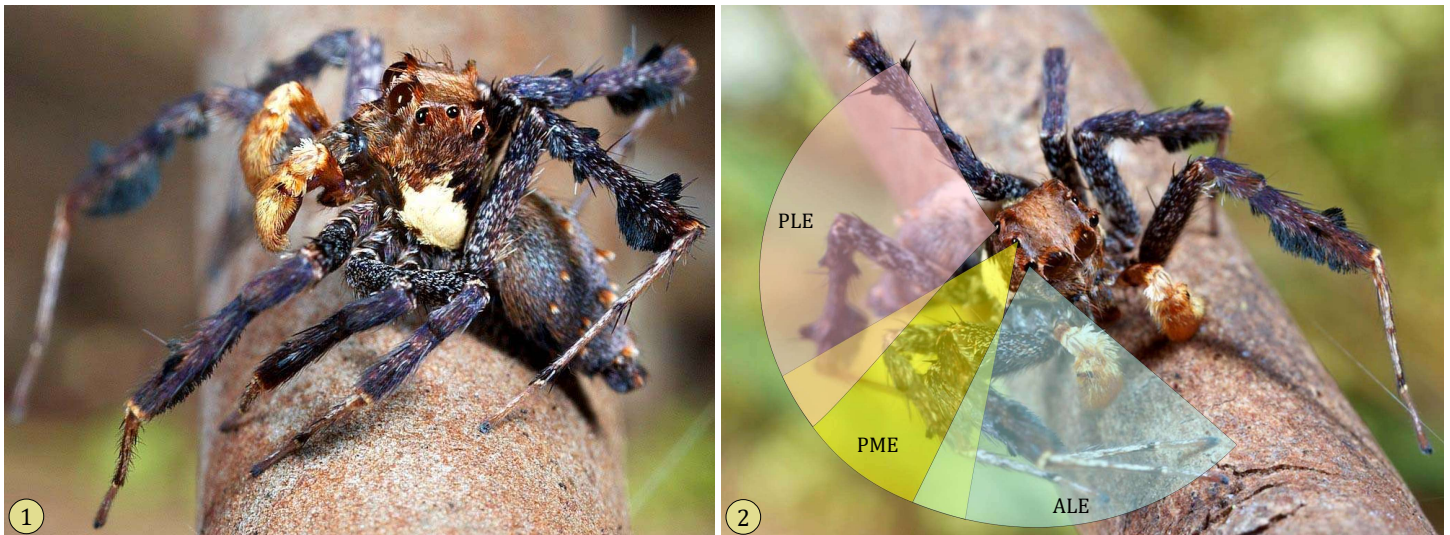


Figure 50. Adult male *Portia fimbriata* from Queensland. The large PME fill a gap (~20°) between the fields of vision of the ipsilateral PLE and ALE (Land 1985). **2,** The irregular-conical, solid angles corresponding to the field of vision of each secondary eye are approximated here with sectors of a single plane. Photographs ©Jürgen Otto, used with permission.

The ALE are longer, primarily forward-directed, with a considerable field of binocular overlap in front, with a narrower field of vision and a much higher density of photoreceptors (corresponding to greater visual acuity) corresponding to the field of binocular vision; in contrast the PLE are shorter, wide angle eyes with a more uniform receptor density, supporting a view to the sides, above, and to the rear of the salticid (Figures 51, 52.1-4; Homann 1928; Land 1969a, 1985a, 1985b; Zurek 2012; Zurek & Nelson 2012; Goté et al. 2019; Nelson 2021). Only a single kind of photoreceptor is known from these eyes, with a wide range of sensitivity and a green (535-540 nm) peak (Figure 52:5-6).

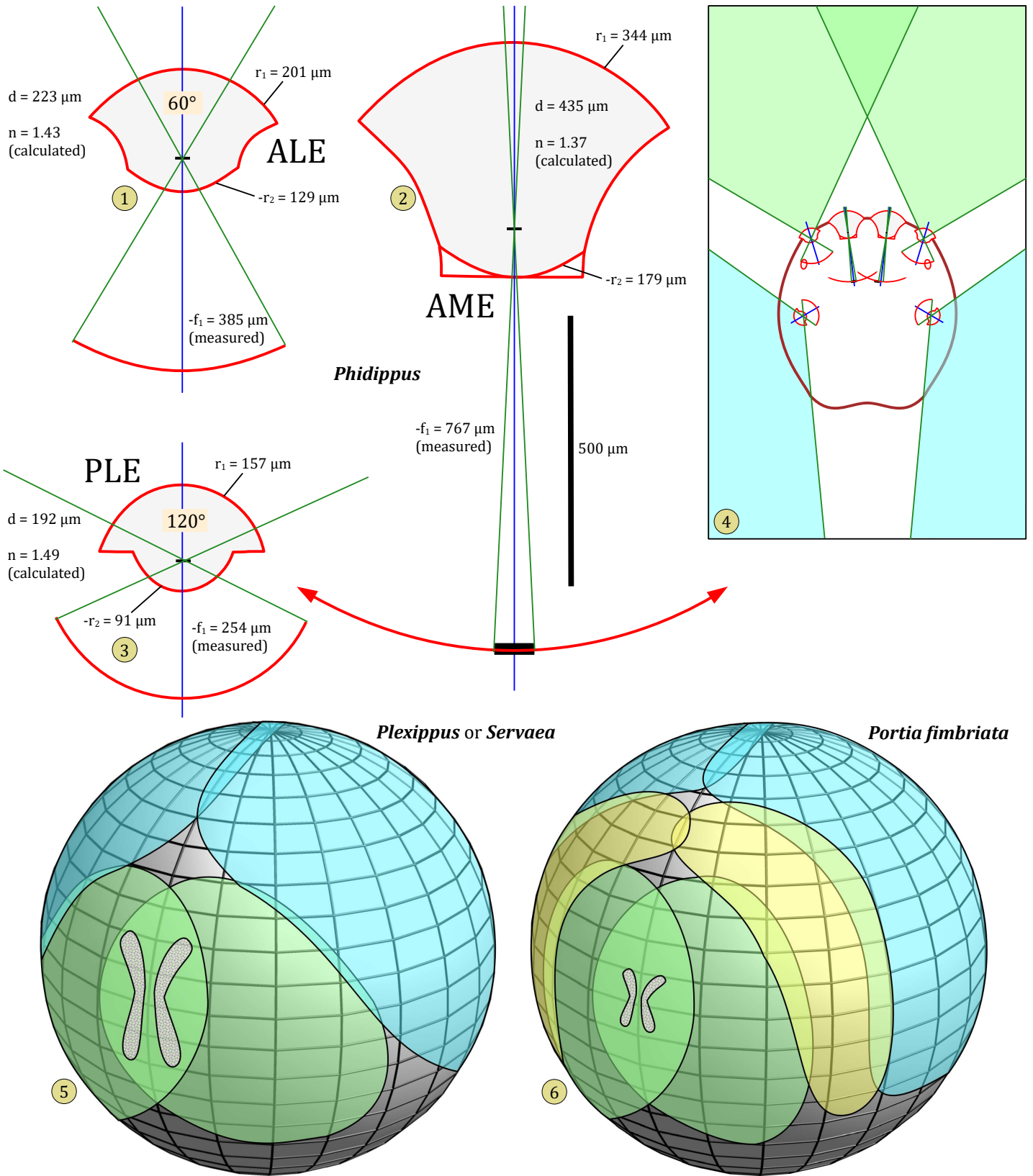


Figure 51. Optics and visual fields of salticid eyes. **1-3**, Scale drawings of respective eyes of *Phidippus johnsoni*, with rays through nodal points (green lines) depicting the width of visual fields, as seen from above (after Land 1969a). The PLE are more symmetrical, with a shorter focal length and much wider field of vision than the ALE. **4**, Horizontal view of the ALE and PLE fields of vision of *Phidippus*. **5-6**, Orthographic projections depicting the fields of vision of the ALE (green), PLE (blue) and, the PME (yellow), surrounding a salticine, either *Plexippus* or *Servaea* (**5**) and the spartaeine *Portia fimbriata* (**6**), after Land (1985a, 1985b).

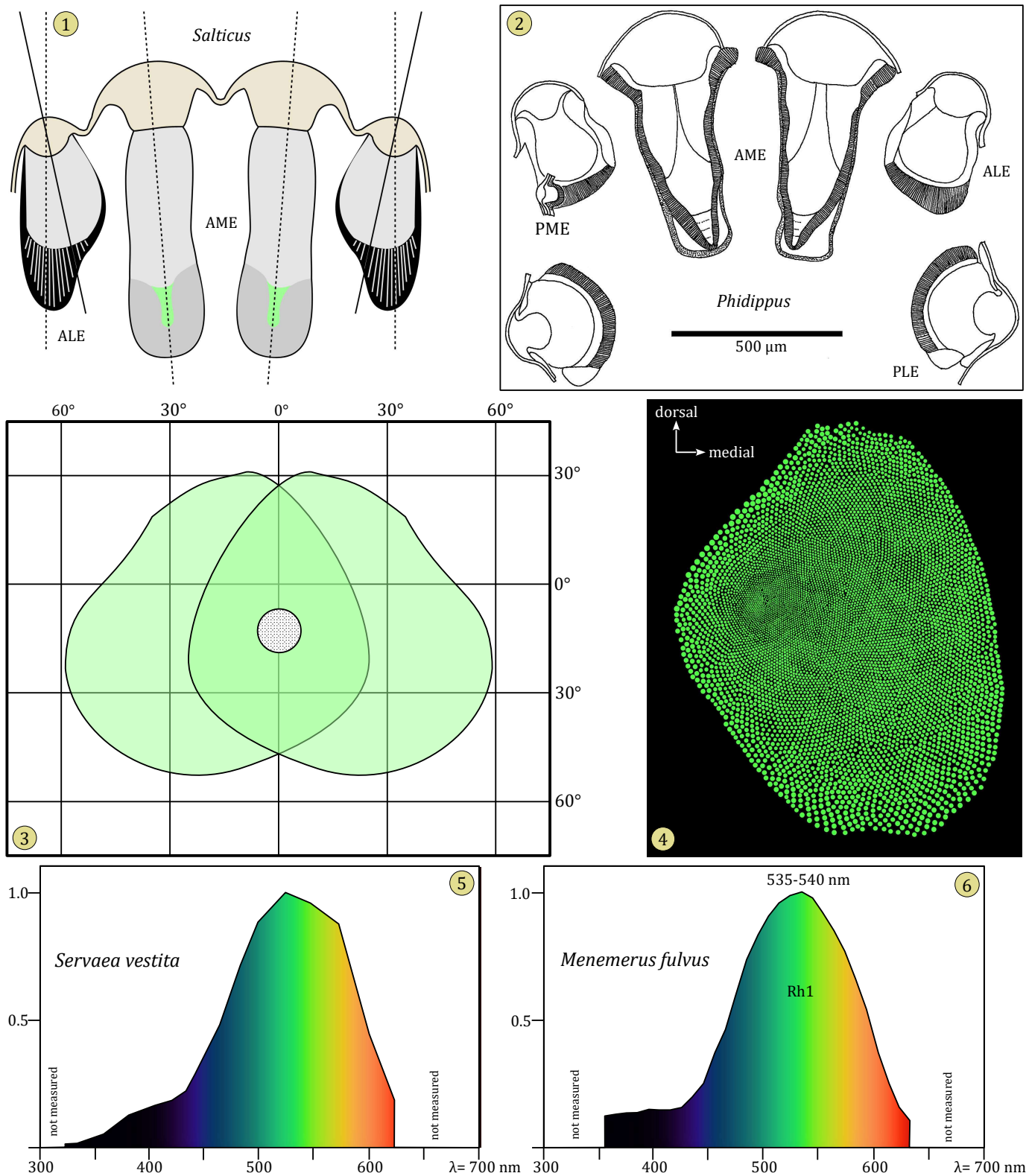


Figure 52. Physical characteristics of the lateral eyes. 1, Schematic horizontal section through the anterior eyes of *Salticus* Latreille 1804, after Homann (1928). 2, Schematic scale drawing of horizontal section through the eyes of *Phidippus johnsoni*. The PME on the right side is not shown. 3, Equirectangular projection of the overlapping ALE visual fields of *Servaea vestita*, with the area of highest-density receptors indicated by a circle, at center. After Zurek 2012; Zurek & Nelson 2012a; Nelson 2021. 4, Plot of ~7000 receptors in the retina of the right ALE of *Phidippus audax* (Hentz 1845), after Goté et al. 2019 (anterior view). 5, Relative spectral sensitivity of the PLE of *Servaea vestita*, after Hardie & Duelli 1978. 6, Average ERG response to monochromatic light for three different ALE preparations, *Menemerus fulvus*, after Yamashita & Tateda 1976.

One more important consideration related to the structure of the secondary eyes lies in the fact that these are not radially symmetrical around the optical axis, although some depictions (e.g., Figure 51:1,3) may suggest this. The fields of vision of these eyes, and the ALE in particular, can be markedly asymmetrical (Figures 51:5,6; 52:3,4). In addition to variation in receptor density (contributing to angular resolution), there may be considerable variation in the length of receptor segments as they pass through the retina of each ALE. Since distal (closer to the lens) parts of each receptor segment should be subject to more intense illumination, long receptor segments could support adaptation to variation in the intensity of incoming light. The proximal parts of these segments might maintain their activity in very bright light, as the distal parts are overwhelmed. With secondary eyes fixed to the carapace, the salticid cannot simply turn away from the sun and must have some way of dealing with direct sunlight.

Unlike the AME, the receptors or sensory neurons of the secondary eyes are unipolar, and the receptor segments (bearing light-sensitive rhabdomeres) of each cell are surrounded in part or completely by the projections of pigmented neuroglia. All receptor segments are arranged in a single layer, in a space-filling array. Based on electron microscopy, three configurations of this array have been described, each corresponding to a different subfamily of salticid spiders (Figure 53; Eakin & Brandenburger 1971; Duelli 1978; Blest & Maples 1979; Blest 1983, 1984, 1985b; Blest & Sigmund 1984). In lyssomanines, pigmented glia lie mostly below the receptor segments (Figure 53:1-2). In spartaeines, pigmented glia completely surround the receptor segments, which are roughly rectangular in cross-section (Figure 53:3-4). The salticines, representing the great majority of living salticid species, have receptor segments that are hexagonal in cross section, also completely surrounded by pigmented glia (Figure 53:5-6).

The ALE and PLE of salticines are also distinguished by the fact that their receptor neuron somata are located just outside of the eye, not in front of the retina as in the lyssomanines and spartaeines. The relationship of the lateral eyes to their associated neuropiles is reviewed in Figures 54-56. Receptor terminals appear to map to the first neuropile (FOG, or AL1 or PL1, respectively) on a 1:1 basis, and each subsequent terminal of the *lame glomerulee* (SOG) appears to map to a single terminal of that first neuropile. For the dendryphantine salticids (*Marpissa*, *Phidippus*), known to have an extensive fiber tract connecting the first neuropile to a lateral eye neuropile, we are not certain if the respective interneurons share the terminals of the first neuropile with interneurons leading to the *lame glomerulee*, but this seems quite likely. In addition to the first neuropile, a separate small neuropile or ganglion (ALx, PLx, and PM1, respectively) has been associated with each secondary eye of dendryphantines, apparently representing a set of receptor terminals. From these originate large fibers of the lateral fiber tract. For the PME of salticines, these ganglia (PM1) are the only known terminus of receptors. Hanstrom (1921) also found neural connections between AL1 or PL1 and the upper lobe of the central body.

Interneurons that originate with an extensive series of synapses in multiple zones along the length of each pedunculate body appear to terminate in the lateral neuropile of the protocerebrum, and a distinct fiber tract (bridge) joins the left and right *corpora pedunculata* (Figure 55). There is also distinct series of transverse fiber tracts penetrating the dense neuropile of each *corpus pedunculatus* (Figure 55:3-4).

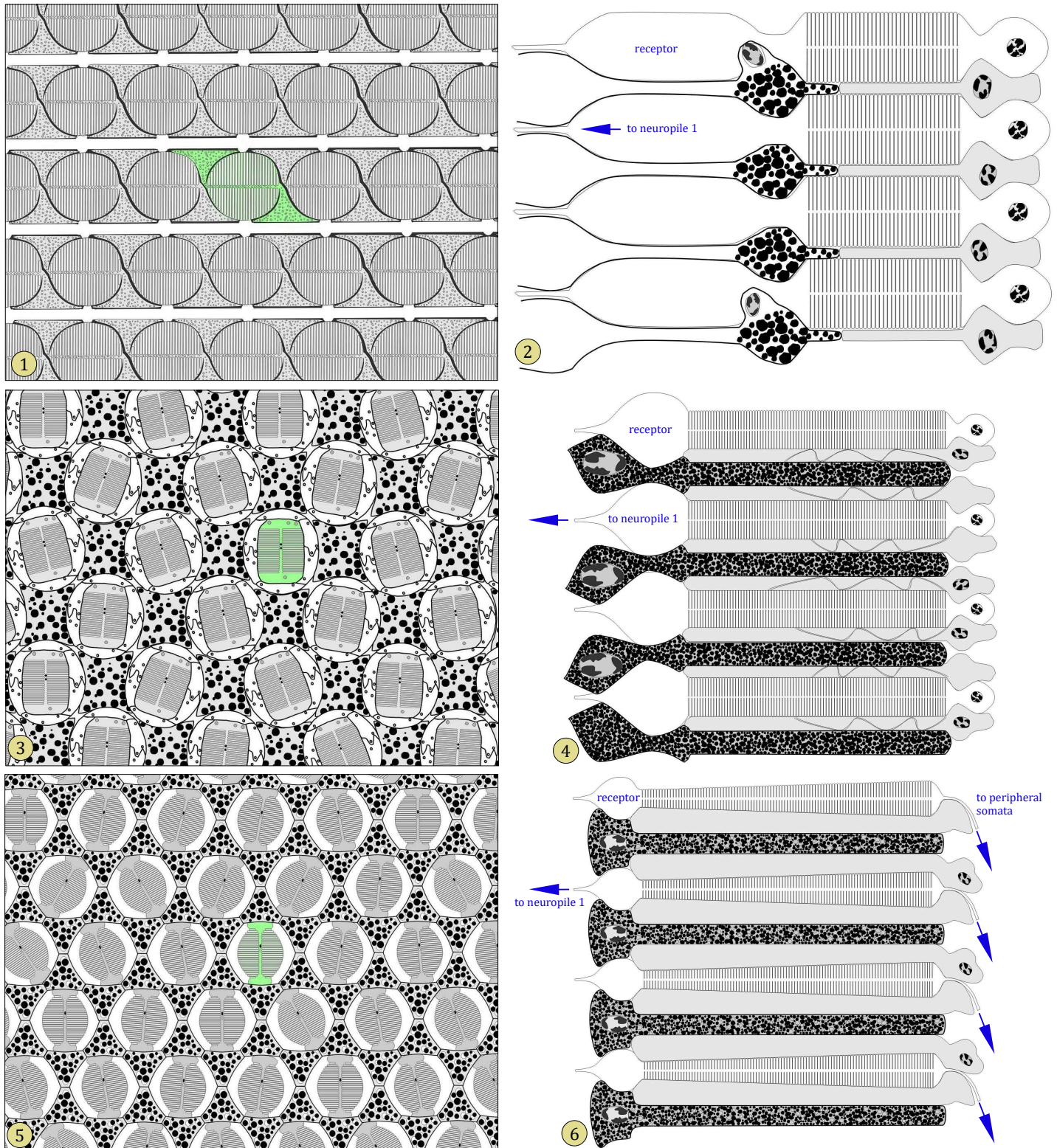


Figure 53. Schematic drawings depicting the arrangement of unipolar sensory cells in the retina of secondary eyes. **1,3,5,** Sections through the plane of the retina, with a single sensory cell highlighted in green in each example. These are surrounded by the processes of both pigmented and unpigmented neuroglial cells. **2,4,6,** Transverse section of each retina showing arrangement of sensory cells and surrounding glial cells. In each example the distal (toward the lens) side of each retina is toward the right. **1-2,** Linear array of *Lyssomanes* (Lyssomaninae; after Blest 1983, 1985b; Blest & Sigmund 1984). **3-4,** Quadrangular array of *Portia* and *Yaginumanis* (Spartaeinae; after Blest 1983, 1984, 1985b; Blest & Sigmund 1984). **5-6,** Hexagonal array of *Euryattus* Thorell 1881, *Evarcha arcuata* (Clerck 1757), *Phidippus*, and *Servaea* (Salticinae; after Eakin & Brandenburger 1971; Duelli 1978, 1980; Blest & Maples 1979; Blest 1983, 1985b; Blest & Sigmund 1984; Harland & Jackson 2012).

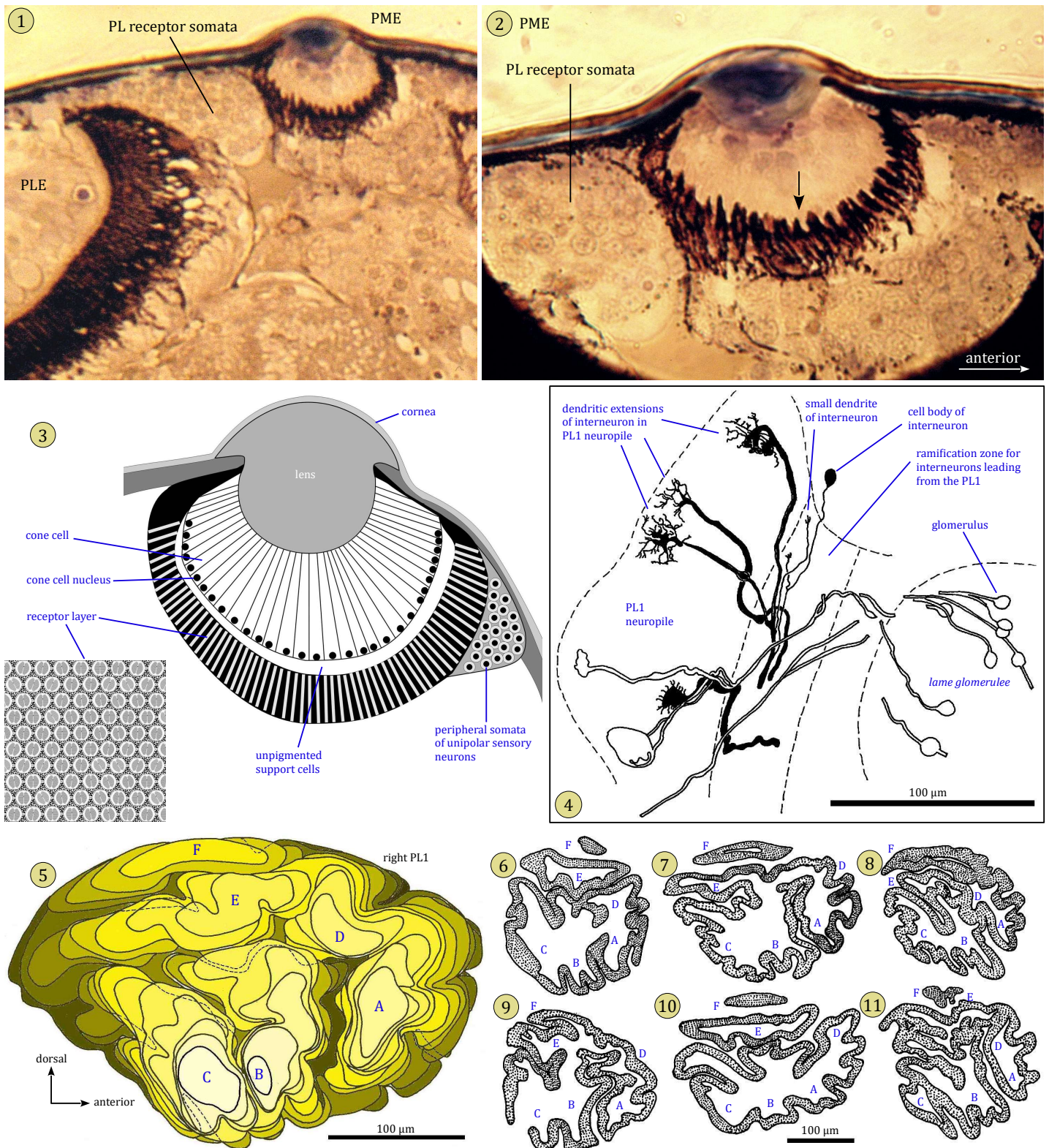


Figure 54. Lateral eyes and associated neuropiles. **1-2**, Horizontal section (5 μm Epon stained with Toluidine Blue) through a PME of a second instar *Phidippus johnsoni*, detail in (2). Note the irregular alignment of pigmented glia near the distal margin (facing the lens) of the retina. **3**, Schematic cross section of a PLE of *Phidippus*, after Eakin & Brandenburger 1971. **4**, Golgi-Kopsch preparation of interneurons in the primary neuropile (PL1) of the left PLE of a sixth instar *P. johnsoni*. Several of the interneurons appeared to synapse in more than one place in the highly-structured PL1, but a larger study of this possibility is needed. **5**, Contour diagram of the right PL1, sixth instar *P. johnsoni* (10 μm intervals). **6-11**, Parasagittal sections through the PL1 of six different sixth instar *P. johnsoni*, showing similar convolutions of this neuropile. 4-11, after Hill 2006

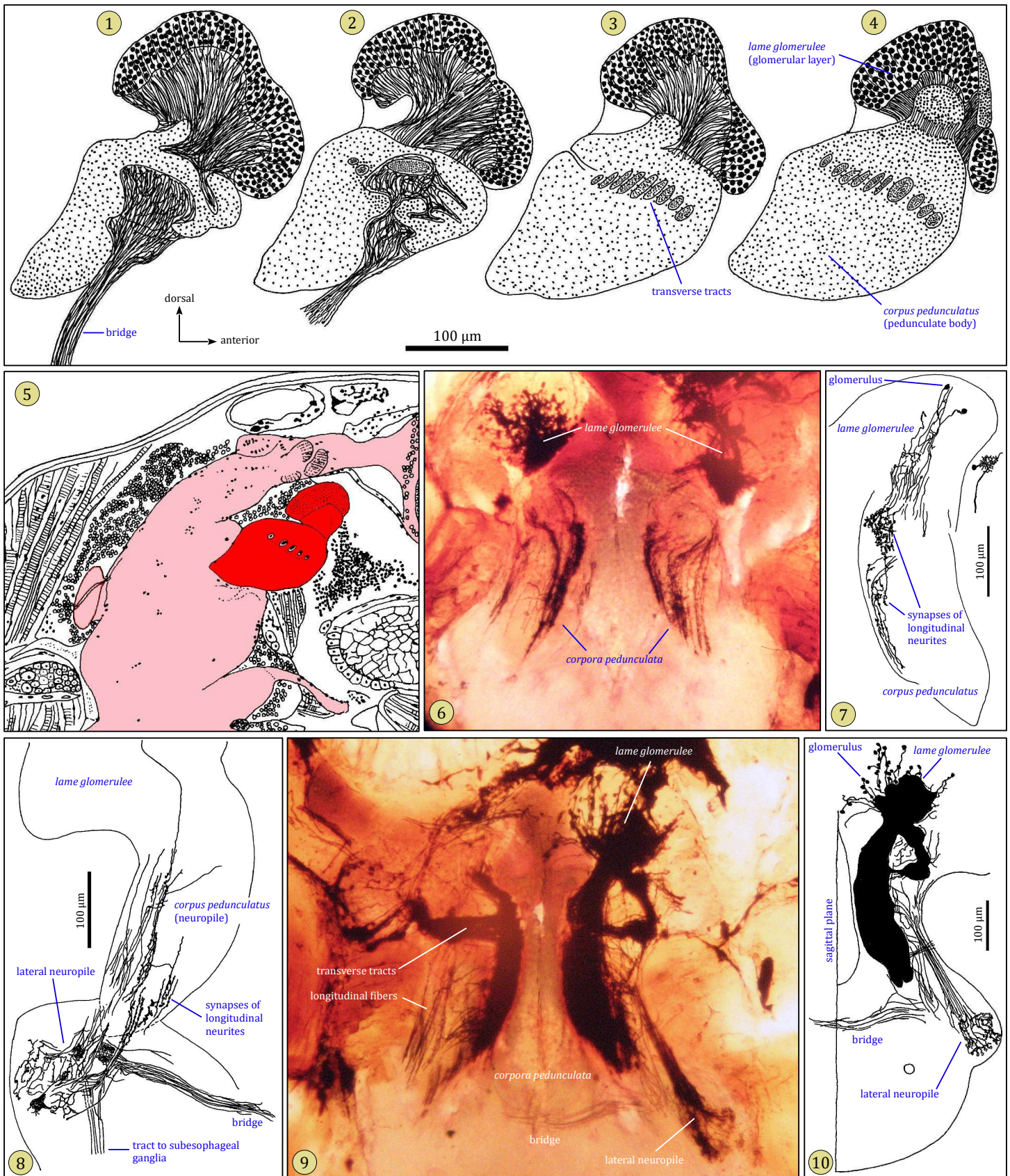


Figure 55. The *corpora pedunculata* (pedunculate bodies). **1-4**, Serial (10 µm) parasagittal sections of the pedunculate body of a sixth instar *Phidippus johnsoni*, in lateral (1) to medial (4) order. **5**, Position of the pedunculate body at the front of the protocerebrum (bright red; parasagittal section of fifth instar *P. clarus*). **6-10**, Photographs and line drawings of thick (80 µm) horizontal sections of Golgi-Kopsch preparations, sixth instar *P. johnsoni*.

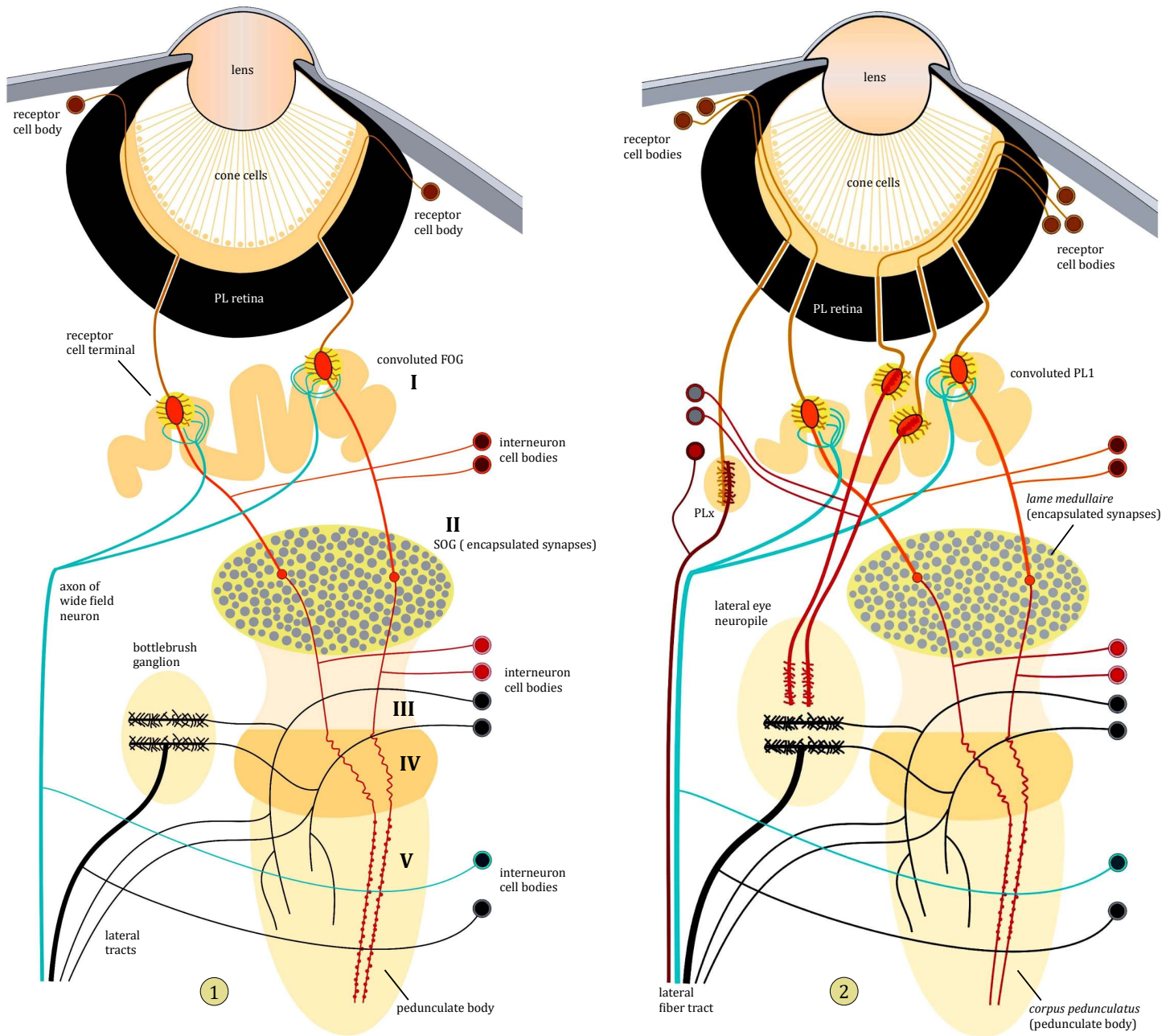


Figure 56. Hypothetical connectivity of PLE receptors with downstream interneurons. **1**, Connectivity based a study of *Evarcha arcuata* and *Servaea vestita* by Duelli (1980). The cell bodies of unipolar receptor neurons are located in groups at the periphery of the eye cup. From each cell body a single axon runs in front of, and then through the retina as a *receptor segment* with photosensitive rhabdoms, terminating in an ovoid, encapsulated synapse, with many local dendrites, at the first optic ganglion (FOG or PL1). Interneurons map these terminals on a 1:1 basis to small spheroid, encapsulated synapses of the second optic ganglion (SOG or *lame medullaire*). Downstream interneurons connect each capsule of the SOG to successive synaptic layers (III-V) of the pedunculate body. Other interneurons with extensive processes in the pedunculate body form bottlebrush-like processes in an adjacent (lateral) bottlebrush ganglion. Lateral tracts include the axons of wide field interneurons originating with terminals of the FOG (PL1), Thick axons connect to bottlebrush synapses in the bottlebrush ganglion, and other neurites originating in the pedunculate body. **2**, Connectivity including suggestions from studies of *Phidippus* and *Marpissa* (Hill 1975, 2006; Long 2016; Steinhoff et al. 2017, 2019). This includes features shown in (1), with the assumption (as suggested by Duelli 1980) that the *bottlebrush ganglion* is the same as the *lateral eye neuropile*. Additional features include direct interneuron connections from PL1 terminals to the lateral eye neuropile (as indicated by silver staining of fiber tracts), and the addition of a small ganglion or neuropile (PLx, corresponding to ALx for the ALE) where some of the receptors may synapse with the large fibers of the *lateral fiber tract*. As shown in Figures 14-15, each receptor terminal may be linked to both the lateral eye neuropile and the *lame glomerulee*. Each salticrine PME is only known to synapse in a small ganglion (PM1) which, like the PLx, appears to be the origin of large fibers that occupy the lateral tract.

Functions of the secondary eyes. Earlier studies of the secondary eyes, and the PLE in particular, focused on their role in directing the rapid facing turns of salticids (Figures 47, 57). Recently there has been more interest in their functions, including the likelihood that the ALE, at least, support some degree of object recognition (Table 10).

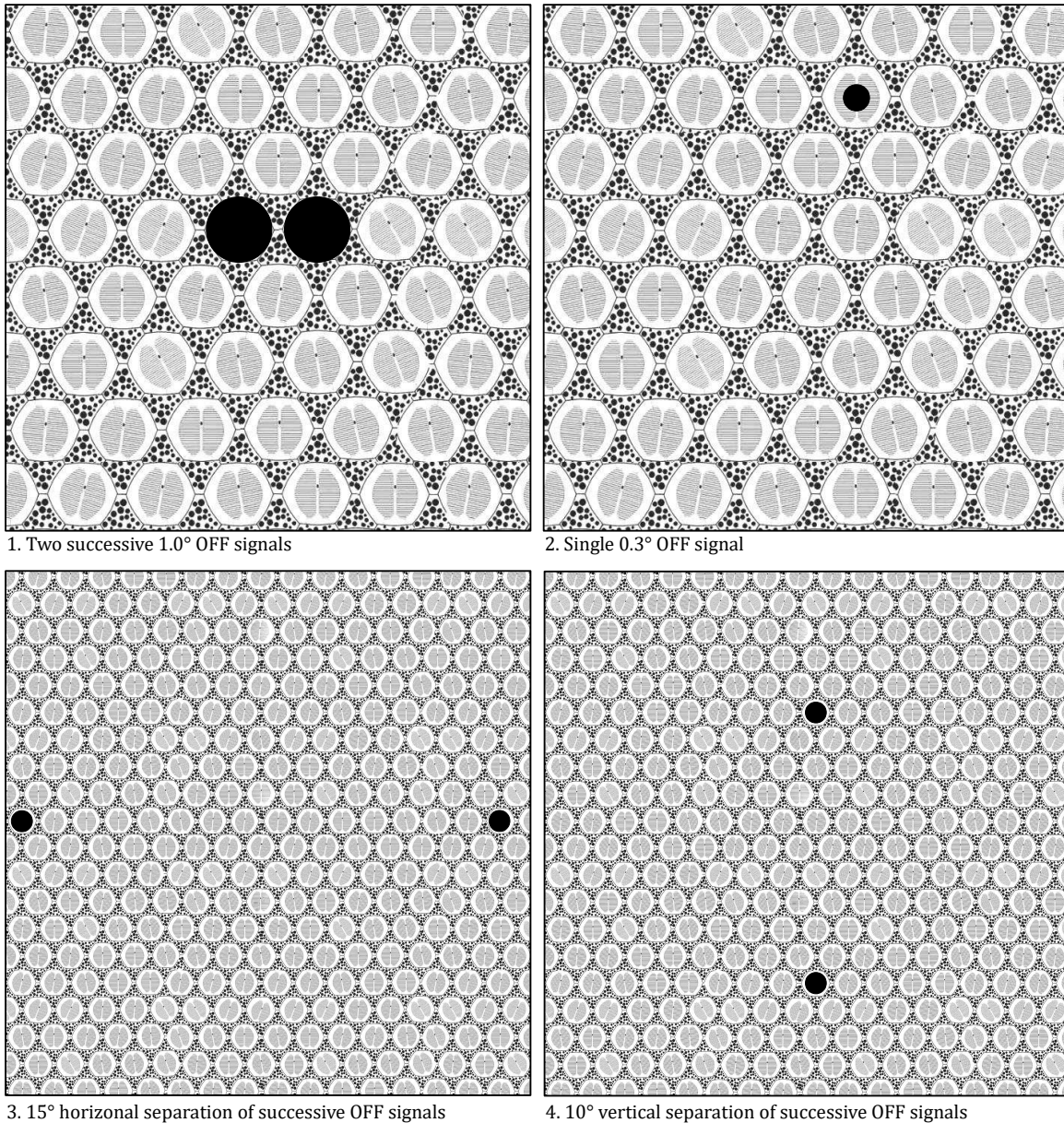


Figure 57. Schematic transverse sections of the PLE retina showing minimal point signals required to elicit facing turns by *Evarcha arcuata* (after Duelli 1978). **1**, Successive OFF signals (dark spot) to two adjacent receptors is sufficient to elicit a facing turn to the second signal. The priming effect of the first OFF signal lasted for about 200 msec. **2**, In some cases a small OFF signal directed at a single receptor was sufficient to elicit a facing turn. **3**, Successive OFF signals directed at receptors separated horizontally by 15° or less elicited facing turns. The effect was not seen, and might be suppressed, with greater separation. **4**, Vertical separation of OFF signals by 10° or less elicited facing turns. These turns are very accurate, taking the shortest path to either the right or to the left in response to stimuli that are presented in any radial direction ($0-360^\circ$) in the surrounding horizontal plane (Land 1971, 1972; Duelli 1975, 1977, 1978; Hill 1978, 2006)

Table 10. Published studies of the function of the secondary eyes of salticid spiders.

#	hypothetical function	references	notes/issues
1	ALE and PLE detect and locate direction of moving objects to drive <i>facing turns</i>	Land 1971, 1972; Duelli 1975, 1977, 1978; Hill 1978, 2006; Yamashita 1985; Komiya, Yamashita & Tateda 1988; Zurek, Taylor, Evans & Nelson 2010; Zurek 2012; Zurek & Nelson 2012b	Stimulus size, contrast, and speed are also factors that determine whether the spider makes a facing turn. Response can be elicited through both off- and on-stimulation of a few receptors. Stimulus displacement smaller than the inter-receptor angle can be detected by the ALE (Zurek 2012; Zurek & Nelson 2012b).
2	Separation of the ALE supports the accurate determination of distance in the relevant 3-20 cm range through superposition of images from both eyes (binocular vision)	Hill 1978, 2010a; Figure 58	Highest angular resolution of the ALE lies in the overlap between fields of the left and right ALE, directly in front of the spider.
3	ALE direct movement (saccades) of AME to a target	Zurek & Nelson 2012a	
4	ALE direct tracking of moving objects by the AME	Jakob et al. 2018	AME would scan stationary objects if ALE were masked.
5	ALE alone can elicit stalking of prey	Zurek, Taylor, Evans & Nelson 2010; Zurek 2012	With only the ALE, <i>Servaea</i> stalked and attacked flies.
6	ALE initiate retreat from objects growing in size (<i>looming</i>) in front of the spider	Spano, Long & Jakob 2012	There was much less reaction to objects as their size was reduced (<i>receding</i>).
7	ALE provide a lower resolution image of recognized objects, subsequently detailed by the AME	Dolev 2016	Object recognition without the AME.
8	ALE redirection of AME varies according to the nature of both <i>primary</i> and <i>distractor</i> stimuli	Bruce, Daye, Long, Winsor, Menda, Hoy & Jakob 2021	Higher-order processing of relevant information appears to determine if the spider is distracted by a second stimulus.
9	Secondary eyes contribute to the evaluation of movement patterns of sighted objects	De Agrò, Rößler, Kim & Shamble 2021	Random patterns of point-to-point movement appeared to elicit a stronger response than those that were deemed <i>biological</i> .
10	Spectral sensitivity of ALE complements spectral sensitivity of AME to extend color discrimination into the red end of the spectrum	(this paper)	Hypothesis only.
11	Secondary eyes entrain circadian rhythm	Tork 2019	For ? <i>Marpissa</i> (<i>M. marina</i> is a <i>nomen dubium</i>), ALE, PME and PLE, but not AME, could entrain a new schedule of activity.

The PME of salticines have often been thought to be *vestigial*, but their structure and connectivity suggests otherwise. In dendryphantines, the receptor somata do not lie outside of the eye cup, but just inside of it adjacent to the retina; unlike the ALE and PLE receptor segments of the PME are not surrounded by pigmented glia (Eakin & Brandenburger 1971). This suggests a specialized function for these eyes, either as a alerting mechanism for overhead movement, or as a driver of circadian rhythms.

The special placement of the ALE should not be overlooked in the discussion of distance determination by a salticid. This, along with receptor spacing, constitutes *prima facie* anatomical evidence for ALE-based *binocular vision* (Table 10, hypothesis 2; Figure 58). The narrow field of binocular overlap in front of the salticid corresponds to a significantly higher density of receptors in each ALE, supporting higher image and distance resolution. Since the positions and orientation of these eyes on the carapace are fixed, each pairing of one receptor from each ALE corresponds to a specific position (both distance and direction), and fixation or turning of both eyes (as in a vertebrate) is not needed for convergence (or superposition) of this kind. Estimates of the accuracy of distance discrimination (depth perception) may be low, as statistical sampling of distance from an object in the overlapping field between both ALE may involve a large number of separate receptors, resulting in *hyperacuity* (Figure 59; Zurek & Nelson 2012b; Shepeleva 2022). Facilitation of this sampling process may explain for the tendency of many salticids to rotate the sagittal plane of the carapace laterally when observing an object (Figure 60; *yaw* or ρ turns; Hill 1978, 2010a).

Whereas information collected from a single AME (relative focus in layers I and II) might support a degree of distance resolution (based on assumed color) in a salticid with occluded ALE (Nagata et al. 2012), in an intact spider with use of the ALE to determine distance, the same information could be used to determine spectral hue within the range of the green-peak receptors (Table 10, hypothesis 10). When combined with sampling by the UV receptors in layers III and IV, this could provide the salticid with something like trichromatic vision.

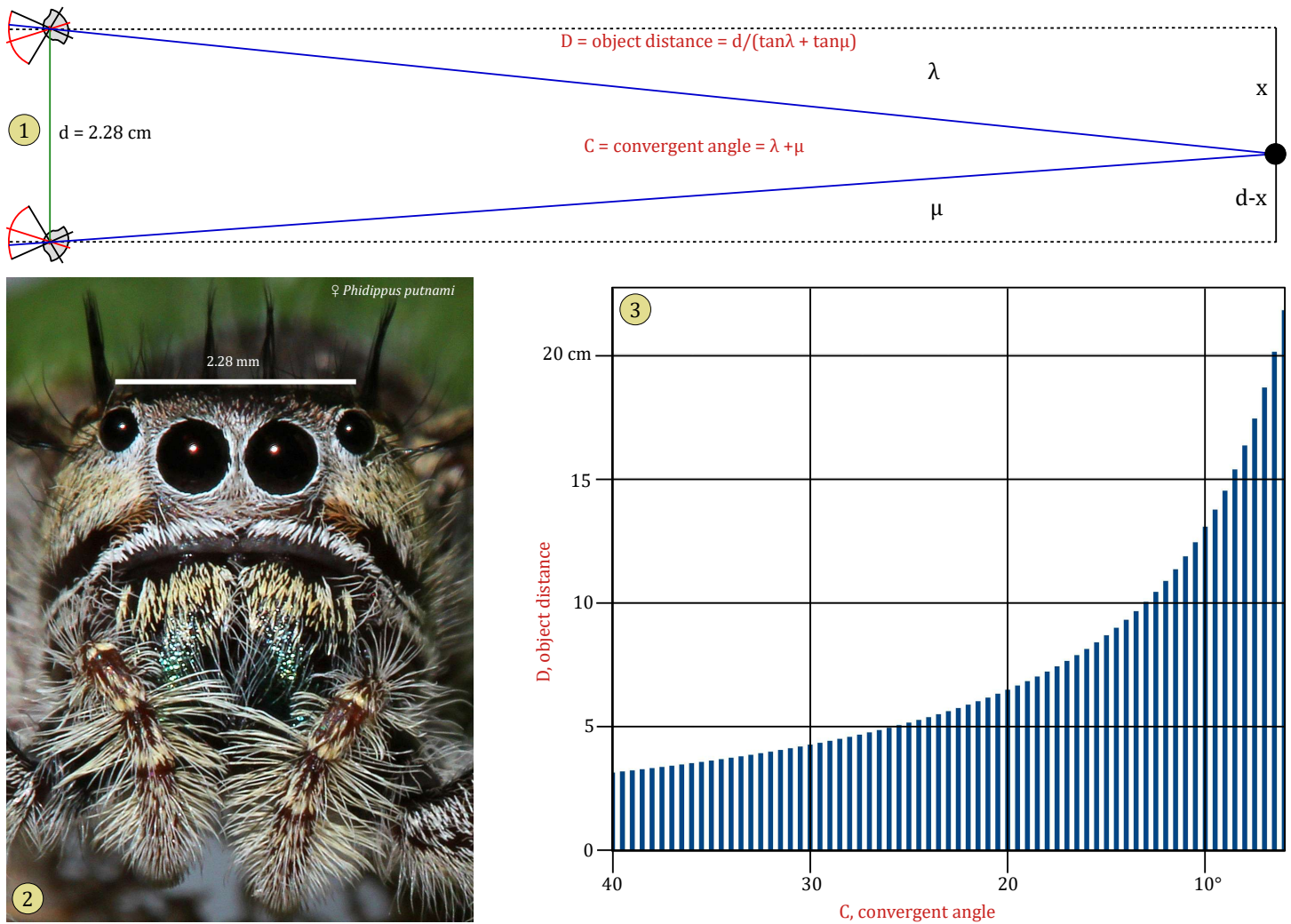


Figure 58. Predicted ability of *Phidippus* to resolve distance through superposition of signals collected from both ALE (binocular vision or *stereopsis*; after Hill 1978, 2010a). **1**, Formula for calculation of distance (D), based on separation of the receptors in each eye (d) and the convergence or angular direction faced by each receptor (λ and μ , respectively). **2**, Face of adult female *Phidippus putnami*, showing separation of ALE. **3**, Calculation of object distance for successive increments (vertical bars) of separation of two receptors, one in each eye (convergent angle, C). This is based on receptor separation of $\sim 0.5^\circ$ of arc within the forward-facing part of each retina, and placement of the object directly in front of the spider. The result is a rather smooth curve, very accurate at a useful distance for a spider that may execute an accurate jump of more than 10 cm to capture its prey (Hill 2010b). With greater distances, the ability to resolve distance is reduced, but other cues such as the perspective afforded by surrounding plants, and the relative size of a familiar object, are also available to the spider.

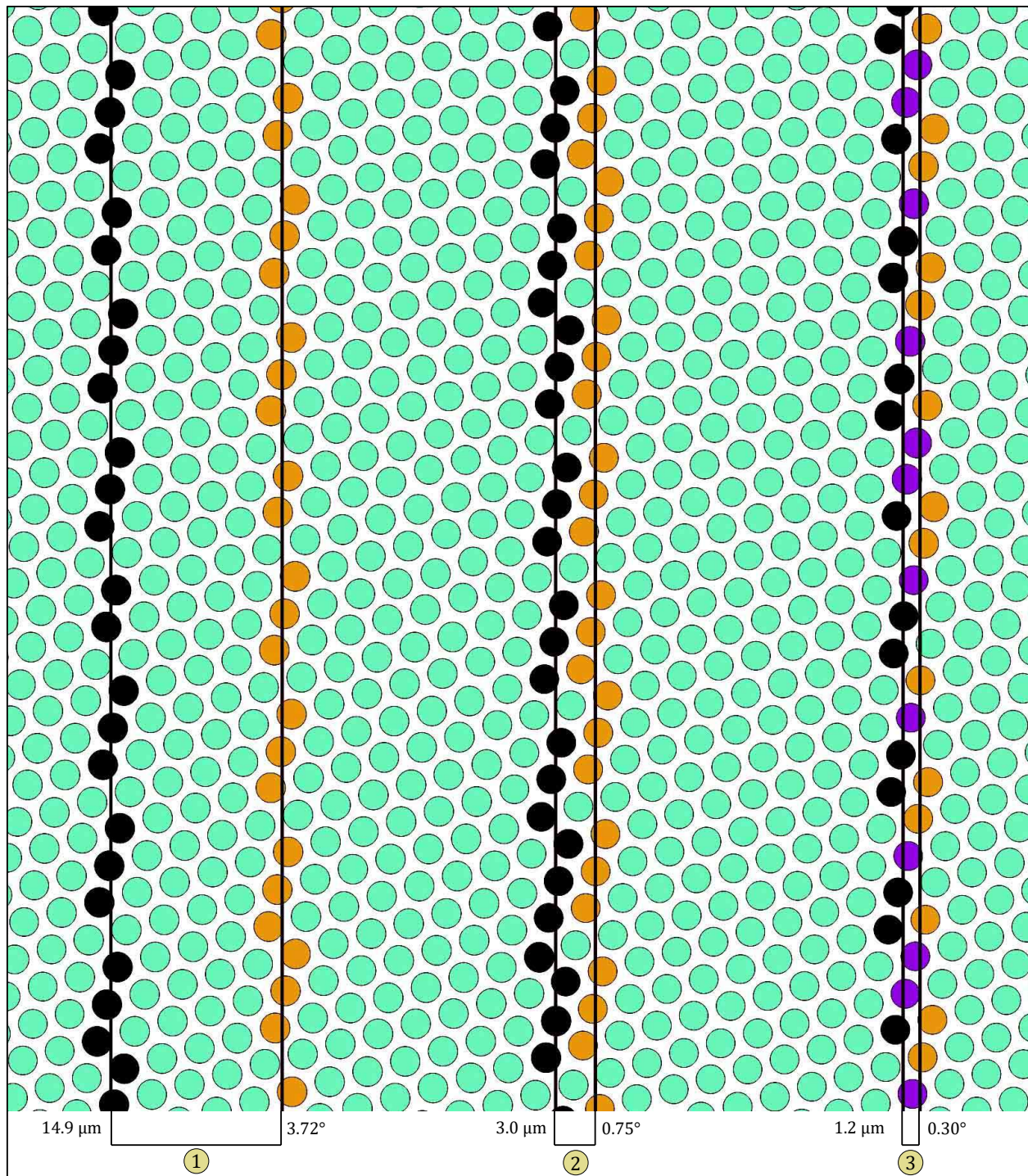


Figure 59. Oversampling effect of signals associated with linear rows of receptors on potential visual acuity, based on the ALE of *Phidippus*. Receptor separation is estimated at $3\ \mu\text{m}$ and 0.75° of arc, based on a count of 80 receptors spanning $250\ \mu\text{m}$ and 60° of arc in the part of the retina that collects light directly in front of the spider. The line of receptors that detect each line is highlighted in black or orange, respectively, or violet if both lines are detected. **1**, Widely separated linear signals affect completely different sets of receptors and pose no limit to their separation, particularly since there are many intervening rows of receptors. **2**, When separation of lines is equal to receptor separation, they may be resolved as a single line, as there are few intervening receptors. But the position of each line could still be resolved at a level of accuracy greater than the width of a receptor. **3**, Even a much smaller shift in position might be detectable, as the set of receptors associated with each position would be different. This may explain salticid *hyperacuity* (Zurek & Nelson 2012b), or what is known as the *Vernier effect* (Hamer, Carvalho & Venture 2013; Gomes, Bartelt & Frazão 2021). Ultimately the visual acuity of these eyes depends on downstream processing in the associated ganglia, much like *cortical magnification* in the human primary visual cortex (Duncan & Boynton 2003).

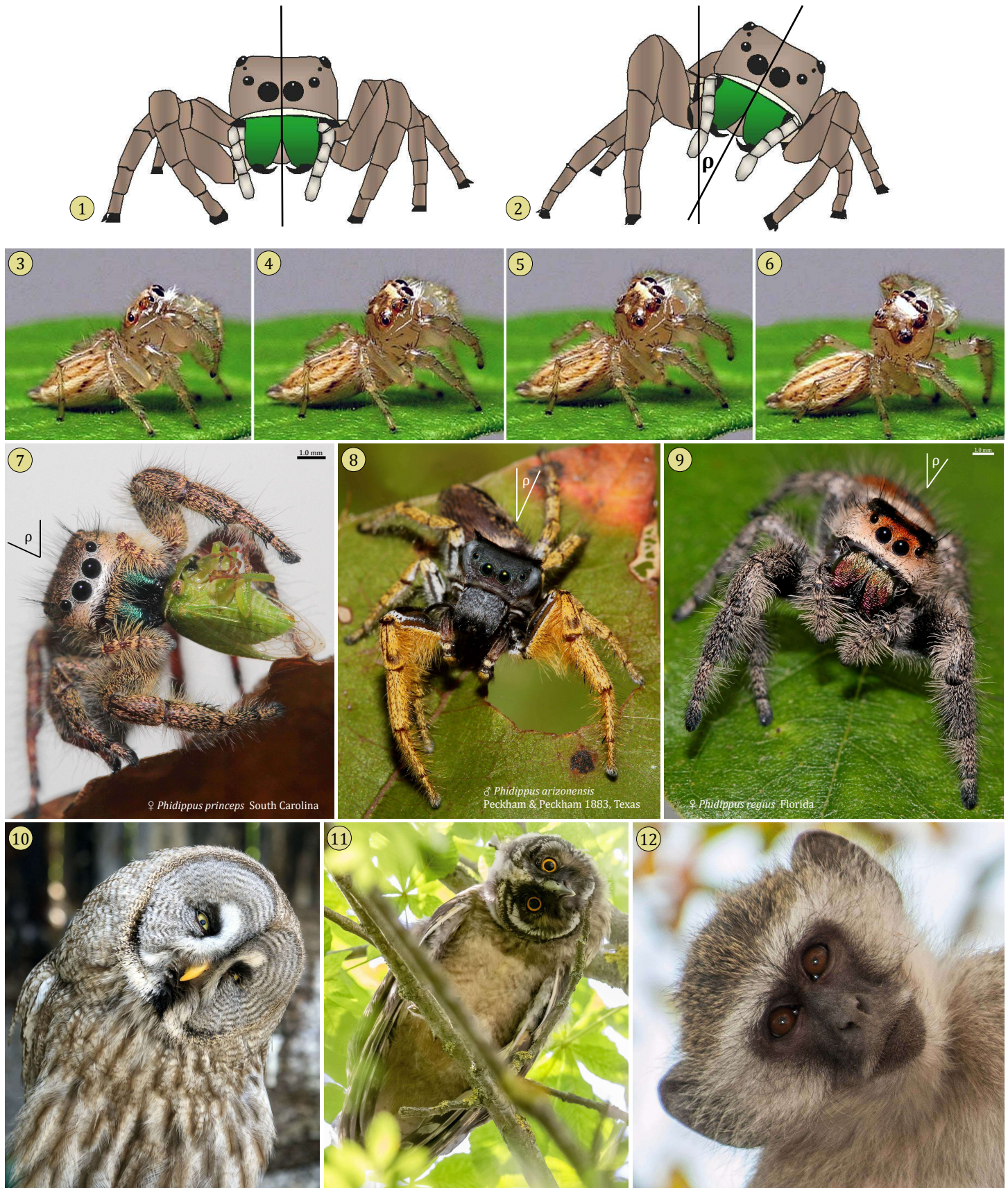


Figure 60. Yaw or ρ turns executed by various animals as they observe a subject of interest. These turns should improve binocular vision by increasing relevant sampling along a line or edge (Lam et al. 2008). **1-2,** Diagram of a ρ turn by a salticid (Hill 2010a). **3-6,** Sequential frames showing execution of a ρ turn by a female *Colonus sylvanus* (South Carolina). **7-9,** Three *Phidippus* species after execution of a ρ turn. **10-12,** Two owls and a monkey similarly engaged.

Other structured neuropiles

The *central (arcuate) body* (Figure 61) has been viewed as a third neuropile of the AME (Babu 1985; Strausfield, Weltzien & Barth 1993; Babu & Barth 1984; Barth 2002; Döffinger 2010; Long 2016), or as a *motor and association center* with control over programmed behavior (Millot 1949; Babu 1985). With a central location, distinctive structuring of its neuropiles, and well-defined medial and lateral connectivity, it seems likely that this structure plays a key role in the organization of behavior.

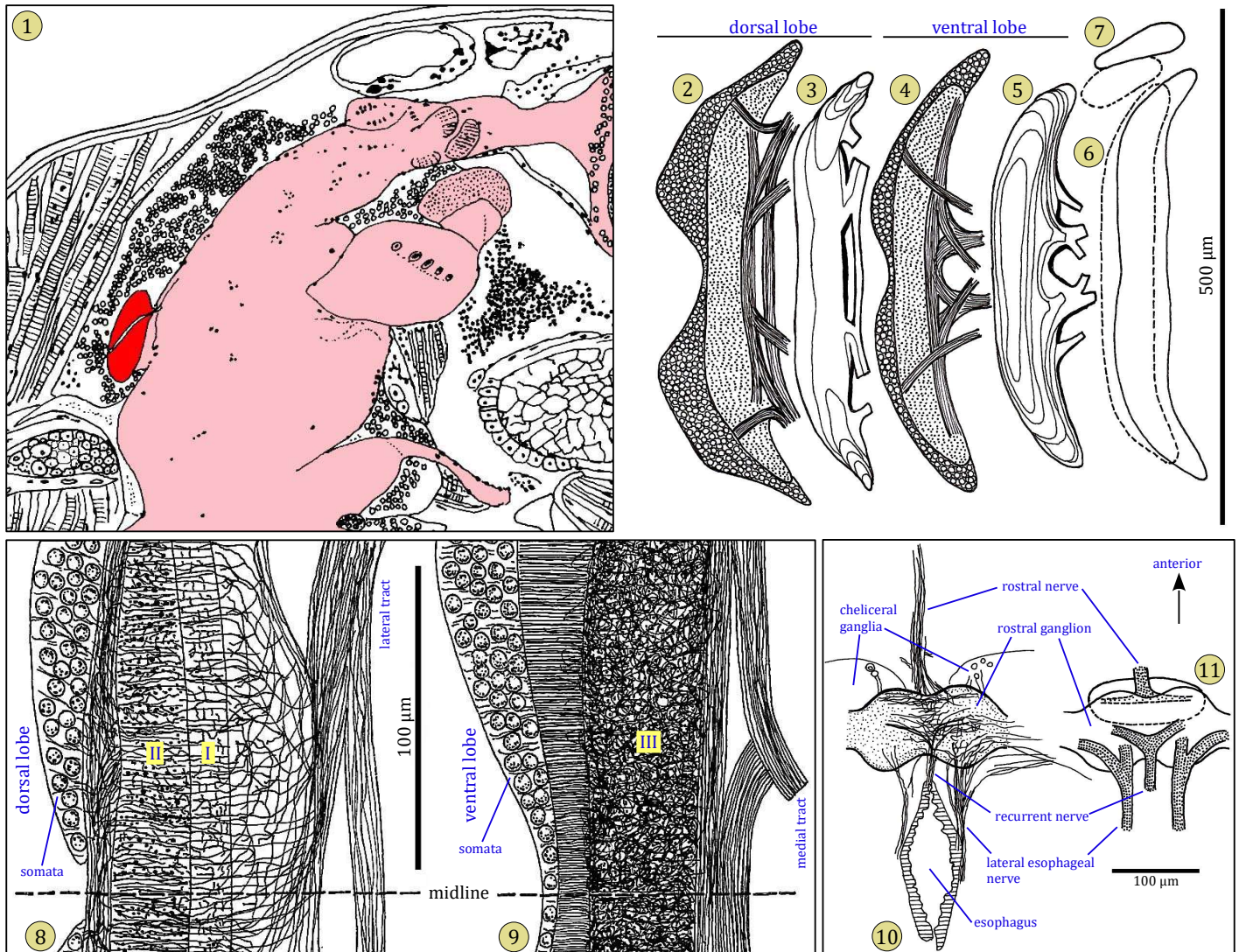


Figure 61. Other features of the protocerebrum or supraesophageal ganglia. **1**, Position of the central (arcuate or curved) body at the rear of the protocerebrum (bright red; parasagittal section of fifth instar *Phidippus clarus*). This is surrounded by the somata (cell bodies) of the interneurons that support the fibrous mass of the CNS. **2-7**, Schematic dorsal views of the central body, based primarily on examination of horizontal sections of sixth instar *P. johnsoni*. **2-3**, Dorsal lobe in section (2) and contour diagram (3) of the respective neuropile. **4-5**, Ventral lobe in section (4) and contour diagram of the respective neuropile (5). **6-7**, Relative positions of the dorsal and ventral lobe neuropiles in dorsal (6) and lateral (7) views. **8-9**, Semi-diagrammatic drawings of sections through the dorsal (8) and ventral (9) lobes of the central body. The wiring of the two lobes is different, and highly structured. Somata of the dorsal lobe are joined to two distinct synapsing zones or neuropiles (I and II) through a largely lateral tract just anterior to those somata. Large, laterally directed tracts lead from these neuropiles to other parts of the CNS, as shown in (2). Somata of the ventral lobe, in contrast, are joined to a more irregular neuropile (III) by parallel back-to-front fibers, and extrinsic fibers leading anteriorly from this neuropile are directed medially as shown in (4). **10-11**, Schematic (10, drawn from serial sections) and diagrammatic (11) views of the rostral ganglion, situated at the median, above the esophagus near the cheliceral ganglia. Note that the commissure of the cheliceral ganglia, like those of the pedipalp and leg ganglia, is subesophageal.

The *rostral ganglion* and its associated nerves (Figure 61:10) is positioned to play a key role with respect to coordination of feeding structures aligned in the sagittal plane (mouth, pharynx and sucking stomach), much like the buccal ganglion of snails (Kater 1974; Murphy 2001). This may involve coordination of the regular and pulsatile expansion of the pharynx and sucking stomach associated with ingestion of fluids (Hill 2011). Legendre (1959) proposed a double origin for the rostral ganglion, whereby the rostral ganglion is formed by the fusion of a pair of rostral neuromeres with a frontal ganglion. A paired origin for this composite structure is suggested by the lateral lobes depicted in Figure 61:10.

Non-visual sensory systems

Clearly the function of the eyes has been the primary subject for the study of salticid neurology. There are few studies of either motor functions or other sensory systems for salticids, although these have received a considerable amount of study in other spider families. The *bulbous setae* or *bulbosae* of certain amycoid salticids, including *Colonus*, have received some attention (Hill 2018a). These appear to be sensors for bioelectricity, perhaps detected through the separation of two fine, parallel processes in response to charging, but this needs to be verified. A reference to sensory systems that have been studied in other spiders is provided here in Table 11. The nature of the *graviceptors* used by salticids and other spiders is not known. Graviceptors are clearly of the greatest importance to salticids, which clearly orient with respect to gravity (Hill 1978, 1979, 2010a, 2010b). There are many possibilities here, ranging from cellular receptors to specific organs, or even the integration of information collected by distributed sensors (Hengstenberg 1993; Anken & Rahmann 2002; Bender & Frye 2009; Grob et al. 2020).

Table 11. Non-visual sensory systems of spiders.

#	system	references	description
1	tactile setae (mechanoreceptors)	Foelix & Chu-Wang 1973a; Harris & Mill 1973, 1977a; Foelix 1985a; Sivertsen 1989; Gronenberg 1990; Hill 2010c; Shamble et al. 2016	Sensitive to tactile stimuli. Sivertsen (1989) recorded CNS response to a <i>light touch</i> . Innervated spines and tenent setae of the feet are included in this category (Foelix 1985).
2	trichobothria	Frings & Frings 1966; Reissland & Görner 1985; Barth 1985b; Gronenberg 1989	Sensitive to airborne vibrations and air currents
3	slit-sensilla and lyriform organs	Pringle 1955; Walcott 1969; Seyfarth & Barth 1972; Seyfarth 1978, 1985; Barth 1985a, 1985b; Gronenberg 1989	Cuticular stress receptors or proprioceptors, sensitive to deformation (compression) by airborne and substrate borne vibrations
4	chemoreceptors	Foelix & Chu-Wang 1973b; Harris & Mill 1973, 1977b; Drewes & Bernard 1976; Hill 1977, 2010c; Foelix 1985a	Whorled or segmented setae, found at ends of legs and pedipalps, are contact chemoreceptors. Foelix (1985a) also reported the presence of <i>taste hairs</i> in <i>Liphistius</i> and <i>pore hairs</i> in <i>Gradulunga</i> .
5	graviceptors	Hill 1978, 1979, 2010a, 2010b; Görner & Claas 1985; Seyfarth, Gnatzy & Hammer 1990	Important but specific receptors not known, may be mechanoreceptors associated with the flexible whorled setae. There are many possibilities.
6	olfaction or hygromoreception	Foelix & Chu-Wang 1973b; Dumpert 1978; Foelix 1985a	Tarsal or pit organs on the dorsum of the tarsus, pheromone receptors in <i>Cupiennius</i> .
7	thermoreceptors	Foelix 1985a	
8	<i>trichoid</i> sensilla	Seyfarth 1985	Sensory hairs or spines bridging joints.
9	internal joint receptors	Foelix & Choms 1979; Seyfarth and Pflügler 1984; Seyfarth 1985	Proprioceptors that respond to strain of the joint membrane.
10	bulbous setae, or <i>bulbosae</i> (bioelectric sensors?)	Hill 2018a	Known only from <i>Colonus</i> and related amycoid salticids, these may be bioelectric sensors.

Other neural systems

A reference list of relevant studies is shown in Table 12.

Table 12. Efferent and neurosecretory systems of some arachnids. Except for entrainment of circadian rhythms by the secondary eyes (Tork 2019; Table 10:11), these have not been investigated in the Salticidae.

#	system	references	notes
1	Schneider's organs I and II, or retrocerebral neuroendocrine system	Babu 1973; Legendre 1985; Bonaric 1995	Function not clear, but may be involved in the regulation of ecdysis.
2	circadian rhythm	Fleissner & Fleissner 1985 (scorpions); Kovoov, Muñoz-Cuevas & Ortega-Escobar 2005; Tork 2019	Large fibers connected to the laminae (neuropile 1) of the secondary eyes of <i>Lycosa</i> connect with axons of neurosecretory cells in the same area.
3	cardiac ganglion	Sherman & Pax 1967, 1968; Sherman, Bursey, Fourtner and Pax 1969; Bursey & Sherman 1970; Sherman 1985	Control of heartbeat. Middorsal position along length of the heart.
4	motor neurons	Root 1985	Based on findings with scorpions, large somata associated with motoneurons, should be below each respective leg ganglion, where each ramifies with many dendrites around a large axon that extends into that leg.

Electrophysiology

There are few available electrophysiological studies of salticid neurons, two related to vision and one related to hearing or sensitivity to airborne vibrations (Table 13).

Table 13. Neurophysiological recordings of individual neurons.

#	reference	description
1	Sivertsen 1989	Recorded responses of 150 units, including 64 responsive to images presented to the anterior eyes, from neuron somata at the front of the protocerebrum of <i>Phidippus</i> spp. Cells driven by the AME (n=18) responded to a stable location relative to the prosoma and a visual field wider than the retina of that eye. Some cells driven by the AME exhibited size-constancy, with a decreasing visual field with increasing distance. Some AME cells were selective for a stimulus moving at 16°/s. Some cells responded according to orientation and direction of movement. Some cells (n=7) responded to touch or a <i>breath of air</i> on the pedipalps.
2	Menda, Shamble, Nitzany, Golden & Hoy 2014	Recorded responses of 53 units for 33 different animals, including responses of 9 neurons from 6 spiders to images presented to the anterior eyes, from neuron somata just behind and below the central body of <i>Phidippus audax</i> . Best response was to 6-25° high contrast bars moved horizontally at 25°/s. One unit had a well-defined <i>spatiotemporal</i> response only when both AME and ALE were unmasked.
3	Shamble et al. 2016	Auditory-sensitive units of <i>Phidippus audax</i> responded to low frequency airborne tones (80/s, ~65 dB) that also led the spiders to stop their movements. Mechanical stimulation of setae on patella I also generated this response, supporting the view that these are tactile receptors.

Sivertsen (1989) recorded responses to front eye (AME and ALE) stimuli from neurons with tungsten microelectrodes inserted into cell bodies *anterior to the protocerebrum* of a *Phidippus*, not correlated however with their location or function (Table 14). Of these responses, *size-constancy* is perhaps the most interesting, although Sivertsen's data pertaining to this subject is limited. Konkle & Oliva (2012) found that neurons in the human occipitotemporal cortex were organized spatially according to their response to *object size*, and it is possible that something similar could be found in salticids.

Electrophysiological recording from single neurons is difficult in salticids, in large part because of the challenge of penetrating the hard cuticle of the carapace (Sivertsen 1989; Menda et al 2014). At the same time, monitoring responses of individual cells that can be marked may represent our best opportunity to learn more about the neurological correlates of information processing.

Table 14. Neuron responses detected by Sivertsen (1989). Of 150 single or multiple units that were monitored, 64 were responsive to visual signals (*light or dark contours*, or a *light bar*). Visual responses were only observed when the microelectrode penetrated 0.9-1.1 mm into the protocerebrum.

#	stimulus applied to	units	description of response
1	AME	22	Average receptive field $\Omega = 234 \text{ deg}^2$ (range 8.7-1255 deg^2). Receptive field, larger than the static field of the retina, was constant with respect to the carapace.
2	ALE or ALE and ipsilateral AME	6	Average receptive field $\Omega = 2375 \text{ deg}^2$ (range 118-1600 deg^2).
3	AME	n=?	Constant receptive field Ω .
4	AME	n=?	Beyond a certain distance response was size-constant, source of distance information may come from plane of focus (Land 1969a).
5	AME	7	Maximum response to stimuli moving at $16^\circ/\text{s}$, corresponding to retinal movements described by Land (1969b, 1971).
6	AME	3	Maximum response to stimuli moving at 128 deg/s , or faster. Stronger response to movement aligned with the long axis of the AME retina.
7	AME and ipsilateral ALE	2	Maximum response to stimuli moving at 128 deg/s , or faster. Stronger response to movement aligned with the long axis of the AME retina.
8	AME	13	Preferred one direction of movement over the opposite direction.
9	AME and 2? ALE	2	Preferred one direction of movement over the opposite direction.
10	2 AME and 2 ALE	1	Not as well-tuned to one direction of movement as a single AME.
11	AME and 0-2 ALE	16	Half (n=8) preferred responded best to upward movement, half of these (n=4) had a second preference for downward movement, and medial to lateral movement was the first or second preference of 5 units.
12	either AME or ALE or both	7	Transient response to termination of a series of flashes of a light bar, delayed by an average 62.9 msec (range 30-95 msec).
13	either AME or ALE or both	15	Transient response to termination of a stimulus, delayed by an average of 125 msec (range 40-255 msec); the delay correlated positively with the degree to which sensitivity was correlated with the direction of movement (high <i>tuning index</i>).
14	pedipalps	7	Active in response to <i>light touch or breath of air</i> .
15	no stimulus	20	Spiking at regular periodicity of ~ 70 msec over intervals of minutes to hours (<i>clock cells</i>), for some the frequency could be increased for ~ 30 sec by visual or other stimulation.
16	no stimulus	?	Rhythmic pulses from 0.5/sec to 5/sec, varying over time, perhaps as a result of motor activity.
17	2 AME and 2 ALE	2	Variable sensitivity and of response over a large field, sensitive to direction, degree and latency of contrast, responding best to the onset of motion of a small (subtending $\sim 1^\circ$) black spot.

Acknowledgements

I am grateful to Christopher J. Bayne for his support of my first studies of salticid neurology at Oregon State University. I am also grateful to Hugh Dingle, Stanley B. Kater, Jonathan R. Reiskind and Thomas Eisner for their support of my later studies of salticid behavior and neurology. Thanks also to Bruce Cutler, G. B. Edwards, Jürgen Otto and David B. Richman for introducing me to many of these remarkable spiders, and to Gio Diaz, Wayne Maddison, Aaron Morales, Jürgen Otto, Sarab Seth and Thomas Shahan for permitting the use and modification of their photographs. Early access to the works of Michael F. Land was an inspiration, as are memories of related conversations in California with Richard M. Eakin, Jean L. Brandenburger, and B. J. Kaston. Finally I thank my dear wife Rose Marie, who has supported me through many years filled with unusual pursuits.

All errors related to representation of information in this paper are my own, and any additional information or corrections will be welcome. As this is a complex and active subject of research on many fronts, it is hoped that the current version will stimulate some thinking and that useful feedback can be incorporated into a subsequent version of this document.

All components of this paper that are not otherwise attributed are ©D. E. Hill and may be used freely under the terms of a [CC BY 4.0](#) license, with attribution to *D. E. Hill*. The entire paper may be freely replicated, posted or distributed under the terms of a [CC BY-NC-ND 4.0](#) license.

References

- Angelini, D. R., P. Z. Liu, C. L. Hughes and T. C. Kaufman. 2005.** Hox gene function and interaction in the milkweed bug *Oncopeltus fasciatus* (Hemiptera). *Developmental Biology* 287: 440-455.
- Anken, R. H. and H. Rahmann. 2002.** Gravitational zoology: how animals use and cope with gravity. In: *Astrobiology The Quest for the Conditions of Life*, eds. G. Horneck and C. Baumstark-Khan, Springer: 315-333.
- Audouin, V. 1826.** Explication sommaire des planches d'arachnides de l'Égypte et de la Syrie. In: *Description de l'Égypte, ou recueil des observations et des recherches qui ont été faites en Égypte pendant l'expédition de l'armée française, publié par les ordres de sa Majesté l'Empereur Napoléon le Grand*. *Histoire Naturelle* 1 (4): 1-339.
- Babu, K. S. 1965.** Anatomy of the central nervous system of arachnids. *Zoologische Jahrbücher, Abteilung für allgemeine Zoologie und Physiologie der Tiere* 82: 1-154.
- Babu, K. S. 1973.** Histology of the neurosecretory system and neurohemal organs of the spider *Argiope aurantia* (Lucas). *Journal of Morphology* 141: 77-98.
- Babu, K. S. 1985.** Patterns of arrangement and connectivity in the central nervous system of arachnids. Chapter I in: *Neurobiology of Arachnids*, ed. F. G. Barth, Springer-Verlag: 3-19.
- Babu, K. S. and F. G. Barth. 1984.** Neuroanatomy of the central nervous system of the wandering spider, *Cupiennius salei*. *Zoomorphology* 104: 344-359.
- Bach, M. 2022.** 147 visual phenomena & optical illusions. *Online at: <https://michaelbach.de/ot/index.html>*
- Banks, N. 1929.** Spiders from Panama. *Bulletin of the Museum of Comparative Zoology* 69: 53-96.
- Barth, F. G. 1985a.** Slit sensilla and the measurement of cuticular strains. Chapter IX in: *Neurobiology of Arachnids*, ed. F. G. Barth, Springer-Verlag: 162-188.
- Barth, F. G. 1985b.** Neuroethology of the spider vibration sense. Chapter XI in: *Neurobiology of Arachnids*, ed. F. G. Barth, Springer-Verlag: 203-229.
- Barth, F. G. 2002.** *A Spider's World: Senses and Behavior*. Springer-Verlag: i-xiv, 1-394.
- Bartos, M. 2000.** Distance of approach to prey is adjusted to the prey's ability to escape in *Yllenus arenarius* Menge (Araneae, Salticidae). *European Arachnology 2000. Proceedings of the 19th European Colloquium of Arachnology*: 33-38.
- Becker, N., S. Prasad-Shreckengast and S. Byosiere. 2021.** Methodological challenges in the assessment of dogs' (*Canis lupus familiaris*) susceptibility of the Ebbinghaus-Titchener illusion using the spontaneous choice task. *Animal Behavior and Cognition*. 8 (2): 138-151.
- Behrens, C., T. Schubert, S. Haverkamp, T. Euler and P. Berens. 2016.** Connectivity map of bipolar cells and photoreceptors in the mouse retina. *eLife* 5 (e20041): 1-20. DOI: 10.7554/eLife.20041.
- Bender, J. and M. Frye. 2009.** Invertebrate solutions for sensing gravity. *Current Biology*, 19 (5): R186-R190.
- Bennett, T. J. and R. D. Lewis. 1979.** Visual orientation in the Salticidae (Araneae). *New Zealand Entomologist* 7 (1): 58-63.
- Blest, A. D. 1983.** Ultrastructure of secondary retinæ of primitive and advanced jumping spiders (Araneae, Salticidae). *Zoomorphology* 102: 125-141.
- Blest, A. D. 1984.** Ultrastructure of the secondary eyes of a primitive jumping spider, *Yaginumanis*. *Zoomorphology* 104: 223-225.
- Blest, A. D. 1985a.** Retinal mosaics of the principal eyes of jumping spiders (Salticidae) in some neotropical habitats: optical trade-offs between sizes and habitat illuminances. *Journal of Comparative Physiology A* 157: 391-404.
- Blest, A. D. 1985b.** The fine structure of spider photoreceptors in relation to function. Chapter V in: *Neurobiology of Arachnids*, ed. F. G. Barth, Springer-Verlag: 79-102.
- Blest, A. D. 1987.** The retinæ of *Euryattus bleekeri*, an aberrant salticid spider from Queensland. *Journal of Zoology, London* 211: 399-408.
- Blest, A. D. 1988.** Post-embryonic development of the principal retina of a jumping spider I. The establishment of retinal tiering by conformational changes. *Philosophical Transactions of the Royal Society of London B* 320: 489-504.
- Blest, A. D. and M. Carter. 1987.** Morphogenesis of a tiered principal retina and the evolution of jumping spiders. *Nature* 328: 152-155.
- Blest, A. D. and M. Carter. 1988.** Post-embryonic development of the principal retina of a jumping spider II. The acquisition and reorganization of rhabdomeres and growth of the glial matrix. *Philosophical Transactions of the Royal Society of London B* 320: 505-515.
- Blest, A. D., R. C. Hardie, P. McIntyre and D. S. Williams. 1981.** The spectral sensitivities of identified receptors and the function of retinal tiering in the principal eyes of a jumping spider. *Journal of Comparative Physiology* 145: 227-239.
- Blest, A. D. and J. Maples. 1979.** Exocytotic shedding and glial uptake of photoreceptor membrane by a salticid spider. *Proceedings of the Royal Society of London B* 204: 105-112.
- Blest, A. D., P. McIntyre and M. Carter. 1988.** A re-examination of the principal retinæ of *Phidippus johnsoni* and *Plexippus validus* (Araneae: Salticidae): implications for optical modelling. *Journal of Comparative Physiology A* 162: 47-56.
- Blest, A. D., D. C. O'Carroll and M. Carter. 1990.** Comparative ultrastructure of Layer I receptor mosaics in principal eyes of jumping spiders: the evolution of regular arrays of light guides. *Cell and Tissue Research* 262: 445-460.

- Blest, A. D. and G. D. Price. 1984.** Retinal mosaics of the principal eyes of some jumping spiders (Salticidae: Araneae): adaptations for high visual acuity. *Protoplasma* 120: 172-184.
- Blest, A. D. and C. Sigmund. 1984.** Retinal mosaics of the principal eyes of two primitive jumping spiders, *Yaginumanis* and *Lyssomanes*: clues to the evolution of salticid vision. *Proceedings of the Royal Society of London B* 221: 111-125.
- Blest, A. D. and C. Sigmund. 1985.** Retinal mosaics of a primitive jumping spider, *Spartaeus* (Salticidae: Araneae): a transition between principal retinae serving low and high spatial acuities. *Protoplasma* 125: 129-139.
- Bloom, M. and M. A. Berkley. 1977.** Visual acuity and the near point of accommodation in cats. *Vision Research* 17 (6): 723-730.
- Bonaric, J. 1995.** Le système neuroendocrine rétro-cérébral des Araignées: structure et fonction. *Proceedings of the 15th European Colloquium of Arachnology*: 27-34.
- Bridgeman, B. 2007.** Efference copy and its limitations. *Computers in Biology and Medicine* 37: 924-929.
- Bruce, M., D. Daye, S. M. Long, A. M. Winsor, G. Menda, R. R. Hoy and E. M. Jakob. 2021.** Attention and distraction in the modular visual system of a jumping spider. *Journal of Experimental Biology* 224: 1-5.
- Burse, C. R. and R. G. Sherman. 1970.** Spider cardiac physiology I, structure and function of the cardiac ganglion. *Comparative and General Pharmacology* 1: 160-170.
- Carroll, J., C. J. Murphy, M. Neitz, J. N. Ver Hoeve and J. Neitz. 2001.** Photopigment basis for dichromatic color vision in the horse. *Journal of Vision* 1: 80-87.
- Caves, E. M. and S. Johnsen. 2018.** AcuityView: an R package for portraying the effects of visual acuity on scenes observed by an animal. *Methods in Ecology and Evolution, British Ecological Society* 9: 793-797, supporting table S1.
- Cerveira, A. M., R. R. Jackson and X. J. Nelson. 2019.** Dim-light vision in jumping spiders (Araneae, Salticidae): identification of prey and rivals. *Journal of Experimental Biology* 222, jeb198069: 1-7.
- Charman, W. N. 1991.** Optics of the human eye. In: *Visual Optics and Instrumentation*, ed. J. Cronley Dillon, CRC Press, Boca Raton: 1-26.
- Chaya, T., A. Mastsumato, Y. Sugita, S. Watanabe, R. Kuwahara, M. Tachibana and T. Furukawa. 2017.** Versatile functional roles of horizontal cells in the retinal circuit. *Scientific Reports* 7 (5540): 1-15.
- Chen, S. and W. Li. 2013.** A color coding amacrine cell may provide a "Blue-Off" signal in a mammalian retina. *Nature Neuroscience* 15 (7): 954-956.
- Clark, D. L. and C. L. Morjan. 2001.** Attracting female attention: the evolution of dimorphic courtship displays in the jumping spider *Maevia inclemens* (Araneae: Salticidae). *Proceedings of the Royal Society London B* 268: 2461-2465.
- Clark, D. L. and G. W. Uetz. 1993.** Signal efficacy and the evolution of male dimorphism in the jumping spider, *Maevia inclemens*. *Proceedings of the National Academy of Sciences of the United States of America* 90 (24): 11954-11957.
- Clerck, C. 1757.** Aranei Svecici. Svenska spindlar, uti sina hufvud-slägter indelte samt under några och sextio särskildte arter beskrefne och med illuminerade figurer uplyste. Laurentius Salvius, Stockholmiae: 1-154.
- Crocker, R. L. and R. B. Skinner. 1984.** Boolean model of the courtship and agonistic behavior of *Hentzia palmarum* (Araneae: Salticidae). *Florida Entomologist* 67 (1): 97-106.
- Curtis, J. L. 1892.** A new jumping spider. *Zoe* 3: 332-337.
- Dacke, M., T. A. Doan and D. C. O'Carroll. 2001.** Polarized light detection in spiders. *The Journal of Experimental Biology* 204: 2481-2490.
- Damen, W. G. M. 2002.** Parasegmental organization of the spider embryo implies that the parasegment is an evolutionary conserved entity in arthropod embryogenesis. *Development* 129: 1239-1250.
- Damen, W. G. M., M. Hausdorf, E. Seyfarth and D. Tautz. 1998.** A conserved mode of head segmentation in arthropods revealed by the expression pattern of Hox genes in a spider. *Proceedings of the National Academy of Sciences, USA* 95: 10665-10670.
- Damen, W. G. M. and D. Tautz. 1999.** Comparative molecular embryology of arthropods: the expression of Hox genes in the spider *Cupiennius salei*. *Invertebrate Reproduction and Development* 36: (1-3): 203-209.
- Davey, M. P., M. V. Srinivasan and T. Maddess. 1998.** The Craik-O'Brien-Cornsweet illusion in honeybees. *Naturwissenschaften* 85: 73-75.
- De Agrò, M., D. C. Rößler, K. Kim and P. S. Shamble. 2021.** Perception of biological motion by jumping spiders. *PLoS Biology* 19 (7, e3001172): 1-16.
- Defrize, J., C. R. Lazzari, E. J. Warrant and J. Casas. 2011.** Spectral sensitivity of a colour changing spider. *Journal of Insect Physiology* 57 (4): 508-513.
- DeVoe, R. D. 1972.** Dual sensitivities of cells in wolf spider eyes at ultraviolet and visible wavelengths of light. *The Journal of General Physiology* 59: 247-269.
- DeVoe, R. D. and J. E. Zvargulis. 1967.** Spectral sensitivities of vision in wolf spiders and jumping spiders. *Federation Proceedings* 26: 655.
- DeVoe, R. D., R. J. W. Small and J. E. Zvargulis. 1969.** Spectral sensitivities of wolf spider eyes. *The Journal of General Physiology* 54: 1-32.
- DeVoe, R. D. 1975.** Ultraviolet and green receptors in principal eyes of jumping spiders. *Journal of General Physiology* 66: 193-207.

- Döffinger, C. M. 2010.** Early steps in ventral nerve cord development in chelicerates and myriapods and formation of brain compartments in spiders. Ph.D. dissertation, Johannes Gutenberg-Universität, Mainz: i-x, 1-161.
- Doleschall, L. 1859.** Tweede Bijdrage tot de kennis der Arachniden van den Indischen Archipel. Acta Societatis Scientiarum Indica-Neerlandica 5: 1-60.
- Dolev, Y. 2016.** Visual perception in jumping spiders. Ph.D. Dissertation, University of Canterbury: i-vii, 1-177.
- Drees, O. 1952.** Untersuchungen über die angeborenen Verhaltensweisen bei Springspinnen (Salticidae). Zeitschrift für Tierpsychologie 9: 169-207.
- Drewes, C. D. and R. A. Bernard. 1976.** Electrophysiological responses of chemosensitive sensilla in the wolf spider. Journal of Experimental Zoology 198: 423-428.
- Duelli, P. 1975.** Bewegungs-Lokalisation in den Posterolateral-Augen von *Evarcha arcuata* (Salticidae, Araneae). Preliminary results, 20.II.75: 1-8.
- Duelli, P. 1977.** Evidence for an off-pass-filter in the movement detecting system of jumping spiders (*Evarcha arcuata*, Salticidae). Proceedings of the Australian Physiological and Pharmacological Society 8: 98.
- Duelli, P. 1978.** Movement detection in the posterolateral eyes of jumping spiders (*Evarcha arcuata*, Salticidae). Journal of Comparative Physiology 124: 15-26.
- Duelli, P. 1980.** The neuronal organization of the posterior lateral eyes of jumping spiders (Salticidae). Zoologisches Jahrbuch, Abteilung Anatomie 103: 17-40.
- Dumpert, K. 1978.** Spider odor receptor: electrophysiological proof. Experientia 34: 754-755.
- Duncan, R. O. and G. M. Boynton. 2003.** Cortical magnification within human primary visual cortex correlates with acuity thresholds. Neuron 38: 659-671.
- Eakin, R. M. and J. L. Brandenburger. 1971.** Fine structure of the eyes of jumping spiders. Journal of Ultrastructure Research 37: 618-663.
- Eberhard, W. G. and W. T. Wcislo. 2011.** Grade changes in brain-body allometry: morphological and behavioural correlates of brain size in miniature spiders, insects and other invertebrates. In: *Advances in Insect Physiology, Volume 40*, ed. Jérôme Casas, Academic Press, Burlington: 155-214.
- Edwards, G. B. 2020.** Description of *Phidippus pacosauritus* sp. nov. (Salticidae: Salticinae: Dendryphantini: Dendryphantina), with a reanalysis of related species in the *mystaceus* group. Peckhamia 221.1: 1-18.
- Einthoven, W. 1885.** Stereoscopie durch Farbendifferenz. Graefe's Archiv für Ophthalmologie 31:211-238.
- Elias, D. O., B. R. Land, A. C. Mason and R. R. Hoy. 2006.** Measuring and quantifying dynamic visual signals in jumping spiders. Journal of Comparative Physiology A 192, 785-797.
- Elias, D. O., W. P. Maddison, C. Peckmezian, M. B. Girard and A. C. Mason. 2012.** Orchestrating the score: complex multimodal courtship in the *Habronattus coecatus* group of *Habronattus* jumping spiders (Araneae: Salticidae). Biological Journal of the Linnean Society 105 (3): 522-547.
- Faubert J. 1994.** Seeing depth in colour: More than just what meets the eyes. Vision Research 34: 1165-1186.
- Field, G. D., J. L. Gauthier, A. Sher, M. Greschner, T. A. Machado, L. H. Jepson, J. Shlens, D. E. Gunning, K. Mathieson, W. Dabrowski, L. Paninski, A. M. Litke and E. J. Chichilnisky. 2010.** Functional connectivity in the retina at the resolution of photoreceptors. Nature 467: 673-678.
- Fite, K. V. 1973.** Anatomical and behavioural correlates of visual acuity in the great horned owl. Vision Research 13: 219-230.
- Fleissner, G. and G. Fleissner. 1985.** Neurobiology of a circadian clock in the visual system of scorpions. Chapter XVIII in: *Neurobiology of Arachnids*, ed. F. G. Barth, Springer-Verlag: 351-375.
- Foelix, R. F. 1985a.** Mechano- and chemoreceptive sensilla. Chapter VII in: *Neurobiology of Arachnids*, ed. F. G. Barth, Springer-Verlag: 118-137.
- Foelix, R. F. 2011.** *Biology of Spiders*. Third Edition. Oxford University Press. i-vii, 1-419.
- Foelix, R. F. and I. W. Chu-Wang. 1973a.** The morphology of spider sensilla. I. Mechanoreceptors. Tissue Cell 5: 451-460.
- Foelix, R. F. and I. W. Chu-Wang. 1973b.** The morphology of spider sensilla. I. Chemoreceptors. Tissue Cell 5: 451-460.
- Foelix, R. F. and B. Erb. 2011.** Microscopical studies on exuviae of the jumping spider *Phidippus regius*. Peckhamia 90.1: 1-15.
- Franze, K, J. Grosche, S. N. Skatchkov, S. Schinkinger, C. Foja, D. Schild, O. Uckermann, K. Travis, A. Reichenbach and J. Guck. 2007.** Müller cells are living optical fibers in the vertebrate retina. Proceedings of the National Academy of Sciences, USA 104 (20): 8287-8292.
- Frings, H. and M. Frings. 1966.** Reactions of orb-weaving spiders (Argiopidae) to airborne sounds. Ecology 47:578 - 588.
- Gabe, M. 1954.** Emplacement et connexions des cellules neurosecretrices chez quelques araneids. Comptes Rendus hebdomadaires des Seances de l'Academie des Sciences Paris 238: 1265-1267.
- Gardner, B. T. 1966.** Hunger and characteristics of the prey in the hunting behavior of salticid spiders. Journal of Comparative Physiology and Psychology 62: 475-478.
- Geisler, W. S. 1984.** Physical limits of acuity and hyperacuity. Journal of the Optical Society of America A 1 (7): 775-782.
- Gerstaecker, A. 1873.** Arachnoidea. In: Die Gliederthier-Fauna des Sansibar-Gebietes. Nach dem von Dr. O. Kersten während der v. d. Decken'schen Ost-Afrikanischen Expedition im Jahre 1862 und von C. Cooke auf der Insel Sansibar im Jahre 1864 gesammelten Material. C. F. Winter, Leipzig: 461-503, pl. 18.

- Girard, M. B., M. M. Kasumovic and D. O. Elias. 2011.** Multi-modal courtship in the Peacock Spider, *Maratus volans* (O.P.-Cambridge, 1874). PLoS ONE 6 (9): e25390: 1-10 (doi:10.1371/journal.pone.0025390).
- Giribet, G., G. D. Edgecombe and W. C. Wheeler. 2001.** Arthropod phylogeny based on eight molecular loci and morphology. *Nature* 413: 157-161.
- Glasser, A., M. T. Pardue, M. E. Andison and J. G. Sivak. 1997.** A behavioral study of refraction, corneal curvature, and accommodation in raptor eyes. *Canadian Journal of Zoology* 75: 2010-2020.
- Glenszyk, M., D. Outomuro, M. Gregorič, S. Kralj-Fišer, J. M. Schneider, D. Nilsson, N. I. Morehouse and C. Tedore. 2022.** The jumping spider *Saitis barbipes* lacks a red photoreceptor to see its own sexually dimorphic red coloration. *The Science of Nature* 109 (6): 1-13 (<https://doi.org/10.1007/s00114-021-01774-6>).
- Gomes, A. D., H. Bartelt and O. Frazão. 2021.** Optical vernier effect: recent advances and developments. *Laser Photonics Review* 2021 (2000588): 1-16.
- Goodman, J. W. 1968.** *Introduction to Fourier Optics*. McGraw-Hill Physical and Quantum Electronics Series. McGraw-Hill, New York. i-xiv, 1-287.
- Gorner, P. and B. Claas. 1985.** Homing behavior and orientation in the funnel-web spider, *Agelena labyrinthica*. Chapter XIV in: *Neurobiology of Arachnids*, ed. F. G. Barth, Springer-Verlag: 275-297.
- Goté, J. T., P. M. Butler, D. B. Zurek and E. K. Buschbeck. 2019.** Growing tiny eyes: how juvenile jumping spiders retain high visual performance in the face of size limitations and developmental constraints. *Vision research* 160: 24-36.
- Gray, H. and W. H. Lewis. 1918.** *Anatomy of the Human Body*, Twentieth Edition. Lea & Febiger, Philadelphia and New York. 1-1396.
- Gregory, R. L. and P. Heard. 1979.** Border locking and the Café Wall illusion. *Perception* 8: 365-380.
- Griswold, C. E. 1979.** New species of *Pellenes* from California (Araneae: Salticidae). *Journal of Arachnology* 7: 129-138.
- Grob, R., C. Tritscher, K. Grübel, C. Stigloher, C. Groh, P. N. Fleischmann and W. Rössler. 2020.** Johnston's organ and its central projections in *Cataglyphis* desert ants. *Journal of Comparative Neurology* 529 (8): 2138-2155.
- Gronenberg, W. 1989.** Anatomical and physiological observations on the organization of mechanoreceptors and local interneurons in the central nervous system of the wandering spider *Cupiennius salei*. *Cell and Tissue Research* 258: 163-175.
- Gronenberg, W. 1990.** The organization of plurisegmental mechanosensitive interneurons in the central nervous system of the wandering spider *Cupiennius salei*. *Cell and Tissue Research* 260: 49-61.
- Gross, H., F. Blechinger, W. Singer and B. Ahtner. 2008.** Human eye. Chapter 36 in: *Handbook of Optical Systems, Vol. 4, Survey of Optical Instruments*, ed. H. Gross. Wiley-Blackwell. 1-1092.
- Halanych, K. M., and A. M. Janosik. 2006.** The state of annelid phylogeny. *Integrative and Comparative Biology* 46: 533-543.
- Hamer, R. D., F. A. Carvalho and D. F. Ventura. 2013.** Effect of contrast and gaps between Vernier stimulus elements on sweep visual evoked potential measurements of human cortical Vernier responses. *Psychology and Neuroscience* 6 (2): 199-212.
- Hanström, B. 1921.** Über die Histologie und vergleichende Anatomie der Sehganglien und Globuli der Araneen. *Kungliga Svenska Vetenskapsakademiens Handlingar* 61 (12): 1-39.
- Hanström, B. 1935.** Fortgesetzte Untersuchungen über das Araneengehirn. *Zoologische Jahrbücher, Abteilung für Anatomie und Ontogenie der Tiere* 59: 455-478.
- Hardie, R. C. and P. Duelli. 1978.** Properties of single cells in the posterior lateral eyes of jumping spiders. *Zeitschrift für Naturforschung* 33c: 156-158.
- Harland, D. P. and R. R. Jackson. 2000.** 'Eight-legged cats' and how they see - a review of recent research on jumping spiders. *Cimbebasia* 16: 231-240.
- Harland, D. P. and R. R. Jackson. 2001a.** Cues by which *Portia fimbriata*, an araneophagic jumping spider, distinguishes jumping-spider prey from other prey. *The Journal of Experimental Biology* 203: 3485-3494.
- Harland, D. P. and R. R. Jackson. 2001b.** Prey classification by *Portia fimbriata*, a salticid spider that specializes at preying on other salticids: species that elicit cryptic stalking. *Journal of Zoology, London* 255: 455-460.
- Harland, D. P. and R. R. Jackson. 2002.** Influence of cues from the anterior medial eyes of virtual prey on *Portia fimbriata*, an araneophagic jumping spider. *The Journal of Experimental Biology* 205: 1861-1868.
- Harland, D. P., D. Li and R. R. Jackson. 2012.** How jumping spiders see the world. Chapter 9 in: *How Animals See the World: Comparative Behavior, Biology, and Evolution of Vision*, eds. O. F. Lazareva, T. Shimizu, & E. A. Wasserman, Oxford University Press: 133-163.
- Harris, D. J. and P. J. Mill. 1973.** The ultrastructure of chemoreceptor sensilla in *Ciniflo* (Araneida, Arachnida). *Tissue Cell* 5: 679-689.
- Harris, D. J. and P. J. Mill. 1977a.** Observations on the leg receptors of *Ciniflo* (Araneida, Dictynidae). I. External mechanoreceptors. *Journal of Comparative Physiology* 119: 37-54.
- Harris, D. J. and P. J. Mill. 1977b.** Observations on the leg receptors of *Ciniflo* (Araneida, Dictynidae). II. Chemoreceptors. *Journal of Comparative Physiology* 119: 55-62.

- Hashimi, H., M. Pakbin, B. Ali, A. Yekta, H. Ostadimoghaddam, A. Asharlous, M. Aghamirsalim and M. Khabazkhoob. 2019.** Near points of convergence and accommodation in a population of university students in Iran. *Journal of Ophthalmic and Vision Research* 14 (3): 306-314.
- Hengstedberg, R. 1993.** Multisensory control in insect oculomotor systems. Chapter 13 in: *Visual Motion and its Role in the Stabilization of Gaze*, eds. F. A. Miles and J. Wallman, Elsevier: 285-298.
- Hentz, N. M. 1846.** Descriptions and figures of the araneides of the United States. *Boston Journal of Natural History* 5: 352-370.
- Hering, E. 1964.** *Outlines of a Theory of the Light Sense*. English translation from the German by L. M. Hurvich and D. Jameson. Harvard University Press, Cambridge, Massachusetts. 1-317.
- Hill, D. E. 1975.** The structure of the central nervous system of jumping spiders of the genus *Phidippus* (Araneae: Salticidae). M.S. thesis, Oregon State University: i-ix, 1-94.
- Hill, D. E. 1977.** The pretarsus of salticid spiders. *Zoological Journal of the Linnean Society* 60 (4): 319-338.
- Hill, D. E. 1978.** Orientation by jumping spiders of the genus *Phidippus* (Araneae: Salticidae) during the pursuit of prey. Ph.D. dissertation, University of Florida: i-v, 1-202.
- Hill, D. E. 1979.** Orientation by jumping spiders of the genus *Phidippus* (Araneae: Salticidae) during the pursuit of prey. *Behavioral Ecology and Sociobiology* 5: 301-322.
- Hill, D. E. 2006.** The structure of the central nervous system of jumping spiders of the genus *Phidippus* (Araneae: Salticidae). Republication Version 1. Peckhamia Epublications: 1-46.
- Hill, D. E. 2010a.** Use of location (relative direction and distance) information by jumping spiders (Araneae, Salticidae, *Phidippus*) during movement toward prey and other sighted objectives. *Peckhamia* 83.1: 1-103.
- Hill, D. E. 2010b.** Targeted jumps by salticid spiders (Araneae: Salticidae: *Phidippus*). *Peckhamia* 84.1: 1-35.
- Hill, D. E. 2010c.** Jumping spider feet (Araneae: Salticidae). *Peckhamia* 85.1: 1-48.
- Hill, D. E. 2011.** The jumping spider mouth (Araneae: Salticidae). *Peckhamia* 97.1: 1-17.
- Hill, D. E. 2018a.** Notes on the jumping spiders *Colonus puerperus* (Hentz 1846) and *Colonus sylvanus* (Hentz 1846) in the southeastern United States (Araneae: Salticidae: Amycoidea: Gophoini). *Peckhamia* 99.2: 1-63.
- Hill, D. E. 2018b.** The jumping behavior of jumping spiders: a review (Araneae: Salticidae). *Peckhamia* 167.1: 1-8.
- Hill, D. E. 2020.** Respiration by jumping spiders (Araneae: Salticidae). *Peckhamia* 225.1: 1-28.
- Hill, D. E. and D. B. Richman. 2009.** The evolution of jumping spiders (Araneae: Salticidae): a review. *Peckhamia* 75.1: 1-7.
- Hill, D. E., D. L. Glaser and E. C. Galvão. 2021.** Extension of fangs during the predatory jumps of jumping spiders (Araneae: Salticidae). *Peckhamia* 242.1: 1-9.
- Hill, D. E. and J. C. Otto. 2011.** Visual display by male *Maratus pavonis* (Dunn 1947) and *Maratus splendens* (Rainbow 1896) (Araneae: Salticidae: Euophryinae). *Peckhamia* 89.1: 1-41.
- Hoefler, C. D. and E. M. Jakob. 2006.** Jumping spiders in space: movement patterns, nest site fidelity and the use of beacons. *Animal Behaviour* 71: 109-116.
- Homann H. 1928.** Beiträge zur Physiologie der Spinnenaugen. I. Untersuchungsmethoden. II. Das Sehvermögen der Salticiden. *Zeitschrift für vergleichende Physiologie* 7: 201-268.
- Homann, H. 1950.** Die Nebenaugen der Araneen. *Zoologische Jahrbücher, Abteilung für Anatomie und Ontogenie der Tiere* 71: 56-144.
- Homann, H. 1952.** Die Nebenaugen der Araneen. Zweite Mitteilung. *Zoologische Jahrbücher, Abteilung für Anatomie und Ontogenie der Tiere* 72: 345-364.
- Howard, S. R., A. Avargue's-Weber, J. E. Garcia, D. Stuart-Fox and A. G. Dyer. 2017.** Perception of contextual size illusions by honeybees in restricted and unrestricted viewing conditions. *Proceedings of the Royal Society B* 284 (20172278): 1-9.
- Hu, Z., F. Liu, X. Xu, Z. chen, J. Chen and D. Li. 2012.** Spectral transmission of the principal-eye corneas of jumping spiders: implications for ultraviolet vision. *The Journal of Experimental Biology* 215: 2853-2859.
- Insausti, T. C., J. Defrize, C. R. Lazzari and J. Casas. 2012.** Visual fields and eye morphology support color vision in a color-changing crab-spider. *Arthropod Structure & Development* 41: 155-163.
- Jackson, R. R. 2000.** Prey preferences and visual discrimination ability of *Brettus*, *Cocalus* and *Cyrba*, araneophagic jumping spiders (Araneae: Salticidae) from Australia, Kenya and Sri Lanka. *New Zealand Journal of Zoology* 27: 29-39.
- Jackson, R. R. and A. D. Blest. 1982.** The distances at which a primitive jumping spider, *Portia fimbriata*, makes visual discriminations. *Journal of Experimental Biology* 97: 441-445.
- Jackson, R. R. and D. P. Harland. 2009.** One small leap for the jumping spider but a giant step for vision science. *The Journal of Experimental Biology* 212 (14): 2129-2132.
- Jakob, E. M., S. M. Long, D. P. Harland, R. R. Jackson, A. Carey, M. E. Searles, A. H. Porter, C. Canavesi and J. P. Rolland. 2018.** Lateral eyes direct principal eyes as jumping spiders track objects. *Current Biology* 28: R1075-R1095.
- Johnson, A. S. and W. Winlow. 2019.** Are neural transactions in the retina performed by phase ternary computation? *Animal Behavior and Neuroscience* 2 (1): 223-236.
- Karsch, F. 1878a.** Exotisch-araneologisches. *Zeitschrift für die Gesamten Naturwissenschaften* 51: 322-333, 771-826.
- Karsch, F. 1878b.** Diagnoses Attoidarum aliquot novarum Novae Hollandiae collectionis Musei Zoologici Berolinensis. *Mittheilungen des Münchener Entomologischen Vereins* 2: 22-32.

- Kashiyama, K., T. Seki, H. Numata and S. G. Goto. 2009.** Molecular characterization of visual pigments in Branchiopoda and the evolution of opsins in Arthropoda. *Molecular Biology and Evolution* 26 (2): 299-311.
- Kästner, A. 1950.** Reaktionen der Hupfspinnen (Salticidae) auf unbewegte farblose und farbige Gesichtsstimuli. *Zoologische Beiträge* 1: 13-50.
- Kater, S. B. 1974.** Feeding in *Helisoma trivolis*: the morphological and physiological bases of a fixed action pattern. *American Zoologist* 14 (3): 1017-1036
- Katz, M. and P. B. Kruger. 2009.** The human eye as an optical system. Chapter 33 in: *Duane's Ophthalmology*, 15th Edition, ed. W. Tasman and E. Jaeger, Lippincott Williams & Wilkins, Philadelphia. 1-63.
- Keyserling, E. 1882.** Die Arachniden Australiens, nach der Natur beschrieben und abgebildet. Erster Theil, Lieferung 29-30. Bauer & Raspe, Nürnberg: 1325-1420, pl. 113-120.
- Keyserling, E. 1885.** Neue Spinnen aus America. VI. Verhandlungen der Kaiserlich-Königlichen Zoologisch-Botanischen Gesellschaft in Wien 34: 489-534.
- Koch, C. L. 1846.** Die Arachniden. J. L. Lotzbeck, Nürnberg. Dreizehnter Band: 1-234, pl. 433-468, figs. 1078-1271; Vierzehnter Band: 1-88, pl. 467-480, figs. 1272-1342.
- Koch, L. 1878.** Japanische Arachniden und Myriapoden. Verhandlungen der Kaiserlich-Königlichen Zoologisch-Botanischen Gesellschaft in Wien 27 (1877): 735-798, pl. 15-16.
- Koch, L. 1879.** Die Arachniden Australiens, nach der Natur beschrieben und abgebildet. Erster Theil, Lieferung 24-25. Bauer & Raspe, Nürnberg: 1045-1156, pl. 91-100.
- Komiya, M., S. Yamashita and H. Tateda. 1988.** Turning reactions to real and apparent motion stimuli in the posterolateral eyes of jumping spiders. *Journal of Comparative Physiology A* 163: 585-592.
- Konkle, T. and A. Oliva. 2012.** A real-world size organization of object responses in occipitotemporal cortex. *Neuron* 74: 1114-1124.
- Kovoor, J., A. Muñoz-Cuevas and J. Ortega-Escobar. 2005.** The visual system of *Lycosa tarentula* (Araneae, Lycosidae): microscopic anatomy of the protocerebral optic centres. *Italian Journal of Zoology* 72: 205-216.
- Koyanagi, M., T. Nagata, K. Katoh, S. Yamashita and F. Tokunaga. 2008.** Molecular evolution of arthropod color vision deduced from multiple opsin genes of jumping spiders. *Journal of Molecular Evolution* 66: 130-137.
- Kuehni, R. G. 2004.** Variability in unique hue selection: a surprising phenomenon. *Color Research and Application* 29: 158-162.
- Kuhne, H. 1959.** Die neurosekretorischen Zellen und der retrocerebrale neuro-endocrine Komplex von Spinne. *Zoologische Jahrbücher, Abteilung für Anatomie und Ontogenie der Tiere* 77: 527-600.
- Labin, A. M. and E. N. Ribak. 2010.** Retinal glial cells enhance human vision acuity. *Physical Review Letters* 158102: 1-4.
- Lam, D. Y. S., T. L. Cheng, D. G. Kirschen and D. M. Laby. 2008.** Effects of head tilt on stereopsis. *Binocular Vision and Strabismus Quarterly Journal* 23 (2): 95-104.
- Land, M. F. 1969a.** Structure of the retinae of jumping spiders (Salticidae: Dendryphaninae) in relation to visual optics. *Journal of Experimental Biology* 51: 443-470.
- Land, M. F. 1969b.** Movements of the retinae of jumping spiders (Salticidae: Dendryphantinae) in response to visual stimuli. *Journal of Experimental Biology* 51: 471-493.
- Land, M. F. 1971.** Orientation by jumping spiders in the absence of visual feedback. *Journal of Experimental Biology* 54: 119-139.
- Land, M. F. 1972.** Stepping movements made by jumping spiders during turns mediated by the lateral eyes. *Journal of Experimental Biology* 57: 15-40.
- Land, M. F. 1985a.** Fields of view of the eyes of primitive jumping spiders. *Journal of Experimental Biology* 119: 381-384.
- Land, M. F. 1985b.** The morphology and optics of spider eyes. Chapter IV in: *Neurobiology of Arachnids*, ed. F. G. Barth, Springer-Verlag: 53-78.
- Latreille, P. A. 1804.** Tableau methodique des Insectes. *Nouveau Dictionnaire d'Histoire Naturelle*, Paris 24: 129-295.
- Legendre, R. 1959.** Contribution à l'étude du système nerveux des aranéides. *Annales des Sciences Naturelles, Zoologie et Biologie Animale* 28: 343-474.
- Legendre, R. 1961.** Sur deux particularités du système nerveux central de la mygale *Scodra calceata* Fabr. *Annales des Sciences Naturelles, Zoologie et Biologie Animale* 30: 767-771.
- Legendre, R. 1971.** Etat actuel de nos connaissances sur le développement embryonnaire et la croissance des araignées. *Annales des Sciences Naturelles, Zoologie et Biologie Animale* 96: 93-114.
- Legendre, R. 1985.** The stomatogastric nervous system and neurosecretion. Chapter III in: *Neurobiology of Arachnids*, ed. F. G. Barth, Springer-Verlag: 38-49.
- Lewis, R. F., B. M. Gaymard and R. J. Tamargo. 1998.** Efference copy provides the eye position information required for visually guided reaching. *Journal of Neurophysiology* 80 (3): 1605-1608.
- Li, D. and M. L. M. Lim. 2005.** Ultraviolet cues affect the foraging behaviour of jumping spiders. *Animal Behaviour* 70: 771-776.
- Li, J., Z. Zhang, F. Liu, Q. Liu, W. Gan, J. Chen, M. L. M. Lim and D. Li. 2008.** UVB-based mate choice cues used by females of the jumping spider *Phintella vittata*. *Current Biology* 18: 699-703.

- Lim, M. L. M. 2006.** UV vision in jumping spiders (Araneae: Salticidae): sexual selection and foraging behaviour. Ph.D. Thesis, National University of Singapore: i-xv, 1-258.
- Lim, M. L. M. and D. Li. 2006a.** Behavioural evidence of UV sensitivity in jumping spiders (Araneae: Salticidae). *Journal of Comparative Physiology A* 192: 871-878.
- Lim, M. L. M. and D. Li. 2006b.** Extreme ultraviolet sexual dimorphism in jumping spiders (Araneae: Salticidae). *Biological Journal of the Linnean Society* 89: 397-406.
- Lim, M. L. M., J. Li and D. Li. 2007.** Effect of UV-reflecting markings on female mate-choice decisions in *Cosmophasis umbratica*, a jumping spider from Singapore. *Behavioral Ecology* 19 (1): 61-66.
- Liu, Y., A. Maas and D. Waloszek. 2009.** Early development of the anterior body region of the grey widow spider *Latrodectus geometricus* Koch, 1841 (Theridiidae, Araneae). *Arthropod Structure & Development* 38: 401-416.
- Locket, N. A. 1992.** Problems of deep foveas. *Australian and New Zealand Journal of Ophthalmology* 20 (4): 281-295.
- Long, S. M. 2016.** Spider brain morphology & behavior. Ph.D. dissertation, University of Massachusetts, Amherst: i-xxiii, 1-215.
- Lucas, H. 1846.** Histoire naturelle des animaux articulés. In: *Exploration scientifique de l'Algérie pendant les années 1840, 1841, 1842* publiée par ordre du Gouvernement et avec le concours d'une commission académique. Aris, Sciences physiques, Zoologie 1: 89-271, pl. 1-17.
- Maddison, W. P. 2009.** New cocalodine jumping spiders from Papua New Guinea (Araneae: Salticidae: Cocalodinae). *Zootaxa* 2021: 1-22.
- Maddison, W. P. 2012.** Five new species of lapsiine jumping spiders from Ecuador (Araneae: Salticidae). *Zootaxa* 3424: 51-65.
- Maddison, W. P. and M. Hedin. 2003.** Jumping spider phylogeny (Araneae: Salticidae). *Invertebrate Systematics* 17: 529-549.
- Martin, G. 2017.** *Sensory Ecology of Birds*. Oxford University Press.
- Martin, G. R. and I. E. Gordon. 1975.** Visual acuity in the Tawny Owl (*Strix aluco*). *Vision Research* 14: 1393-1397.
- Masland, R. H. 2001.** The fundamental plan of the retina. *Nature Neuroscience* 4 (9): 877-886.
- Masland, R. H. 2011.** Cell populations of the retina: The Proctor Lecture. *Investigative Ophthalmology and Visual Science* 52 (7): 4581-4591.
- McCourt, M. E. 1982.** A spatial-frequency dependent grating-induction effect. *Vision Research* 22: 119-134.
- Meier, F. 1967.** Beiträge zur Kenntnis der postembryonalen Entwicklung der Spinnen (Araneida, Labidognatha) unter besonderer Berücksichtigung der Histogenese des Zentralnervensystems. *Revue Suisse de Zoologie* 74: 1-114.
- Melin, A. D., D. W. Kline, C. Hiramatsu and T. Caro. 2016.** Zebra stripes through the eyes of their predators, zebras, and humans. *PLOS One* (DOI:10.1371/journal.pone.0145679): 1-18.
- Menda, G., P. S. Shamble, E. I. Nitzany, J. R. Golden and R. R. Hoy. 2014.** Visual perception in the brain of a jumping spider. *Current Biology* 24: 2580-2585.
- Mikellidou, K. and P. Thompson. 2013.** The vertical-horizontal illusion: assessing the contributions of anisotropy, abutting, and crossing to the misperception of simple line stimuli. *Journal of Vision* 13 (8)(7): 1-11.
- Miller, P. E. 2001.** Vision in animals - What do dogs and cats see? Waltham/OSU Symposium, Small Animal Ophthalmology, online at: <https://www.vin.com/apputil/content/defaultadv1.aspx?pld=11132&id=3844144>
- Miller, P. E. and C. J. Murphy. 1995.** Vision in dogs. *Journal of the American Veterinary Medical Association* 207 (12): 1623-1634.
- Millot, Jacques. 1949.** Ordre des araneides (Araneae). In: *Traite de Zoologie*, ed. P. Grasse, 6: 589-743.
- Monnier, P. and S. K. Shevell. 2003.** Large shifts in color appearance from patterned chromatic backgrounds. *Nature Neuroscience* 6: 801-802.
- Morehouse, N. I., D. B. Zurek, L. A. Taylor, T. Cronin. 2017a.** Repeated evolution of color vision underlies rapid diversification of salticid male coloration. In: *Proceedings of the Abstract of the Annual Meeting of SICB, New Orleans, LA, USA, 4-8 January 2017*.
- Morehouse, N. I., E. K. Buschbeck, D. B. Zurek, M. Steck and M. L. Porter. 2017b.** Molecular evolution of spider vision: new opportunities, familiar players. *Biological Bulletin* 233: 21-38.
- Murphy, A. D. 2001.** The neuronal basis of feeding in the snail, *Helisoma*, with comparisons to selected gastropods. *Progress in Neurobiology* 63 (4): 383-408.
- Nagata, T., K. Arikawa and M. Kinoshita. 2019.** Photoreceptor projection from a four-tiered retina to four distinct regions of the first optic ganglion in a jumping spider. *Journal of Comparative Neurology* 527: 1346-1361.
- Nagata, T., M. Koyanaga, H. Tsukamoto, S. Saeki, K. Isono, Y. Shichida, F. Tokunaga, M. Kinoshita, K. Arikawa and A. Terakita. 2012.** Depth perception from image defocus in a jumping spider. *Science* 335: 469-471, supporting material online at www.sciencemag.org/cgi/content/full/335/6067/469/DC1
- Nagata, T., M. Koyanaga, H. Tsukamoto and A. Terakita. 2010.** Identification and characterization of a protostome homologue of peropsin from a jumping spider. *Journal of Comparative Physiology A* 196: 51-59.
- Nakamura, T. and S. Yamashita. 2000.** Learning and discrimination of colored papers in jumping spiders (Araneae, Salticidae). *Journal of Comparative Physiology A* 186: 897-901.

- Nakano, M., C. M. Lockhart, E. J. Kelly and A. E. Rettle. 2014.** Ocular cytochrome P450s and transporters: roles in disease and endobiotic and xenobiotic disposition. *Drug Metabolism Reviews*, Informa Healthcare (ISSN 1097-9883): 1-14.
- Nelson, X. J. 2010.** Visual cues used by ant-like jumping spiders to distinguish conspecifics from their models. *The Journal of Arachnology* 38: 27-34.
- Nelson, X. J. 2021.** Visual processing in a unique modular system. *Posted online at:* <https://www.ximenanelson.com/spider-vision.html>, accessed 12 DEC 2021: 1-6.
- Nelson, X. J. and R. R. Jackson. 2007.** Vision-based ability of an ant-mimicking jumping spider to discriminate between models, conspecific individuals and prey. *Insectes Sociaux* 54: 1-4.
- Nelson, X. J. and R. R. Jackson. 2009.** Prey classification by an araneophagic ant-like jumping spider (Araneae: Salticidae). *Journal of Zoology* 279: 173-179.
- Ninio, J. and K. A. Stevens. 2000.** Variations on the Hermann grid: an extinction illusion. *Perception* 29 (10): 1209-1217.
- Nolte, A. 2015.** Lab report: Investigating jumping spider vision. *Published online at:* https://www.esa.int/gsp/ACT/doc/BIO/AlekeNolte_FinalReport.pdf
- Nolte, A., D. Hennes, D. Izzo, C. Blum, V. V. Hafner and T. Gheysens. 2017.** A note on the depth-from-defocus mechanism of jumping spiders. *Biomimetics* 2 (3): 1-14.
- Oberdorfer, M. D. 1975.** The neural organization of the first optic ganglion of the principal eyes of jumping spiders (Salticidae). *Journal of Comparative Neurology* 174: 95-118.
- Otto, J. C. and D. E. Hill. 2012.** Contests between male *Maratus vespertilio* (Simon 1901) (Araneae: Salticidae). *Peckhamia* 98.1: 1-17.
- Otto, J. C. and D. E. Hill. 2016.** Seven new peacock spiders from Western Australia and South Australia (Araneae: Salticidae: Euophryini: Maratus). *Peckhamia* 141.1: 1-101.
- Patterson, S. S., M. Neitz and J. Neitz. 2021.** Seminars in Cell and Developmental Biology (<https://doi.org/10.1016/j.semcdb.2021.05.004>): 1-4.
- Peaslee, A. G. and G. Wilson. 1989.** Spectral sensitivity in jumping spiders (Araneae, Salticidae). *Journal of Comparative Physiology A* 164: 359-363.
- Peckham, G. W., and E. G. Peckham. 1883.** Descriptions of new or little known spiders of the family Attidae from various parts of the United States of North America. Milwaukee. 1-35.
- Peckham, G. W., and E. G. Peckham. 1885.** On some new genera and species of Attidae from the eastern part of Guatamala. *Proceedings of the Natural History Society of Wisconsin* 1885: 62-86.
- Peckham, G. W., and E. G. Peckham. 1888.** Attidae of North America. *Transactions of the Wisconsin Academy of Sciences, Arts and Letters* 7: 1-104.
- Peckham, G. W., and E. G. Peckham. 1895.** The sense of sight in spiders with some observations on the color sense. *Transactions of the Wisconsin Academy of Sciences, Arts, and Letters* 10: 231-261.
- Peters, H. M. 1969.** Maturing and coordination of webbuilding activity. *American Zoologist* 9: 223-227.
- Pichaud, F., A. Briscoe and C. Desplan. 1999.** Evolution of color vision. *Current Opinion in Neurobiology* 9: 622-627.
- Pickard-Cambridge, F. O. 1901.** Arachnida - Araneida and Opiliones. In: *Biologia Centrali-Americana*, Zoology. London 2: 193-312.
- Pickard-Cambridge, O. 1869.** Descriptions and sketches of some new species of Araneida, with characters of a new genus. *Annals and Magazine of Natural History* (4) 3 (13): 52-74, pl. 4-6.
- Poggio, T., M. Fahle and S. Edelman. 1992.** Fast perceptual learning in visual hyperacuity. *Science* 256 (5059): 1018-1021.
- Pridmore, R. W. 2013.** Cone receptor sensitivities and unique hue chromatic responses: correlation and causation imply the physiological basis of unique hues. *PLOS One* 8 (10): e77134: 1-13.
- Pringle, J. W. S. 1955.** The function of the lyriform organs of arachnids. *Journal of Experimental Biology* 32: 270-278.
- Pumphrey, R. J. 1948.** The theory of the fovea. *The Journal of Experimental Biology* 25: 299-312.
- Quesada, R., E. Triana, G. Vargas, J. K. Douglass, M. A. Seid, J. E. Niven, W. G. Eberhard and W. T. Wcislo. 2011.** The allometry of CNS size and consequences of miniaturization in orb-weaving and cleptoparasitic spiders. *Arthropod Structure and Development* 40 (6): 521-529.
- Rempel, J. G. 1957.** The embryology of the black widow spider, *Latrodectus mactans* (Fabr.). *Canadian Journal of Zoology* 35: 35-74.
- Reissland, A. and P. Görner. 1985.** Trichobothria. Chapter VIII in: *Neurobiology of Arachnids*, ed. F. G. Barth, Springer-Verlag: 138-161.
- Reymond, L. 1985.** Spatial visual acuity of the eagle *Aquila audax*: a behavioural, optical and anatomical investigation. *Vision Research* 25: 1477-1491.
- Richman, D. B. 1982.** Epigamic display in jumping spiders (Araneae, Salticidae) and its use in systematics. *Journal of Arachnology* 10: 47-67.
- Richman, D. B. and R. R. Jackson. 1992.** A review of the ethology of jumping spider (Araneae, Salticidae). *Bulletin of the British Arachnological Society* 9 (2): 33-37.
- Robinson, M. H. and C. E. Valerio. 1977.** Attacks on large or heavily defended prey by tropical salticid spiders. *Psyche* 84 (1, 048480): 1-10.

- Root, T. M. 1985.** The central and peripheral organization of scorpion locomotion. Chapter XVII in: *Neurobiology of Arachnids*, ed. F. G. Barth, Springer-Verlag: 337-347.
- Rosenzweig, M. R., S. M. Breedlove and A. L. Leiman. 2002.** *Biological Psychology*. Third Edition. Sinauer Associates, Inc. Sunderland, Massachusetts. i-xx, 1-651, A1-A8, G1-G26, R1-R36, AI1-AI7, I1-I12, IC1-IC2.
- Ross, C. F. 2004.** The tarsier fovea: functionless vestige or nocturnal adaptation? Chapter 19 in: *Anthropoid Origins: New Visions (Advances in Primatology)*, eds. C. F. Ross and R. F. Kay, Kluwer/Plenum: 1-747.
- Roth, L. S. V., A. Balkenius and A. Kelber. 2007.** Colour perception in a dichromat. *The Journal of Experimental Biology* 210: 2795-2800.
- Saint Remy, G. 1890.** Contribution à l'étude du cerveau chez les Arthropodes trachéates. Thèse présentée à la Faculté des Sciences de Paris. 1-274, pl. 1-14.
- Scheiner, R., A. Weiss, D. Malun and J. Erber. 2001.** Learning in honey bees with brain lesions: how partial mushroom-body ablations affect sucrose responsiveness and tactile antennal learning. *Animal Cognition* 4: 227-235.
- Scheuring, L. 1914.** Die Augen der Arachnoideen II. *Zoologische Jahrbücher. Abteilung für Anatomie und Ontogenie der Tiere* 37: 369-464.
- Schmidt, B. P., M. Neitz and J. Neitz. 2014.** Neurobiological hypothesis of color appearance and hue perception. *Journal of the Optical Society of America, A, Optics, Image Science, and Vision* 31 (4): A195-A207.
- Schrauf, M., B. Lingelbach and E. R. Wist. 1997.** The scintillating grid illusion. *Vision Research*. 37 (8): 1033-1038.
- Schwager, E. E. 2008.** Segmentation of the spider *Achaearanea tepidariorum* investigated by gene expression and functional analysis of the gap gene hunchback. Ph.D. dissertation, Universität zu Köln: i-viii, 1-181.
- Schwager, E. E., M. Schoppmeier, M. Pechmann and W. G. M. Damen. 2007.** Duplicated Hox genes in the spider *Cupiennius salei*. *Frontiers in Zoology* 4 (10): 1-11.
- Seyfarth, E.-A. 1978.** Lyriform slit sense organs and muscle reflexes in the spider leg. *Journal of Comparative Physiology* 125: 45-57.
- Seyfarth, E.-A. 1985.** Spider proprioception: receptors, reflexes, and control of locomotion. Chapter XII in: *Neurobiology of Arachnids*, ed. F. G. Barth, Springer-Verlag: 231-248.
- Seyfarth, E.-A. and F. G. Barth. 1972.** Compound slit sense organs on the spider leg: mechanoreceptors involved in kinesthetic orientation. *Journal of Comparative Physiology* 78: 176-191.
- Seyfarth, E.-A., W. Gnatzy and K. Hammer. 1990.** Coxal hair plates in spiders: physiology, fine structure, and specific central projections. *Journal of Comparative Physiology A*, 166 (5): 633-642.
- Seyfarth, E.-A. and H. J. Pflüger. 1984.** Proprioceptor distribution and control of a muscle reflex in the tibia of spider legs. *Journal of Neurobiology* 15: 365- 374.
- Shamble, P. S., G. Menda, J. R. Golden, E. I. Nitzany, K. Walden, T. Beatus, D. O. Elias, I. Cohen, R. N. Miles and R. R. Hoy. 2016.** Airborne acoustic perception by a jumping spider. *Current Biology* 26: 1-8.
- Shapley, R. and M. Hawken. 2002.** Neural mechanisms for color perception in the primary visual cortex. *Current Opinion in Neurobiology* 12: 426-432.
- Shepeleva, I. P. 2022.** A comparative analysis of the camera-like eyes of jumping spiders and humans. *Vision* 6 (2): 1-16 (<https://doi.org/10.3390/vision6010002>).
- Sherman, R. G. 1985.** Neural control of the heartbeat and skeletal muscle in spiders and scorpions. Chapter XVI in: *Neurobiology of Arachnids*, ed. F. G. Barth, Springer-Verlag: 319-336.
- Sherman, R. G., C. R. Bursey, C. R. Fournier and R. A. Pax. 1969.** Cardiac ganglia in spiders (Arachnida: Araneae). *Experientia* 25: 438-439.
- Sherman, R. G. and R. A. Pax. 1967.** A physiological and morphological study of a spider heart. *American Zoologist* 7: 190-191.
- Sherman, R. G. and R. A. Pax. 1968.** The heartbeat of the spider, *Geolycosa missouriensis*. *Comparative Biochemistry and Physiology* 26: 529-536.
- Simon, E. 1868.** Monographie des espèces européennes de la famille des Attides (Attidae Sundewall. - Saltigradae Latreille). *Annales de la Société Entomologique de France* (4) 8: 11-72, 529-726, pl. 5-7.
- Simon, E. 1885.** Matériaux pour servir à la faune arachnologiques de l'Asie méridionale. I. Arachnides recueillis à Wagra-Karoor près Gundacul, district de Bellary par M. M. Chaper. II. Arachnides recueillis à Ramnad, district de Madura par M. l'abbé Fabre. *Bulletin de la Société Zoologique de France* 10: 1-39, pl. 10.
- Simon, E. 1900.** Descriptions d'arachnides nouveaux de la famille des Attidae. *Annales de la Société Entomologique de Belgique*, 44: 381-407.
- Simon, E. 1901.** Histoire naturelle des araignées. Deuxième édition, tome second. Roret, Paris: 381-668.
- Sivertsen, D. W. 1989.** The physiology of high-order visual neurons in the jumping spider (Salticidae) and the vocalizations of free ranging owl monkeys. Ph.D. dissertation, California Institute of Technology: i-ix, 1-140.
- Snyder, A. W. and W. H. Miller. 1978.** Telephoto lens system of falconiform eyes. *Nature* 275 (5676): 127-129.
- Solomon, S. G. and P. Lennie. 2007.** The machinery of colour vision. *Nature Reviews, Neuroscience* 8: 276-286.
- Spano, L., L. M. Long and E. M. Jakob. 2012.** Secondary eyes mediate the response to looming objects in jumping spiders (*Phidippus audax*, Salticidae). *Biology Letters* 8 (6): 949-951.

- Steinhoff, P. O. M., A. Sombke, J. Liedtke, J. M. Schneider, S. Harzsch, and G. Uhl. 2017.** The synganglion of the jumping spider *Marpissa muscosa* (Arachnida: Salticidae): insights from histology, immunohistochemistry and microCT analysis. *Arthropod Structure and Development* 46 (2): 156–170.
- Steinhoff, P. O. M., G. Uhl, S. Harzsch and A. Sombke. 2020.** Visual pathways in the brain of the jumping spider *Marpissa muscosa*. *Journal of Comparative Neurology* 2020 (<https://doi.org/10.1002/cne.24862>): 1-20.
- Stong, C. L. 1974.** The Amateur Scientist. How to create visual illusions. *Scientific American* 231 (5): 126.
- Strausfield, N. J., P. Weltzien and F. G. Barth. 1993.** Two visual systems in one brain: neuropils serving the principal eyes of the spider *Cupiennius salei*. *The Journal of Comparative Neurology* 328 (1): 63-75.
- Surridge, A. K., D. Osorio and N. I. Mundy. 2003.** Evolution and selection of trichromatic vision in primates. *Trends in Ecology and Evolution* 18 (4): 198-205.
- Szűts, T. and N. Scharff. 2009.** Revision of the living members of the genus *Tomocyra* Simon, 1900 (Araneae: Salticidae). *Contributions to Natural History* 12: 1337-1372.
- Taylor, P. W., O. Hasson and D. L. Clark. 2000.** Body postures and patterns as amplifiers of physical condition. *Proceedings of the Royal Society, London B* 267: 917-922
- Taylor, P. W., O. Hasson and D. L. Clark. 2001.** Initiation and resolution of jumping spider contests: roles for size, proximity, and early detection of rivals. *Behavioral Ecology and Sociobiology* 50: 403-413.
- Taylor, P. W., R. R. Jackson and M. W. Robertson. 1998.** A case of blind spider's buff?: prey-capture by jumping spiders (Araneae, Salticidae) in the absence of visual cues. *The Journal of Arachnology* 26: 369-381.
- Telford, M. J. and R. H. Thomas. 1998.** Expression of homeobox genes shows chelicerate arthropods retain their deutocerebral segment. *Proceedings of the National Academy of Sciences, USA* 95: 10671-10675.
- Terakita, A. and T. Nagata. 2014.** Functional properties of opsins and their contribution to light-sensing physiology. *Zoological Science* 31: 653-659.
- Thorell, T. 1881.** Studi sui Ragni Malesi e Papuani. III. Ragni dell'Austro Malesia e del Capo York, conservati nel Museo civico di storia naturale di Genova. *Annali del Museo Civico di Storia Naturale di Genova* 17: 1-720.
- Thoreson, W. B. and D. M. Dacey. 2019.** Diverse cell types, circuits, and mechanism for color vision in the vertebrate retina. *Physiology Reviews* 99: 1527-1573.
- Tork, P. 2019.** Pathways of ocular entrainment in *Marpissa marina* (Araneae, Salticidae). *New Zealand Journal of Zoology* 46 (4): 321-333.
- Tucker, V. A. 2000.** The deep fovea, sideways vision and spiral flight paths in raptors. *The Journal of Experimental Biology* 203: 3745-3754.
- Tuthill, J. C., M. E. Chiappe and M. B. Reiser. 2011.** Neural correlates of illusory motion perception in *Drosophila*. *Proceedings of the National Academy of Science, USA* 108 (23): 9685-9690.
- Veilleux, C. C. and E. C. Kirk. 2014.** Visual acuity in mammals: effects of eye size and ecology. *Brain, Behavior and Evolution* 83: 43-53.
- Walckenaer, C. A. 1837.** Histoire naturelle des insectes Aptères. Tome premier. Roret, Paris: 1-682, pl. 1-15.
- Walcott, C. 1969.** A spider's vibration receptor: it's anatomy and physiology. *American Zoologist* 9: 133-144.
- Walls, G. L. 1937.** Significance of the foveal depression. *Archives of Ophthalmology* 18: 912-919.
- Wanless, F. R. 1981.** A revision of the spider genus *Phaecius* (Araneae: Salticidae). *Bulletin of the British Museum of Natural History, Zoology* 41: 199-212.
- Wanless, F. R. 1982.** A revision of the spider genus *Cocalodes* with a description of a new related genus (Araneae: Salticidae). *Bulletin of the British Museum of Natural History, Zoology* 42: 263-298.
- Wesołowska, W. 1981.** Salticidae (Aranei) from North Korea, China and Mongolia. *Annales Zoologici, Warszawa* 36: 45-83.
- Westheimer G. L. 1981.** Visual hyperacuity. In: *Progress in Sensory Physiology*, vol. 1, eds. H. Autrum, E. R. Perl, R. F. Schmidt and D. Ottoson, Springer, Berlin, Heidelberg.
- Westheimer, G. L. 2010.** Visual acuity and hyperacuity. Chapter 4 in: *Handbook of Optics*, Third Edition: 4.1-4.17, online at: https://cgvr.cs.uni-bremen.de/teaching/cg_literatur/visual_acuity.pdf
- Williams, D. S. and P. McIntyre. 1980.** The principal eyes of a jumping spider have a telephoto component. *Nature* 288: 578-580.
- Winkler, P. 2010.** The nerve cells of the retina. *The Science Journal of the Lander College of Arts and Sciences* 3 (1): 78-94.
- Wu, C. Q. 2010.** A neuroanatomically-based model for human color vision. *BMC Neuroscience* 11. Supplement 1 (P143): 1-2.
- Yaginuma, T. 1967.** Three new spiders (*Argiope*, *Boethus* and *Cispus*) from Japan. *Acta Arachnologica* 20: 50-64.
- Yamashita, S. 1985.** Photoreceptor cells in the spider eye: spectral sensitivity and efferent control. Chapter VI in: *Neurobiology of Arachnids*, ed. F. G. Barth, Springer-Verlag: 103-117.
- Yamashita, S. and H. Tateda. 1976.** Spectral sensitivities of jumping spider eyes. *Journal of Comparative Physiology* 105: 29-41.
- Yamashita, S. and H. Tateda. 1978.** Spectral sensitivities of the anterior median eyes of the orb web spiders *Argiope bruennichii* and *A. amoena*. *Journal of Experimental Biology* 74: 47-57.
- Yan, W., M. A. Laboulaye, N. M. Tran, I. E. Whitney, I. Benhar and J. R. Sanes. 2020.** Mouse retinal cell atlas: molecular identification of over sixty amacrine cell types. *The Journal of Neuroscience* 40 (27): 5177-5195.

- Young, T. 1802.** Bakerian lecture: On the theory of light and colours. Philosophical Transactions of the Royal Society, London 92: 12-48.
- Zhang, J. X. and W. P. Maddison. 2012.** New euophryine jumping spiders from Southeast Asia and Africa (Araneae: Salticidae: Euophryinae). Zootaxa 3581: 53-80.
- Zurek, D. B. 2012.** The function of the anterior lateral eyes in the modular vision system of jumping spiders (Araneae, Salticidae). Ph.D. dissertation, Macquarie University: i-xi, 1-152.
- Zurek, D. B., T. W. Cronin, L. A. Taylor, K. Byrne, M. L. G. Sullivan and N. I. Morehouse. 2015.** Spectral filtering enables trichromatic vision in colorful jumping spiders. Current Biology 25: R403-R404.
- Zurek, D. B. and X. J. Nelson. 2012a.** Saccadic tracking of targets mediated by the anterior-lateral eyes of jumping spiders. Journal of Comparative Physiology A 198 (6): 411-417.
- Zurek, D. B. and X. J. Nelson. 2012b.** Hyperacute motion detection by the lateral eyes of jumping spiders. Vision Research 66: 26-30.
- Zurek, D. B., A. J. Taylor, C. S. Evans and X. J. Nelson. 2010.** The role of the anterior lateral eyes in the vision-based behaviour of jumping spiders. The Journal of Experimental Biology 213: 2372-2378.